Use Authorization

In presenting this thesis in partial fulfillment of the requirements for an advanced degree at Idaho State University, I agree that the Library shall make it freely available for inspection. I further state that permission to download and/or print my thesis for scholarly purposes may be granted by the Dean of the Graduate School, Dean of my academic division, or by the University Librarian. It is understood that any copying or publication of this thesis for financial gain shall not be allowed without my written permission.

Signature _____

Date _____

Optimization of the Thermal Treatment Process for the Removal of ^{14}C from Irradiated Graphite for Waste Volume Reduction and Bulk Graphite Recycle

by

Katherine Jeanne Nelson

A Thesis

submitted in partial fulfillment

of the requirement for the degree of

Master of Science in the Department of Nuclear Engineering

Idaho State University

July 2014

Committee Approval

To the Graduate Faculty:

The members of the committee appointed to examine the thesis of Katherine Nelson find it satisfactory and recommend that it be accepted.

_____

Dr. Mary Lou Dunzik-Gougar
Major Advisor

_____

Dr. Jason Harris
Committee Member

_____

Dr. Rene Rodriguez
Graduate Faculty Representative

Acknowledgements

I am so very grateful to the wonderful individuals who surrounded me with their love, prayers, encouragement and expertise. First, to God, for the dream, the inspiration, the ability and the guidance. Next, to the love of my life, my husband, Troy. You gave your love, support, electrical tape, band wrench and knowledge of flow systems. To my most amazing children, Kristie Jo and Noah, Kassidie and Ben, and Tyler, for their encouragement, and skill in Excel, Word, and in editing and formatting. Time with you was my reward for reaching a goal! Kalli Jo, you are my joy! To the many family and friends who showed interest, said prayers and cheered me on. Everyone deserves cheerleaders like you, thank you! To my boss, Mike Popovich and the entire First Baptist Church team, for your incredible enthusiasm and support. To Lindsay Bennett for her knowledge and wise counsel to take the first step. To Dr. Jay Kunze for believing in me, early on, and advising me through classes. To Dr. Mary Lou Dunzik-Gougar for your direction and expertise in this thesis project. Special thanks to Dr. Jason Harris and Dr. Rene Rodriguez for sitting on my defense committee. To Kevin Claver and the boys in Lab B108. Thanks for allowing me access to the digital scale. To Mark Cherry for your help in mixing aqueous solutions and the DI water. Finally, to Mike Banyas, you are the greatest IT-guy, ever! Thank you so much, everyone, for your part in making this dream come true.

Table of Contents

List of Figures

List of Tables

List of Abbreviations

^{12}C - Carbon 12

^{14}C- Carbon 14

^{14}N – Nitrogen 14

^{17}O - Oxygen 17

Ar - Argon

AVR - Albeitsgenminschaft Versuchsreaktor

CO - Carbon monoxide

CO_2 - Carbon dioxide

CP- 1 - Chicago Pile 1

Gen-IV - Generation IV Concepts

HTGR - High Temperature Gas Cooled Reactor

ILW - Intermediate Level Waste

IR - Infra-red

LLW - Low Level Waste

LSC - Liquid Scintillation Counting

M - Molarity

Merlin - Forschungsreaktor Jülich 1 (FRJ-1)

O_2 – Oxygen

R&D - Research and Development

sccm - Standard cubic centimeters per minute

Optimization of the Thermal Treatment Process for the Removal of ^{14}C from Irradiated Graphite for Waste Volume Reduction and Bulk Graphite Recycle

Thesis Abstract—Idaho State University (2014)

The burden of irradiated graphite waste has been compounding throughout the world for many years. The isotope of greatest concern is carbon-14. Carbon-14 is proven un-removable in current chemical purification treatments since it cannot be differentiated from carbon-12. More successful removal treatments have been demonstrated, by Fachinger et al. (2006), using pyrolysis and oxidation. Developing a feasible waste management strategy for irradiated graphite components would reduce the large volume of long-term deep geological repository storage by allowing the bulk of the graphite to be recycled. An effective treatment process will be significant with the development of the High Temperature Gas Cooled Reactors which utilize many graphite components. This thesis is an optimization of previously studied thermal treatment methods developed at Idaho State University incorporating oxygen pre-loading and elevated temperatures prior to thermal treatment temperatures.

Chapter 1.0: Introduction

1.1 Problem Being Considered

In 1942, the first man-made nuclear reactor, Chicago Pile 1, used graphite blocks to moderate neutrons. Small pieces of uranium metal and uranium oxide were strategically placed inside a matrix of 45,000 graphite bricks in order to achieve criticality (U.S. DOE 1982). From that day forward, graphite has been used as a major component of nuclear reactors, worldwide. More than 250,000 metric tons of irradiated graphite waste has been generated from reactor components (Fachinger et al., 2007). Presently, the world lacks a viable waste-management strategy for irradiated graphite (EPRI, 2006; IAEA, 2006). Long-term storage is the current plan for managing the high volume, low level waste material.

The United States Department of Energy's recent interest in the High Temperature Gas Cooled Reactor (HTGR) has prompted even greater concern as HTGR's utilize many graphite components: graphite coated fuel particles, graphite neutron reflectors, and graphite core structural components. As the demand for cleaner energy drives the growth of the nuclear energy industry, this increase in reactors, and thereby, irradiated graphite, will greatly burden waste storage repositories.

Long-term storage of irradiated graphite poses concern, as a major isotope in irradiated graphite, ^{14}C, is readily mobile in ground water and atmospheric systems (Podruhzina, 2004). Carbon-14 is a long-lived radioisotope with a half-life of 5,730 years. Therefore, attempts to remove ^{14}C from irradiated graphite through pyrolysis, oxidation and thermal treatment are currently being explored. Removal of ^{14}C from large irradiated graphite reactor components may prevent costly disposal or allow recycling of this very pure nuclear grade material (Fachinger et al., 2007).

1.2 Objective of Thesis Work

Thermal treatment, the use of high-temperature environments to liberate surface species of graphite, has been explored as a suitable waste management processes for irradiated nuclear graphite: oxidation and pyrolysis, steam and oxygen thermal treatment. Yet these processes require refinement before consideration for a large scale application.

Building upon the preliminary experimental work conducted at Idaho State University by T. Smith (2012) and J. Cleaver (2011) in the area of thermal treatment of irradiated graphite, the objective of this work is to further refine the process towards maximizing the quantity of ^{14}C removed from the bulk graphite material, while minimizing the quantity of bulk graphite remaining after thermal treatment. An optimum thermal treatment process would demonstrate an effective waste management strategy for HTGR components and contribute to better understanding of nuclear graphite behavior during the reactor operation (Smith, 2012).

1.3 Work Performed

In previous studies, it has been shown that thermal treatment of irradiated graphite is most effective at slow oxidation rates, i.e. low temperatures and low availability of oxidizing agent (Smith, 2013; Fachinger et al., 2007). Based on the preliminary work by Smith (2013), the thermal treatment temperature of 700°C was used for all experiments. However, to improve the efficiency of treatment at this temperature, a pre-treatment step was added to the process. Pre-treatment consisted of very low (150°C or 300°C) temperature heating in the presence of oxygen. The objective of this step was to encourage chemisorption of oxygen to the graphite surface, such that this oxygen would be available for oxidation reactions during the higher temperature (700°C) treatment. Pre-treatment temperatures and oxidant concentrations were varied and the

resulting effects determined via measurement of both selective release and absolute release of ^{14}C. Two nuclear grades of irradiated graphite were studied: NBG-18 and NBG-25.

Chapter 2.0: Literary Review

2.1 Nuclear Graphite

Today, nuclear graphite, by design, has very few impurities, which minimizes the activation products formed by neutron irradiation (Marsden, 2002). Since the first graphite pile used in Chicago Pile (CP-1) in 1942, strides have been taken to produce very pure grades of graphite so as to reduce impurities that contribute to neutron interaction, as well as, to the waste management difficulties.

Graphite is formed from a high temperature process combining raw coke particles and a binder that provides cohesion for the raw particles. Nuclear grade graphite uses petroleum coke products selected for their crystallographic structure rather than an amorphous form of carbon. By heating these carbon materials to high temperatures, but below the melting point, in an air environment (calcination), impurities are removed from the petroleum products. These purified coke particles are mixed with the pitch binder and formed into blocks through various methods of extrusion, molding (isostatic or vibrational) or pressing. This formed material is heated for several weeks to temperatures near 1000°C, to expel impurities in the binder phase. The material is then impregnated with coal tar pitch in an attempt to fill in open pores produced by the release of impurities, and then again calcined. This process also aids in increasing the overall density of the block and adding to irradiation resistance (Marsden, 2002). Graphitization occurs at temperatures of 2500-3000^{o}C, whereby the carbon material transforms into a crystalline layered structure, Figure 2.1 Eventually, the graphite is cleansed and metals removed using fluorine gas (EPRI, 2006; IAEA 1154, 2000).

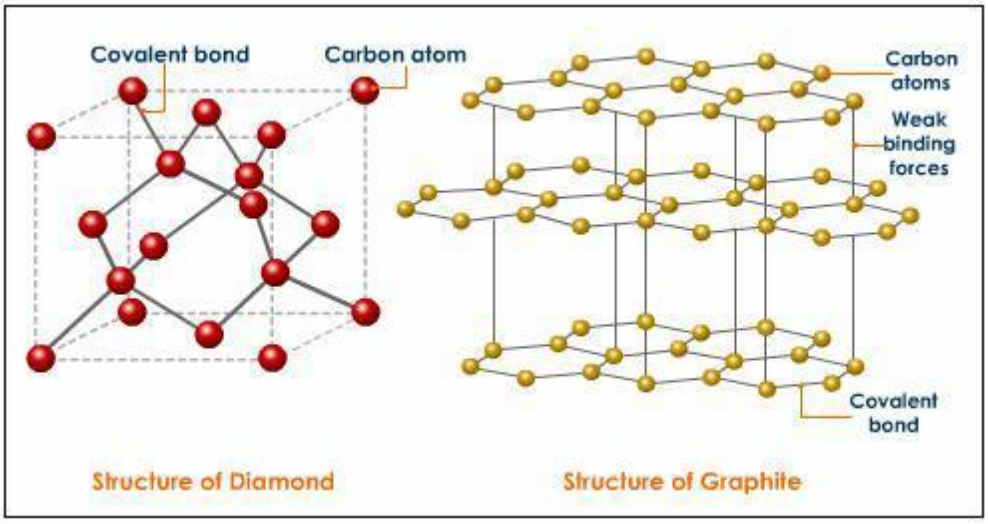

Figure2.1: Crystallographic Structure of Graphite (Mantell, 1968)

New grades of nuclear graphite are being tested for specific use in future HTGRs, with the understanding that much of the graphite will be subjected to higher dose levels of neutron radiation, as well as, to higher temperatures (LaBrier, 2013).

2.2 Neutron Irradiated Graphite

Nuclear grade graphite is a major building material used in reactors worldwide for reflecting and moderating neutrons, as well as, for core structural components. Some examples of types of graphite reactors, which have been or are currently in service, are shown in Table 2.1.

Table 2.1: Graphite reactors currently or previously in service (IAEA 1521, 2006)

Reactor Design/Type	Reactor Deployments
Air-cooled plutonium production graphite piles	X-10 (Oak Ridge National Laboratory, USA) Windscale Piles (UK) G1 (France)
Light water cooled graphite-moderated piles	Plutonium-production plants (Hanford, USA, and Russia) Power reactors such as RBMKs and AMB (Russia)
Carbon dioxide cooled reactors	Magnox and AGRs (UK) UNGG (France)
Helium cooled reactors	Albeitsgenminschaft Versuchsreaktor, or AVR (Germany), Dragon (UK), Thorium Hochtemeratur Reaktor, or THTR (Germany), Fort St. Vrain (USA), and new development reactors such as HTTR (Japan) and HTR-10 (China)

HTGRs are expected to be one of the next-generation nuclear reactors built in the United States. These reactors propose to offer increased proliferation resistance, high burn-up fuel cycles with growth potential for advanced fuels and cycles, and provide deep burn cycles with LWR spent fuel (INL, 2010). Along with their high performance will be the added irradiated graphite waste burden.

Currently, there are more than 250,000 metric tons of irradiated graphite worldwide. This material is classified as intermediate-level waste (ILW) by most countries (IAEA, 2006; Banford, 2008), although the United States does not have this classification. Due to the production of long-lived radioisotopes within irradiated graphite, all must be

managed as radioactive waste. As neutrons interact with graphite, changes occur in the chemical, mechanical and physical properties of the graphite (IAEA, 2006). In addition to these changes, impurities in the graphite and possibly radioisotopes from fuel interact with neutrons to form many long-lived and environmentally harmful radioisotopes. Some of these isotopes originating from minor impurities and corrosion products include: ^{3}H, ^{60}Co, ^{41}Ca, ^{55}Fe, ^{63}Ni, ^{110m}Ag, and ^{109}Cd (IAEA, 2006). Those originating in the fuel or from traces of fuel material outside the fuel particles include the fission products: ^{90}Sr, ^{3}Zr, ^{99}Tc, ^{107}Pd, ^{113m}Cd, ^{121m}Sn, ^{129}I, ^{133}Ba, ^{134}Cs, ^{147}Pm, ^{151}Sm, $^{152,154,155}Eu$, etc. (IAEA, 2006). Radioisotopes coming from uranium and transuranic origins include $^{238\text{-}241}Pu$, $^{241,\ 243}Am$ and $^{242\text{-}244}$ Cm species (IAEA, 2006). However, the most significant long-lived radionuclides of concern are ^{14}C and ^{36}Cl, due to their long half-lives and environmental mobility.

2.3 Carbon-14 in Irradiated Graphite

In nature, the majority of ^{14}C is continually produced in the upper atmosphere by ^{14}N capture of a neutron (National Council on Radiation Protection and Measurement, 1985). Eventually, an equilibrium concentration of ^{14}C is maintained between its production and decay. Plants, animals and ocean life take up ^{14}C as it bonds with oxygen to form carbon dioxide. As plants utilize the carbon dioxide through photosynthesis, animals ingest the plant life, yielding a constant ratio of ^{14}C to ^{12}C in their bodies. Upon death, ^{14}C is no longer taken into the plant or animal, but the ^{14}C continues to decay. This process is the basis for carbon dating.

2.3.1 Formation of ^{14}C in Irradiated Graphite

Carbon-14 is most commonly produced when neutrons from the core interact with ^{13}C, ^{14}N, and ^{17}O. In nuclear reactors, ^{14}C is produced through one of the following reactions:

1. ^{13}C (n, γ) ^{14}C

2. ^{14}N (n, p) ^{14}C

3. ^{17}O (n, α) ^{14}C

The formation of ^{14}C on and within graphite reactor components is highly dependent on the impurities within the graphite and the reactor coolant. In HTGRs, the two dominant ^{14}C production processes are reactions (1) and (2). Nitrogen, carbon, and oxygen can be found either as constituents or as impurities in all reactors (IAEA, 2004; Davis Jr., 1977). ^{13}C is present naturally in the graphite components, and nitrogen impurities can diffuse within the graphite structure, or adsorb to the graphite surface and within the pore structure (LaBrier, 2013). Studies by Marsden (2002) suggest that the majority of ^{14}C present in some irradiated graphites can be attributed to nitrogen that was either absorbed or trapped along the surface and within the graphite structure, on the order of 70% of total ^{14}C. Table 2.2 shows the precursors for carbon-14 production and their isotopic abundance. Nitrogen can enter the graphite during the process of fabricating the components or as an impurity in the coolant. While ^{17}O is also present as an impurity in the graphite and coolant, it contributes less than 1% of the total inventory of ^{14}C in HTGRs (Davis Jr. 1977). Therefore, the most probable contributor to ^{14}C found on irradiated graphite surfaces is ^{14}N, while ^{14}C found homogeneously distributed throughout the graphite body is mostly likely produced from ^{13}C.

Table 2.2: Prominent Precursors for ^{14}C Production and Isotopic Abundance in HTGR Systems

Species	Thermal Absorption Cross Section (Barns)	Isotopic Abundance (%)
^{14}N	1.8	99.63 ^{14}N/Nitrogen
^{13}C	0.0015	1.07 ^{13}C/Carbon
^{17}O	0.235	0.04 ^{17}O/Oxygen

2.3.2 Concentration Levels of ^{14}C in Irradiated Graphite

Several recent studies have concluded that ^{14}C contamination in irradiated graphite has higher concentration levels on the surface rather than within the core graphite (Bradbury, 2004; Podruhzina, 2004; Fachinger, 2006, 2008; von Lensa, 2010; Vulpius, 2013; LaBrier, 2013). Thermal treatment has been demonstrated as an effective method for the removal of surface and sub-surface ^{14}C-bearing contamination (Smith, 2013; LaBrier, 2013). Therefore, knowing the release mechanisms for carbon-14 will better facilitate its removal.

2.3.3 Release of Carbon Oxides on Graphite Surfaces

In inert environments, such as argon, small amounts of air will adsorb onto the surface and pores of the irradiated graphite, allowing carbon-oxygen bonds to form. As oxidation temperatures are achieved, <600°C, these compounds desorb into carbon species of CO and CO_2. The rate at which the oxidation takes place can be increased by introducing an oxidizing component, such as oxygen, steam, or carbon dioxide. Desorption of surface species can affect the morphology and microstructure of the surface, which in turn can affect the rate, pathways, and speciation of future desorption candidates (Smith, 2013). It has been shown that the majority of ^{14}C species liberated from irradiated graphite are carbon oxides, either carbon monoxide (^{14}CO) or carbon dioxide ($^{14}CO_2$) (Fachinger, 2006; Vulpius, 2013; LaBrier, 2013). Thermal treatment studies performed at Idaho State University have similarly demonstrated the preferential removal of ^{14}C from irradiated nuclear graphite based on specific experimental parameters which vary oxygen concentrations during thermal treatment (Smith, 2013).

2.4 Irradiated Graphite Waste Management Solutions

There are social and environmental concerns with the disposal practices for neutron irradiated graphite due to the presence of ^{14}C. Carbon-14 has a long half-life of 5730 years and is fairly mobile throughout the biosphere. Many long-term disposal

strategies have been proposed from near surface storage to deep geological storage, as well as deep sea storage. Difficulties ranging from predicted future human intrusion to regulations forbidding such practices keep the nuclear industry searching for a viable, long-term waste management solution. Alternate options for managing ^{14}C inventories include removal techniques such as radioisotope concentration minimization through incineration, removal by steam, and recycling of the bulk graphite after thermal treatment.

Reactor graphite radionuclide inventories are unique to each reactor due to the purity of the initial graphite, possible contamination during its use in the reactor, as well as to the radial and axial neutron fluxes, all of which factor into the formation of ^{14}C. For example, the average ^{14}C concentrations found on AVR graphite were ~3.51 μCi/g, whereas the average ^{14}C content in the I-1 Russian production reactor was 32.4 μCi/g (EPRI, 2006). These inventories will have bearing on the types of treatment exercised to remove the radionuclides while maintaining the bulk of graphite for recycle, as the demand for higher and purer grades of graphite escalates due to HTGR deployment.

As HTGRs are decommissioned and decontaminated, large volumes of irradiated nuclear graphite will be among the numerous waste forms to be disposed or remediated. Each newly decommissioned HTGR facility is expected to contribute another 2000 tonnes of waste in the form of irradiated graphite. In the UK, industrial efforts are currently geared towards housing irradiated graphite on-site to allow some of the short-term radioisotopes, such as ^{3}H and ^{60}Co, to decay for a few half-lives, as well as mitigating some of internal (Wigner) energy release (EPRI, 2006). Graphite blocks and components are then packed in concrete and sent to a repository for temporary or permanent disposal.

More recently, the European Commission's CARBOWASTE Consortium (2008-2012) collected information for treatment and disposal advances from the principals in remediating irradiated graphite waste, such as the UK National Nuclear Laboratory and the German Jülich Laboratory. As of yet, no consensus among these groups for the disposal of irradiated graphite has been determined.

Technological advances such as thermal treatment, are being investigated that would reduce the volume of high-level waste, allowing the treated graphite to be stored as intermediate-level or low-level waste. Regardless of the method employed for long-term disposal, further understanding of the fundamental physical and chemical processes related to each waste type is required.

2.5 Thermal Treatment

Thermal treatment is being investigated as a viable waste management option because the fractional release of ^{14}C-bearing species is greater than the fractional release of ^{12}C-bearing species when only a small portion of the surface is oxidized (LaBrier, 2013; Podruzhina, 2004; Fachinger et al., 2006, 2008; Vulpius, 2008; Cleaver, 2011). Thermal treatment as a waste management strategy for irradiated nuclear graphite has been researched by Fachinger et al. (2004) as a part of an overall effort by the European Commission to manage contaminated nuclear graphite. Its goal was to selectively remove ^{14}C from irradiated graphite by combining oxidation and pyrolysis at high temperatures (Fachinger et al., 2006; Vulpius et al., 2008; Podruzhina, 2004). Thermal treatment studies were performed at Idaho State University to better understand the speciation and reactions of the preferential release of ^{14}C from neutron-irradiated graphite (Smith, 2013).

2.5.1 Oxidation of Graphite

Studies performed at Idaho State University reveal that a temperature near 700^{o}C results in a greater percentage release of ^{14}C species (Smith, 2013) compared to carbon-12. Oxidation is the means by which carbon species, namely, ^{14}C, is released from the bulk graphite in the form of CO or CO_2. The oxidation of graphite by O_2 primarily occurs via three governing reactions shown in Equation 1 – Equation 3 (IAEA, 2000; Propp, 1998; Backreedy et al., 2001).

$$C_{(s)} + O_{2(g)} \rightarrow CO_{2(g)} \qquad \Delta H_{298} = -393 \text{ kJ/mol} \qquad \text{Equation 1}$$

$$C_{(s)} + \tfrac{1}{2}O_{2(g)} \rightarrow CO_{(g)} \qquad \Delta H_{298} = -110 \text{ kJ/mol} \qquad \text{Equation 2}$$

$$CO_{(g)} + \tfrac{1}{2}O_{2(g)} \rightarrow CO_{2(g)} \qquad \Delta H_{298} = -283 \text{ kJ/mol} \qquad \text{Equation 3}$$

Carbon monoxide and carbon dioxide are the two main carbon species that desorb from the graphite when heat is introduced at temperatures greater than 400^{o}C. The adsorption and interaction of oxygen with a carbon active site occurs spontaneously. While all three reactions occur, the kinetics affect the rate of each reaction. ΔH^{298} denotes the heat of formation of the products at room temperature. An exothermic reaction is indicated with negative values. Each governing reaction is a multistep step process involving the adsorption of the oxidizing component onto the graphite surface where it reacts and then desorbs a carbon-oxygen species (IAEA, 2000; Podruhzina, 2004; Propp, 1998). While the reactions shown in Equations 1-3 are thermodynamically favored, the rates of reaction are highly influenced by the kinetics (IAEA, 2000).

2.5.2 Kinetics of Graphite Oxidation

The kinetics refers to the speed with which oxidation occurs and the limiting mechanism in each regime. Three main categories of factors can influence the kinetics of oxidation (Table 2.3): the characteristics of the type of graphite, the flow parameters of the oxidizing agent, and the environmental temperature during oxidation (Smith, 2013). Exposure to air will adsorb oxygen on to the graphite which will in turn, allow oxidation to occur in an inert environment. Temperature seems to greatly influence the oxidation rate of graphite. Graphite has three unique kinetic regimes dictated by temperature (Propp, 1998; IAEA, 2000, 2006; Marsden et al., 2002; Snead and Burchell, 2002; Podruzhina, 2004; EPRI, 2005; Cleaver, 2011; Smith, 2013).

Table 2.3: Factors that can affect the rate of a graphite oxidation reaction

Factors Impacting Rates of Reaction	Factors Affecting Oxidation	References
Graphite Properties	*Graphite Surface*	
	Reactive surface area available to oxygen	Propp, 1998; IAEA, 2000; Snead and Burchell, 2002
	Surface roughness	Propp, 1998
	Graphite Structure	
	Amount of porosity and characteristics of pores	Propp, 1998; Snead and Burchell, 2002
	Perfection of the crystal structure	Podruzhina, 2004
	History of the Graphite	
	Irradiation dose level and neutron damage	IAEA, 2000; Snead and Burchell, 2002
	Pre-oxidation from radiolytic or thermal burn-off	IAEA, 2000
	Graphite Composition	
	Concentrations of impurities	Eto and Growcock, 1981
	Presence of catalytic impurities, especially metals	IAEA, 2000; Snead and Burchell, 2002; Binford, 1958
Effects of Oxidizing Agent Flow Parameters	*Reaction Products*	
	Rate of product removal	IAEA, 2000; Marsden *et al.*, 2002
	Creation of a surface layer of reaction products	Marsden *et al.*, 2002
	Reacting Gas (Oxygen)	
	Partial pressure	IAEA, 2000
	Rate supplied	Eto and Growcock, 1981; Propp, 1998; IAEA, 2000; Snead and Burchell, 2002
	Effective diffusion coefficient (diffusion constant)	Propp, 1998; IAEA, 2000
Effects of the Environmental Temperature	*Reaction Conditions*	
	Temperature	Propp, 1998; IAEA, 2000; Marsden *et al.*, 2002; Snead and Burchell, 2002

Within each kinetic regime the oxidation reaction rate increases as the temperature is increased (see Figure 2.2) (Propp, 1998). Kinetic regime 1, the chemical controlled regime, is dictated by the chemical reaction between the oxidation species and the graphite. Regime 2, the diffusion controlled regime, is controlled by the in-pore gas diffusion rate. Regime 3, is boundary layer controlled (United States Department of Energy Office of Environmental Management Spent Fuel Management Office, 1998).

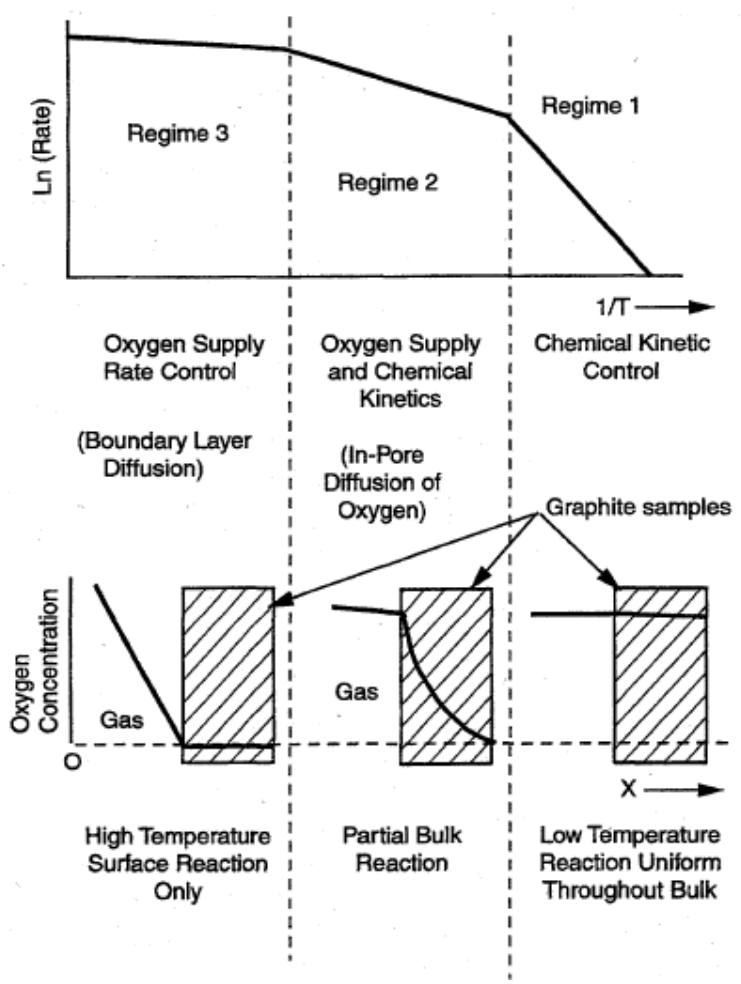

Figure 2.2: Graphite Oxidation Kinetic Regimes ((Propp, 1998)

During oxidation occurring in regime 1 the reaction rate is low, which allows reactant gases containing oxygen to enter and gaseous products (CO and CO_2) to leave the bulk of the solid graphite. This allows for oxidation of all surfaces and in the open porosity (IAEA, 2000; Marsden et al., 2002; Snead and Burchell, 2002; Podruzhina, 2004; EPRI, 2005; United States Department of Energy Office of Environmental Management Spent Fuel Management Office, 1998). In this regime catalysts, such as metallic impurities, are most likely to provide an alternate reaction pathway that may lower the activation energy, consequently affecting the reaction rate (IAEA, 2000, 2006). Oxidation occurring

within regime 2 is affected by the decreased ability of reaction gases to move through the entire graphite. The decreased diffusion causes a concentration gradient to form (IAEA, 2000, 2006; Marsden et al., 2002; Snead and Burchell, 2002; Podruzhina, 2004; EPRI, 2005; United States Department of Energy Office of Environmental Management Spent Fuel Management Office, 1998). Due to the high temperatures in regime 3, reactions occur quickly causing the reaction rate to be controlled by the mass transport of reactant gases across the boundary layer and by the transport of gaseous products away from the graphite. The boundary layer effect causes reactions to occur at the graphite surface (Propp, 1998; IAEA, 2000, 2006; Marsden et al., 2002). The availability of the oxidation component is most influential during regime 3 (Propp, 1998; Snead and Burchell, 2002; IAEA, 2006; EPRI, 2005; United States Department of Energy Office of Environmental Management Spent Fuel Management Office, 1998).

The transition between kinetic regimes is altered by the grade of graphite and experimental conditions (oxidizing agent type and flow rate) (Propp, 1998). Approximated regime transition temperatures are displayed in Table 2.4 (United States Department of Energy Office of Environmental Management Spent Fuel Management Office, 1998; IAEA, 2000; Xiaowei et al. 2004). It should be noted that the oxidation of graphite is not significant at temperatures below 400°C (Podruhzina, 2004).

Table 2.4: Expected Temperature Regime Boundaries

Regime I	Regime II	Regime III	Reference
< 700-825°C	Between I and III	>1371°C	Propp, 1998
Less than II	600-900°C	Greater than II	IAEA, 2000
< 500°C	Between I and III	>900°C	Snead and Burchell, 2002
O_2: < 500°C Steam: < 850°C	O_2: 500-900°C Steam: 850-1350□C	O_2: >900°C Steam: >1250-1400°C	Podruzhina, 2004
Starts at 350-400°C	-	-	EPRI, 2005

The adsorbed oxygen functional groups and active sites on the graphite surface have different stabilities and activities. Consequently, carbon oxides, primarily CO or CO_2, will desorb at different rates upon heating (El-Genk and Tournier, 2011; Podruhzina, 2004). Surface characterization of the graphites studied for this thesis has identified

fragments consistent with the El-Genk and Tournier (2011; 2012) model shown in Figure 2.3 (McCrory, 2011). However, as stated earlier, irradiation changes the chemical properties of graphite and, until recently, most graphite oxidation studies have been performed on unirradiated materials.

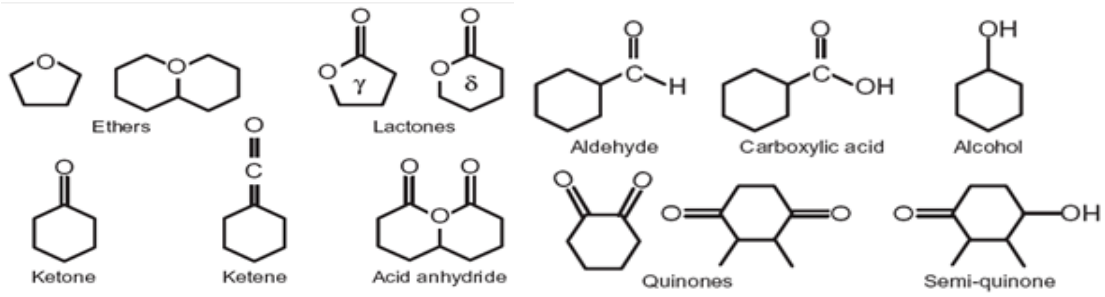

Figure 2.3: Plausible Compounds Formed by Oxygen Adsorption on Graphite Surface as Incorporated in the Model by El-Genk and Tournier (2011, 2012)

The graphite structure undergoes changes as oxidation continues. These structural changes may affect the desorption rate, pathway, and speciation. The avulsion of CO typically results from the direct release from an ether or carbonyl; after the decomposition of an ether, ketene, or aldehyde; or when released after the gasification of carbon atoms neighboring ethers, lactones, and anhydrides (El-Genk and Tournier, 2011). CO_2 could separate from esters, C_2O_2 complexes, and carboxyl-anhydrides. However, the majority of CO_2 likely desorbs after surrounding carbon-carbon bonds are weakened by the chemisorption of an oxygen atom on a neighboring quinone or semi-quinone complex. While CO could also desorb from a quinone complex, the activation energy required to remove CO from the quinone complex is quite high (Yates et al., 1978). More recently, LaBrier (2013) proved that the primary source for CO_2 release during thermal treatment of irradiated NBG-25, comes from the formation of caboxylates. These carboxylates were found on neutron irradiated NBG-25 samples.

2.5.3 Previous Thermal Treatment Work

The inhomogeneous distribution of ^{14}C throughout some irradiated graphites allows thermal treatment to be effective. Characterization studies have concluded that

^{14}C accumulates on the surface of the irradiated graphite making it more conducive to oxidation than the ^{12}C bulk graphite matrix (Podruzhina, 2004; Fachinger et al., 2006, 2008; Vulpius et al., 2008). A study also found that oxidation opens the graphite pores, allowing the oxygen to reach the ^{14}C that may be trapped (Eto and Growcock, 1981).

Over the years, research conducted by Fachinger and Podruzhina (2004) and later Vulpius and Fachinger (2008), using argon and steam, and later nitrogen with oxygen and steam, respectively, to oxidize bulk graphite samples has increased understanding of graphite behavior. Their efforts resulted in ^{14}C enriched off-gas steam. In 2011, Cleaver performed inert thermal treatment on POCOFoam graphite. A summary of the results are shown below in Table 2.5, including Smith's (2013) results from adding varying temperatures and oxidant flow rates of O_2 to the argon carrier gas in the treatment of NBG18.

Table 2.5: Previous Thermal Treatment Results

	Podruhzhina, 2004	**Vulpius et al., 2008**	**Cleaver, 2011**	**Smith, 2013**
Mass loss ^{14}C (%)	20 (Ar) 24 and 65 (Ar + $H_2O_{(g)}$)	79 (N_2 + O_2, 3 hours) 93 (N_2 + $H_2O_{(g)}$, 7 hours)	22 (Ar, 900°C) 38 (Ar, 1400°C)	NBG18: 46(Ar, 700°C, 13hrs) POCO: 97(Ar+3%O_2, 700°C)
Mass loss ^{12}C (%)	1.36 (Ar) 42 and 4 (Ar + $H_2O_{(g)}$)	2.9 (N_2 + O_2, 3 hours) 5.4 (N_2 + $H_2O_{(g)}$, 7 hours)	0.53 (Ar, 900°C) 0.78(Ar, 1400°C)	NBG18: 0.66(Ar, 700°C, 13hrs) POCO: 9(Ar+3%O_2, 700°C)

2.5.4 Previous Thermal Treatment Experiment Designs

The thermal treatment experiments conducted by Fachinger et al. (2006, 2008) and Podruzhina (2004) used the apparatus shown in Figure 2.4.

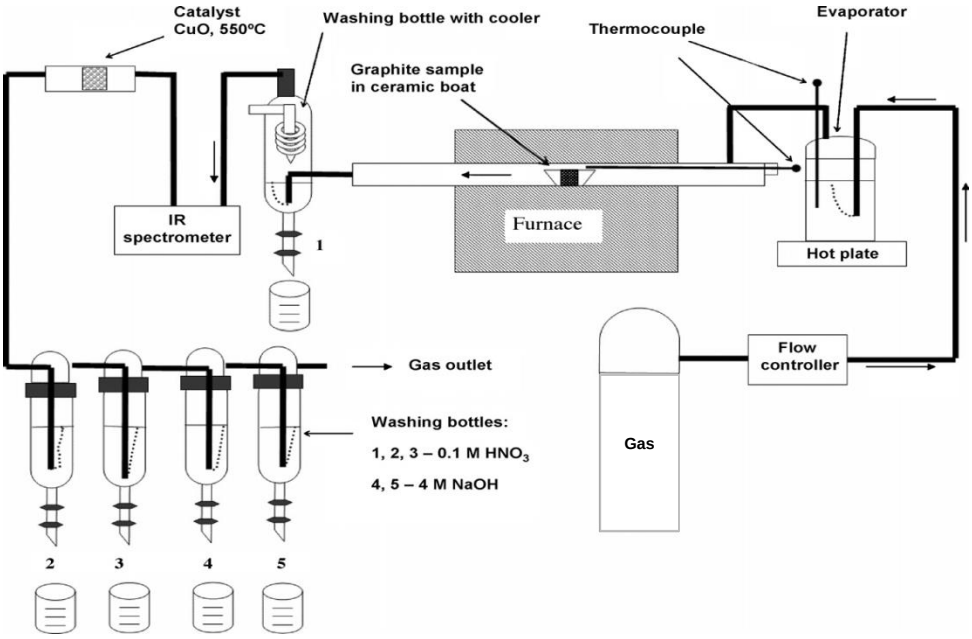

Figure 2.4: Experimental Apparatus for the Thermal Treatment Process to Remove ^{14}C from Irradiated Graphite (Podruzhina, 2004; Fachinger et al., 2006, 2008; Vulpius et al., 2008)

The experiments conducted by Fachinger et al. (2006, 2008) employed argon (Ar) as the carrier gas mixed with steam, and later N_2 mixed with steam, and N_2 mixed with O_2. These mixtures flowed through a furnace across a pre-weighed graphite sample. The flow path then passed through an IR-spectrometer where CO and CO_2 levels were detected, and then through an oxidation furnace, where copper oxide (CuO), at 500°C, converted all remaining CO into CO_2 for capture in washing bottles of 4M NaOH. The first collection bottle contained HNO_3 for collecting tritium (Podruzhina, 2004; Fachinger et al., 2006, 2008; Vulpius et al., 2008). From the washing bottles and throughout the experiment, 1 ml samples were taken and placed in a vial containing 1 ml of distilled water and 18 ml of HIONIC FLUOR™ scintillation cocktail for analysis in a Liquid scintillation counting (LSC) machine. This would count the activity of the ^{14}C in each sample. Upon completion of the thermal treatment, each sample was weighed and placed back into the furnace for complete oxidation. New solutions of NaOH and HNO_3 were used for the oxidation collection which gave the total amount of ^{14}C in each sample.

In 2011, at Idaho State University, Cleaver (2011) performed similar experiments with irradiated POCOFoam® using argon as the carrier gas. Other differences from those conducted by Fachinger et al. (2006, 2008) included an increased oxidation furnace temperature of 800°C from 500°C, and no tritium collection bottle Cleaver's (2011) experimental setup is shown in Figure 2.5.

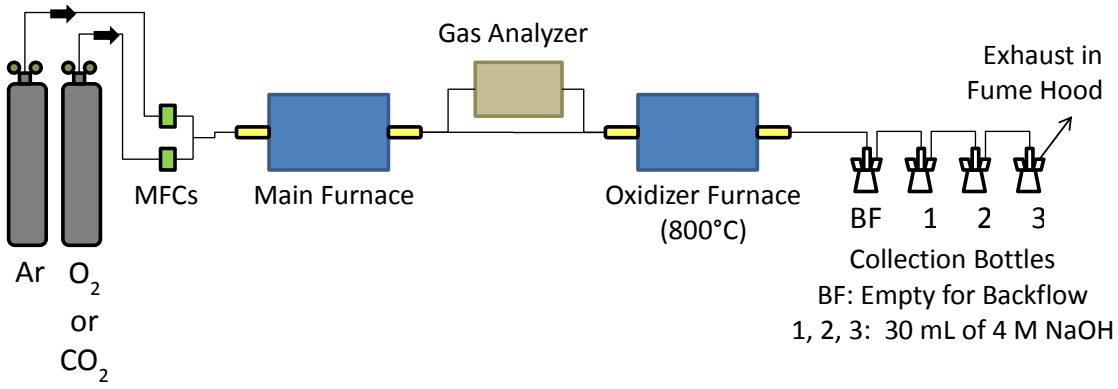

Figure 2.5: Cleaver (2011) Experimental Setup

In 2012, Smith used the very same experimental set up and added back in the tritium collection bottle (Smith, 2103). A summary of the previous thermal treatment experimental parameters can be seen in Table 2.6.

Table 2.6: Summary of Previous Thermal Treatment Work Parameters

	Podruzhina, 2004; Fachinger et al., 2006, 2008	Vulpius et al., 2008	Cleaver 2011	Smith 2013
Temperature (°C)	400-1070	900-1300	900-1400	700 & 1400
Gas	Ar and Ar + $H_2O_{(g)}$	N_2 + O_2 (Max. 1.2 vol. %) N_2 + $H_2O_{(g)}$	Ar	Ar +O_2 (0, 3, & 5 vol. %)
Flow rate (L/min)	0.08-0.175 and 0.08-0.66	(no mention)	0.05	0.05
Partial pressure of H_2O (kPa)	2.3-7.0	(no mention)	--	--
Treatment time (hours)	9-18 and 5-25	3 (O_2) and 7 ($H_2O_{(g)}$)	10-12	2-13
Graphite form	Powder and Bulk	Powder and Bulk	Foam	PocoFoam & NBG18
Graphite quantity (g)	0.15-0.459	(no mention)	0.522 (avg)	PocoFoam 0.51 NBG18 0.18 (avg)

2.5.5 Results and Calculations from Previous Thermal Treatments

Results from thermal treatment experiments are presented as release rates, defined by Equation 4 (Podruzhina, 2004; Fachinger et al., 2006, 2008; Cleaver, 2011; Smith, 2013) See Appendix A for release rate data.

$$R_i = \frac{X_i(t_j) - X_i(t_{j-1})}{m(t_{j-1}) \cdot (t - t_{j-1})} \qquad \text{Equation 4}$$

R_i is the release rate of a nuclide *i* (mol/gh),
$X_i(t_j)$ is the amount of nuclide *i* (mol) released at time *j*,
t_j is the time at moment *j* (h), and
$m(t_j)$ is the mass of the graphite sample at time t_j (g).

After applying a normalizing factor, f_i (the molar fraction of nuclide *i* in the graphite, see Equatio), the normalized release rate, NR_i, can be determined as seen in Equation 5. The NR_j allows the release rate of a radionuclide to be compared to another species released on a per mass released basis (Smith, 2013).

$$NR_i = \frac{R_i}{f_i} \qquad \text{Equation 5}$$

$$f_i = \frac{v_i}{v_{12_C}} \qquad \text{Equation 6}$$

v_i is the amount of radionuclide *i* (mol)

The selective release of a radionuclide (*i* denotes ^{14}C for this thesis) is determined by comparing the normalized release rate of the radionuclide to that of the bulk material (^{12}C) as seen in Equation 7.

$$K_i = \frac{NR_i}{NR_{12_C}} \qquad \text{Equation 7}$$

Table 2.7 shows comparisons of selective release ratios from previous experimental studies. As can be seen, nuclear graphite grades respond differently to thermal treatment and are affected by structure (powder, solid) temperature and oxidant concentration. All results confirm that selective release of ^{14}C decreases as temperature increases (Fachinger et al., 2006, 2008; Cleaver, 2011; Smith, 2013).

Table 2.7: Selective Release Ratio, K, Summary

Summary of Previous Selective Release Ratios, K ($\%^{14}C$ to $\%^{12}C$)						
Podruhzina 2004	**Cleaver 2011**		**Smith 2013**			
Merlin, AVR 1060°C, Ar	POCOFoam® 900°C, Ar	POCOFoam® 1400°C, Ar	POCOFoam®		NBG18	
			700°C	1400°C	700°C	1400°C
26.9	42.14	38.49	Ar + 3% 8.08	Ar + 3% 2.85	Ar 195.49	--
--	--	--	Ar + 5% 5.89	Ar + 5% 1.57	Ar + 5% 11.17	Ar +5% 2.55

A selective release ratio value of greater than 2 shows that ^{14}C is released faster than the bulk material and indicates that thermal treatment is expected to be an effective waste management strategy for irradiated graphite waste (Fachinger et al., 2008; Cleaver, 2011). However, it is agreed that further study is needed to optimize and verify experimental conditions (Podruzhina, 2004; Fachinger et al., 2006, 2008; Vulpius et al. 2008; Cleaver, 2011, Smith, 2013).

Chapter 3.0: Experimental

3.1 Graphite Characteristics

In order to fulfill the objective of this thesis, two types of nuclear grade graphite were studied, NBG-18 and NBG-25.

3.1.1 NBG-18 Irradiation

Nuclear grade graphite, NBG-18, was liquid nitrogen immersed prior to irradiation in order to ensure detectable amounts of ^{14}C on the graphite sample surfaces. After liquid nitrogen immersion, the samples were sealed, in an air environment, in an irradiation vessel. These samples were irradiated in MURR at the University of Missouri where they were exposed to a flux of 6.7E+13 neutrons/(cm^2s) for 120 days. Sample sizes averaged height of 0.5cm by diameter of 0.5cm.

3.1.2 NBG-25 Irradiation

Nuclear grade graphite, NBG-25, did not undergo liquid nitrogen immersion prior to irradiation. These spacers were irradiated under a flowing He gas environment in the Advanced Test Reactor, ATR, at Idaho National Laboratory. The cylinder shaped graphite samples (Figure 3.1) were exposed to a flux of 3E+14 neutrons/(cm^2s) for between 350 and 400 days and have dimensions as follows: diameter of 25 mm; height of 10 mm. For analysis, small pieces of each spacer were cut or sliced apart to provide adequate sized samples.

Figure 3.1: Irradiated NBG-25 Sample

For ease of comparison, Tables 3.1 and 3.2 display sample characteristics and irradiation conditions, respectively.

Table 3.1: Sample Characteristics (SGL, 2013)

Graphite	Density (g/cc)	Impurity Level (ppm)	Average Porosity (%)	Sample Geometry Size H(cm) x D (cm)
NBG-18	1.85	<100	17-18	0.5 x 0.5
NBG-25	1.82		10-15	Varied

Table 3.2: Summary of Sample Irradiation Conditions

Type	Irradiation Time (days)	Flux (n/cm2-s)	Facility	Liquid Nitrogen Immersed Prior to Irradiation?
NBG-18	120	6E+13	MURR	Yes
NBG-25	< 400	3E+14	ATR	No

For the NBG-25 samples, reference will be made to 'high, mid, low' in each sample identification number. For example, AE11-0-N25-2150-L, refers to a sample from a spacer (used in an experimental reactor to separate test samples in a sample tube) located farther away from the flux source (low flux relative to the other spacers). This refers to

their location within the reactor at the time of irradiation and in reference to one another. In the ATR material test assembly, the spacers were placed between test materials, also being irradiated. Surface activity and dose information on the three samples was made available by the Idaho National Laboratory and is summarized in Table 3.3 (LaBrier, 2013). Spacers toward the center of the reactor core received a higher flux than those near the outer edges. This difference in radiation dose between NBG-25 samples may be noteworthy, because as concluded by El Genk (2012), changes in the crystal structure, density, and pore system of irradiated graphite would make it less reactive to oxygen complex formation than unirradiated graphite.

Table 3.3: Surface Swipe Activities and Dose Levels for Irradiated NBG-25 Spacers (LaBrier, 2013)

Spacer Name	Dose Imparted (dpa)	Beta/gamma (smear) (dpm/100 cm^2)	Alpha (smear) (dpm/100 cm^2)
END-4PB16	6.63	7063	< 20
4PB16-4PB17	6.62	12115	< 20
4PB17-4PB18	6.60	15730	< 20

3.2 Thermal Treatment Apparatus/Equipment

The thermal treatment equipment setup can be seen in the schematic drawn in Figure 3.2 and the photo seen in Figure 3.3.

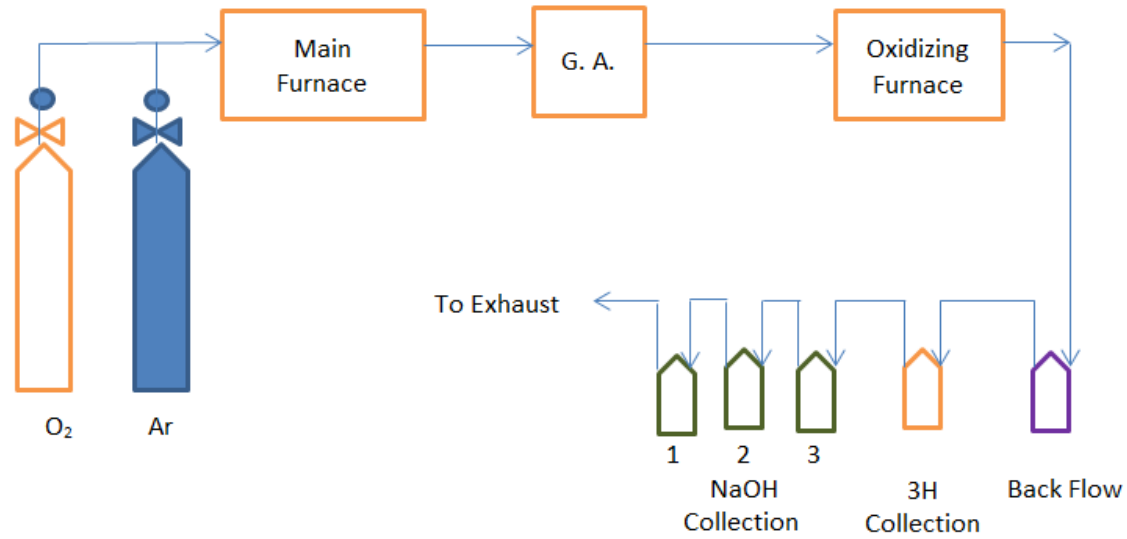

Figure 3.2: Thermal Treatment Equipment Schematic

Figure 3.3: Photo of Thermal Treatment Apparatus at Idaho State University Lab

For this study, the same experimental apparatus was utilized as for experiments conducted by Smith (2013). During the thermal treatment process, argon (flowing at 50 sccm) functioned as the inert carrier gas, which transported any gases released from the graphite and carried them to gas collection bottles. In some experiments, oxygen gas (0 vol%, 2 vol%, or 5 vol%) was added to the argon to serve as the oxidant, flowing at 0 sccm (pyrolysis), 1 sccm or 2.6 sccm, respectively. A mass flow controller regulated the gas levels as they flowed across the graphite samples placed in the center of the main furnace.

All samples for this thesis were thermally treated at 700°C for 8 hours. Experimental variables were pre-heating temperatures, pre-heating times and levels of oxygen. These parameters were chosen as likely to improve the thermal treatment results from previous work at ISU.

As the carrier gas leaves the main furnace, a small sample of the gas is syphoned off of the main flow stream for analysis in the Hiden Quadrapole Mass Spectrometer Gas Analyzer (QGA) and then returned to the main gas flow stream.

The gas flow then enters the oxidizing furnace, set at a temperature of 800°C, where any CO is oxidized to CO_2 by copper oxide wrapped in copper mesh. This gas flow enters the series of collection bottles where the CO_2 is captured in the NaOH solution (Figure 3.4).

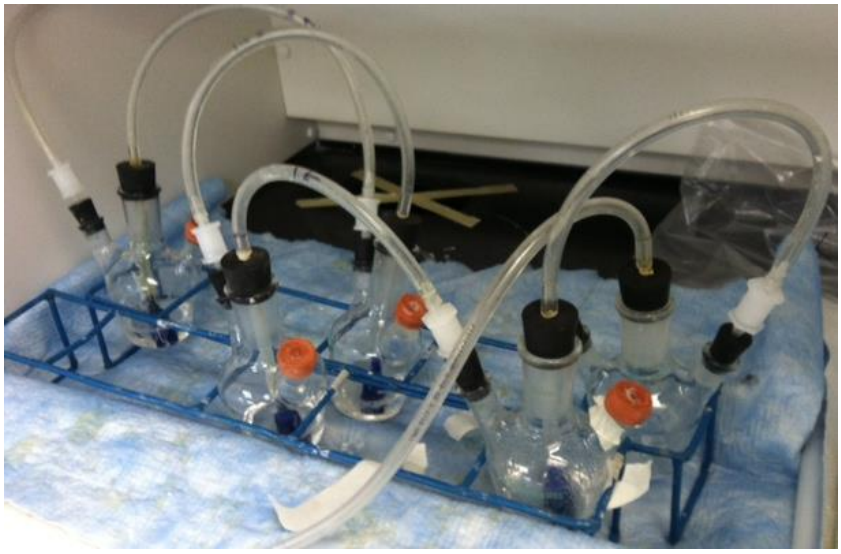

Figure 3.4: Gas Collection Bottles

The first bottle in line is deliberately empty and serves to catch any back flow from subsequent bottles in the event of a quick pressure change in the system. Next is the 'tritium getter' filled with 41mL of 0.1 M HNO_3 for collecting ^3H. Finally, the gas enters a series of three washing bottles filled with 41 mL of 4 M NaOH, which collects the CO_2. Lab-made diffusors (Figure 3.5) were used to bubble the gas into the NaOH to ensure

complete collection of CO_2 via the reaction yielding sodium carbonate and eventually, sodium bicarbonate ($2NaHCO_3$).

Figure 3.5: Lab Made Diffusor

From these air tight collection bottles, and at specified times, 1 mL samples of the solution are drawn off, using a syringe and needle penetrating a rubber septum on the bottles. These 1 mL draws are placed into 20 mL glass vials with 19 mL of liquid scintillation fluid (Fisher ScintSafe Plus Cocktail). The mixtures were analyzed for ^{14}C using a Beckman LS 6500 multi-purpose scintillation counter. A detailed list of all experimental items and equipment is provided in Appendix B.

After thermal treatment, the graphite samples were allowed to cool and then weighed to determine total mass loss (essentially the same as carbon-12 loss). All thermally treated graphite samples were eventually returned to the main furnace to be completely oxidized at 800^{o}C and 50 sccm pure O_2 gas. CO_2 was collected as previously described and collection solutions were analyzed to determine total quantity of ^{14}C in the sample.

3.3 Experimental Parameters

Smith's (2013) thermal treatment study indicated an ideal temperature of 700°C for removing ^{14}C. Therefore, all experiments were performed at a set point temperature of 700˚C, nominally in the in-pore diffusion kinetic regime for oxidation. Three gas flow compositions were selected to evaluate the effects of different oxidation levels for NBG-25, as well as, to compare to Smith's results from thermally treating NBG-18. Volumetric flow rates of the carrier gas components are listed in Table 3.4.

Table 3.4: Experiment Gas Types and Concentrations

Gas Mixture	Argon (sccm)	Oxygen (sccm)
Argon Only	50	0
Argon + 2vol% Oxygen	50	1.0
Argon + 5vol% Oxygen	50	2.6
Complete Oxidation	0	50

Smith (2013) concluded that thermal treatment of NBG-18 at 700°C in argon (pyrolysis) produced preferential conditions for removing ^{14}C. In other words, any oxidation that did occur used oxygen species that were already sorbed on the graphite surface. Therefore, experiments performed for this thesis used 700°C for thermal treatment and added a pre-treatment step to optimize the process. Pre-treatment consisted of heating the sample at a temperature low enough that oxidation would not occur but high enough to increase oxygen sorption to the sample surface. Pre-treatment was performed with no oxidant (as a baseline for comparison) and two low oxidant levels (2 and 5 volume %). Two different pre-loading temperatures (150°C and 300°C) were held for 2 hours before the furnace was heated to 700°C for 8 hours. These experiments are summarized in Table 3.5.

Table 3.5: Experiments Performed

O_2 Pre-Loading Time & Temp	2 Hours at 150°C			2 Hours at 300°C	
Ar + vol% O_2	0%	2%	5%	0%	2%
Graphite Type	Number of Experiments Performed				
NBG-18	2	2	2	2	2
NBG-25	2	2	2	2	2

3.3.1 Temperature Profile

For this thesis, all irradiated graphite samples were thermally treated for 8 hours at 700°C. Due to a limited number of NBG-18 samples, only duplicate experiments were performed for each unique set of pre-treatment parameters. Due to the potential for thermal shock, the alumina tube in the main furnace was heated and cooled at a rate of 200°C/hr. The overall experimental temperature profile is shown in Figure 3.6.

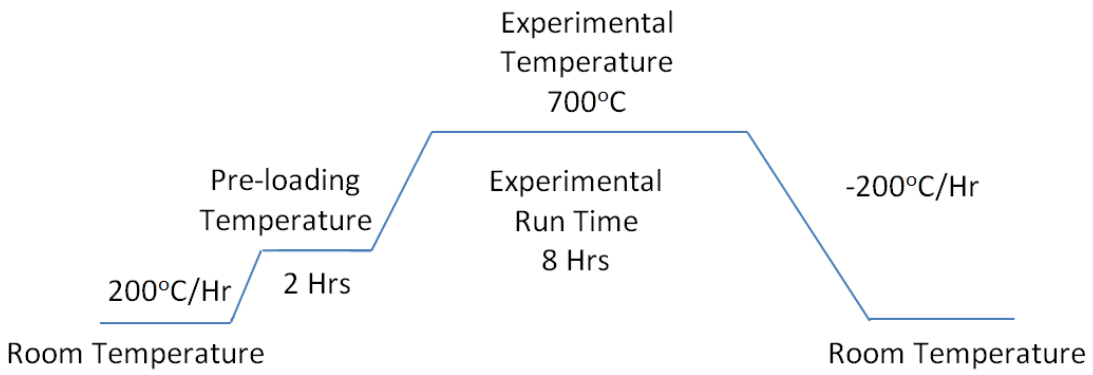

Figure 3.6: Programed Experimental Temperature Profile for Main Furnace

As previously stated, thermally treated samples were weighed to determine mass loss due to treatment and subsequently were returned to the main furnace and fully oxidized. This process took place at 800°C for 2 hours, which was more than sufficient time to burn up the sample. In fact, most samples were fully oxidized by the time the

furnace reached 800°C. The time and temperature profile for the full oxidation experiments is shown in Figure 3.7.

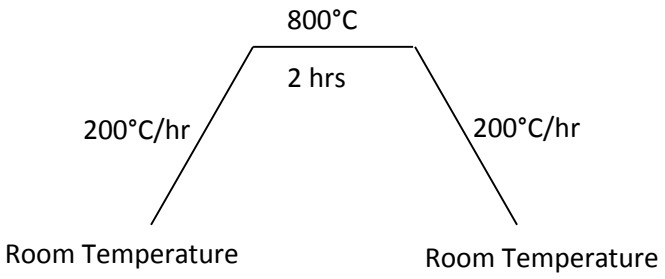

Figure 3.7: Programed Complete Oxidation Temperature Profile for Main Furnace

3.3.2 Experimental Run Time

In previous experiments, thermal treatment time at temperature varied from 2 to 25 hours (see Tables 2.6) however, because each set of experiments was unique there was not a direct correlation. Experiments performed for this thesis were to optimize the method of thermal treatment used by Smith (2013), whose results indicated that 45-75% of all ^{14}C was removed from NBG-18 by 7 hours. Therefore, the dwell time at experimental temperature (experimental run time) for these experiments was chosen to be 8 hours.

3.4 Off-Gas Analysis

The Hiden QGAPro was chosen for its ability to monitor up to 16 masses less than 200 amu provided there is no significant fractional overlap in the masses monitored and for the ability to distinguish between CO and CO_2 (Cleaver, 2011; Smith 2013). During the gasification, it was anticipated that hydrogen and oxygen (from water and other surface

impurities) would form compounds with the carbon and desorb into the gas flow. Consequently, the species selected for monitoring are shown in Table 3.6.

Table 3.6: Gaseous Species Monitored

Gas	Molecular Weight (g/mole)
Argon	40
Oxygen	32
Carbon Dioxide	44
Carbon Monoxide	28
Methane	16
Water	18
Nitrogen	28
$^{14}CO_2$	46
^{14}CO	30

It should be noted that Cleaver (2011) and Smith (2013) believed the gas analyzer or the gas flow system to contain non-removable impurities. Cleaver's attempts to bake out detectable water in the system were unsuccessful. Appendix D describes the calculations the gas analyzer software uses to resolve masses.

Three different gas cylinders were used to calibrate the gas analyzer software: argon, dry air, and a mixture created to include species of greatest interest to the experiments. To increase sensitivity of the gas analyzer measurements, the gas analyzer software was calibrated using mixtures of known quantities of the gases seen in Appendix C. The argon cylinder was the same as used for experiment carrier gas. Dry air with 20.95 ± 0.45% O_2 (balance N_2) was used to calibrate the software for O_2. A mixture of 70% N_2, 10% CO_2, 10% CO, and 10% CH_4 was used to calibrate for the remaining gases identified in table of calibration factors in Appendix D. The gas analyzer software was not calibrated for water due to a lack of calibration source and to minimize the amount of water in the gas analyzer.

Slightly acidic DI water was used to rinse all glassware, diffusors and connections between runs. It is assumed that an equilibrium of absorption and desorption of ^{14}C within

the system has been achieved. While it has been shown that the tubing and equipment contain removable ^{14}C, dismantling and cleaning the system between runs was shown to be unnecessary (Cleaver, 2011).

3.5 Relevant Thermal Treatment Calculations for Data Analysis

For this thesis, all experimental samples were irradiated graphite from two different sources. The NBG-18 samples were liquid nitrogen immersed prior to irradiation at MURR where they were exposed to a flux of 6.7E+13 neutrons/(cm^2s) for 120 days. The NBG-25 samples were irradiated at ATR where they were exposed to a flux of 3E+14 neutrons/(cm^2s) for between 350 and 400 days. The rate at which carbon species were released from the graphite during thermal treatment was recorded by the gas analyzer. In addition, rough rates of release of ^{14}C were determined via LSC analysis of solutions drawn from the collection bottles at precise time intervals throughout each experimental run. Pre and post thermal treatment weights provided mass loss due to the treatment and therefore calculation of percentage mass (^{12}C) loss. Collection of off gas during oxidation allowed for activity totals per graphite sample to be calculated and thereby calculation of percentage activity (^{14}C) loss.

The QGA gas analyzer results are given in terms of partial pressures (torr), which are then summed and a mole fraction calculated by Equations 8 and 9.

Dalton's Law of Partial Pressures

$$P_T = \Sigma P_i \qquad \text{Equation 8}$$

Mole fraction

$$x_i = \frac{P_i}{P_T} \qquad \text{Equation 9}$$

Equation 10 calculates the molar flow rate using the carrier gas volume flow rate, density and molar mass. Molar flow rate is multiplied by the time difference to obtain

the number of moles that passed through the system instantaneously at a given time interval in Equation 11.

Molar flow rate

$$\dot{n} = \frac{\dot{Q} d}{M}$$ Equation 10

Instantaneous Total Moles in System over Δt

$$x(t) = \dot{n}(\Delta t)$$ Equation 11

P_T = total pressure
P_i = partial pressure of the gas of interest
$\dot{Q}$ = volume flow rate
d = density
M = molar mass
Δt = change in time
$x(t)$ = Instantaneous moles in system of species i

Next, the carbon species were grouped according to the time period when samples were drawn from the collection bottles and the instantaneous moles of carbon species were summed (Equation 12). The total moles released during the time periods were summed to determine the total quantity of carbon released (Equation 13).

Sum of Moles of i Within a Time Period

$$X_{t_{j-z}}{}^{i} = \sum_{z}^{j} x(t) * x_i$$ Equation 12

Sum of Total Moles of i during Experiment

$$X_t{}^{i} = \sum X_{t_{j-z}}{}^{i}$$ Equation 13

X = sum of the instantaneous moles
t = experimental time
j-z = a period of time within the experimental time
i = gas of interest
(t) = Instantaneous Total Moles in System
x_i = mole fraction of the gas of interest

Equations 12 and 13 were combined to calculate the percent carbon released during the experiment with respect to time, and the total mass loss determined by weighing the graphite before and after thermal treatment. Due to the uncertainty associated with the gas analyzer data, the total mass loss of the graphite sample was more accurately determined by weighing the sample before and after the experiment. The mass loss measured allowed the gas analyzer results to be corrected by Equation 14.

$$\%C\ Released_{t_{j-z}} = \left(\frac{X_{t_{j-z}}}{X_t}\right)\left(\frac{\Delta W}{W_0}\right) * 100 \qquad \text{Equation 14}$$

ΔW = mass released during thermal treatment determined with the pre- and post-graphite weight
W0 = the graphite weight at the start of the experiment

The carbon release rate is described Equation 15.

$$R'_{\ {}^{i}C} = \frac{X_{\ {}^{i}C}(t_j) - X_{\ {}^{i}C}(t_{j-1})}{m(t_{j-1}) \cdot (t - t_{j-1})} \qquad \text{Equation 15}$$

$X_{\ {}^{i}C}(t_j)$ is the amount (mol) of ^{i}C released at time *j*
i = specific carbon isotope
t_j is the time at moment *j*
m_{t_j} is the mass of the graphite sample (g) at time t_j

In order to directly compare the rate of release of ^{14}C with that of ^{12}C, normalization for total activity, $f_{^{14}C}$, must be performed as shown by Equations 16 and 17.

$$f_{^{14}C} = \frac{v_{^{14}C}}{v_{^{12}C}} \qquad \text{Equation 16}$$

$$f_{^{12}C} = \frac{v_{^{12}C}}{v_{^{12}C}}$$ Equation 17

$f_{^{14}C}$ is the molar fraction of ^{14}C in the graphite sample
$v_{^{14}C}$ is the amount of ^{14}C remaining in the graphite at each experiment time step
$v_{^{12}C}$ is the amount of ^{12}C (mol) remaining in the graphite at each experiment time step

The normalized release rate, $NR_{^{i}C}$, of ^{i}C is determined by Equation 18.

$$NR'_{^{i}C} = \frac{R'_{^{i}C}}{f_{^{i}C}}$$ Equation 18

The ratio of the normalized rate of release of ^{14}C to that of ^{12}C, shown in Equation 19 can be used to evaluate the selective removal of ^{14}C.

$$K_{^{14}C} = \frac{NR'_{^{14}C}}{NR'_{^{12}C}}$$ Equation 19

K = ^{14}C selective release of factor

Chapter 4.0: Results and Analysis

The objective of this study was to optimize the thermal treatment process that has been the subject of previous experimentation at Idaho State University. To achieve this objective, oxidant pre-loading concentrations and temperature were varied. Maximizing the percentage of ^{14}C released during treatment and minimizing the percentage of bulk graphite, ^{12}C, that is released simultaneously, would demonstrate a more effective method of thermal treatment for NBG-18 and NBG-25.

4.1 Experimental Sample Identification Number

Each experiment is identified in the form of "Experiment Number-Oxygen Level-Graphite Type-Hours at Pre-Loading at Temp". For example, AE1-0-N18-2150 would denote Active Experiment #1 (AE1) 0% oxygen level (0) NBG-18 Graphite Type (N18) 2 hours at 150^{o}C Pre-Loading Time and Temp (2150). (This naming protocol is continued from previous experiments at ISU, some of which included use of unirradiated samples. Hence, the term "Active" in the Experiment Number term refers to the fact that all samples in this work were irradiated and active as a result. Averaged experimental results reported in this section do not include the Experiment Number.) NBG-25 experiments will have one of the following letters appearing at the end of the ID#: L, M, H. These letters, reference the positions of the NBG-25 spacers (source of experimental sample) in the irradiation test assembly and therefore, the flux received during irradiation. L (low) denotes low exposure compared to the H (high) sample which was in the higher flux region of the core. All experiments were thermally treated for 8 hours at 700^{o}C.

4.2 Pre-loading Temperatures

For this thesis, the pre-loading temperature refers to a temperature sustained for 2 hours prior to raising the furnace to the thermal treatment temperature of 700^{o}C. Pre-loading temperatures were 150^{o}C and 300^{o}C. The gas mixture levels remained constant throughout the entire run for each sample. Gases were not turned on and off during the ramp up to pre-loading temperature (150^{o}C, 300^{o}C), nor during ramp up to thermal treatment temperature (700^{o}C).

4.3 Molar Flow Rate

The sum of the mass flow controller settings for argon and oxygen was used as the total volumetric, and after conversion, molar flow rate ($\dot{n}$). The gas analyzer gives data results in terms of the partial pressure (torr) of the gases monitored which are converted from partial pressure to mole fraction (see Equations 8 through 11). The quantity of carbon species off gas was very small in comparison with the total gas flow (approx. 1.34E-2 over 17 hours). Therefore summing only the argon and oxygen flows was deemed sufficient to approximate the total gas flow. Table 4.1 shows the molar flow rates for the gas mixtures used in the experiments.

Table 4.1: Molar Flow Rates used in Experiments

Gas Mixture	Total Molar Flow Rate (mol/min)
Argon Only	2.23E-03
Argon + 2vol% O_2	2.41E-03
Argon + 5vol% O_2	2.47E-03

4.4 Graphite Experiments with Pre-Loading for 2 Hours at 150°C

4.4.1 Experimental Parameters

Experimental parameters are shown in Table 4.2 for all tests conducted with a pre-loading for 2 hours at 150°C. The argon and oxygen mixture for each experiment was allowed to flow through the system for approximately 30 minutes, prior to the start of the treatment, as the system was being checked and collection bottles were observed to function properly. Oxygen levels of 0 vol%, 2 vol% and 5 vol% were evaluated.

Table 4.2: Experimental Parameters for O_2 Pre-Loading for 2 hr at 150°C

Experimental ID	Graphite Type	Pre-Loading Time at Temp (hr) at (°C)	Thermal Treatment Time at Temperature (hr) at (°C)
Argon			
AE1-0-N18-2150	N18	2 at 150	8 at 700
AE2-0-N18-2150	N18	2 at 150	8 at 700
AE11-0-N25-2150-L	N25	2 at 150	8 at 700
AE12-0-N25-2150-L	N25	2 at 150	8 at 700
Argon + 2vol% O_2			
AE5-2-N18-2150	N18	2 at 150	8 at 700
AE6-2-N18-2150	N18	2 at 150	8 at 700
AE15R-2-N25-2150-H	N25	2 at 150	8 at 700
AE16-2-N25-2150-L	N25	2 at 150	8 at 700
Argon + 5vol% O_2			
AE3R-5-N18-2150	N18	2 at 150	8 at 700
AE4R-5-N18-2150	N18	2 at 150	8 at 700

These conditions were chosen for comparison with Smith's (2013) NBG-18 results from "pre-loading" conditions of 2 hours at room temperature (38°C) to observe any noticeable changes in release rates of either ^{14}C or the bulk graphite. The purpose of increasing the pre-loading temperature in these experiments was to increase the presence of oxygen on the surface of the graphite sample. Oxygen availability for adsorption during thermal treatment would possibly increase the amount of carbon-oxygen species for desorption.

NBG-25 was not previously tested at the various oxygen levels, however, two graphite samples studied by LaBrier (2013) were available for comparison. LaBrier treated these NBG-25 samples at 0vol% O_2, for 13 hours at 700^oC with a pre-loading at room temp (38^oC) for 2 hours, Results from this treatment provided an opportunity to compare data from this study which incorporated a parameter change of oxidant concentration and/or pre-loading temperature. Experimental parameters for these NBG-25 samples are shown in Table 4.3

Table 4.3: NBG-25 Summary of Experimental Results for 2 hr at 38^oC; thermally treated for 13 hr at 700^oC (LaBrier, 2013)

Experimental ID	Initial Mass (g)	Final Mass (g)	%Mass Loss	Mass Loss (g)
Argon				
DNBG25-0-238-H	0.0823	0.0705	14.34	0.0118
KNBG25-0-238-M	0.0710	0.0705	0.7000	0.0005

4.4.2 Experimental Results

The overview of the results for all experiments conducted under the parameters for pre-loading for 2 hours at 150^oC and then thermally treating for 8 hours at 700^oC can be seen in Table 4.4.

Table 4.4: Summary of Experimental Results for 2 hr at 150°C Pre-loading

Experimental ID	Initial Mass (g)	Final Mass (g)	%Mass Loss	Mass Loss (g)
Argon				
AE1-0-N18-2150	0.0363	0.0358	1.38	0.0005
AE2-0-N18-2150	0.0443	0.0437	1.35	0.0006
AE11-0-N25-2150-L	0.0613	0.0611	0.33	0.0002
AE12-0-N25-2150-L	0.0731	0.0725	0.82	0.0006
Argon +2vol% O_2				
AE5-2-N18-2150	0.0962	0.0837	12.99	0.0125
AE6-2-N18-2150	0.0915	0.0817	10.71	0.0098
AE15-2-N25-2150-H	0.0296	0.0124	58.11	0.0172
AE16-2-N25-2150-L	0.0182	0.0078	57.14	0.0104
Argon +5vol% O_2				
AE3-5-N18-2150	0.1257	0.0788	37.31	0.0469
AE4-5-N18-2150	0.0442	0.0034	92.31	0.0408

4.4.3 Gas Analyzer Data for Experiments with 2 hours at 150°C Pre-Loading

The corrected gas analyzer data for the experiments with argon only (0% O_2) and a pre-loading of 2 hours at 150°C and a thermal treatment for 8 hours at 700°C can be seen in Figures 4.1-4.4. Corrected Data is in partial pressure (Torr).

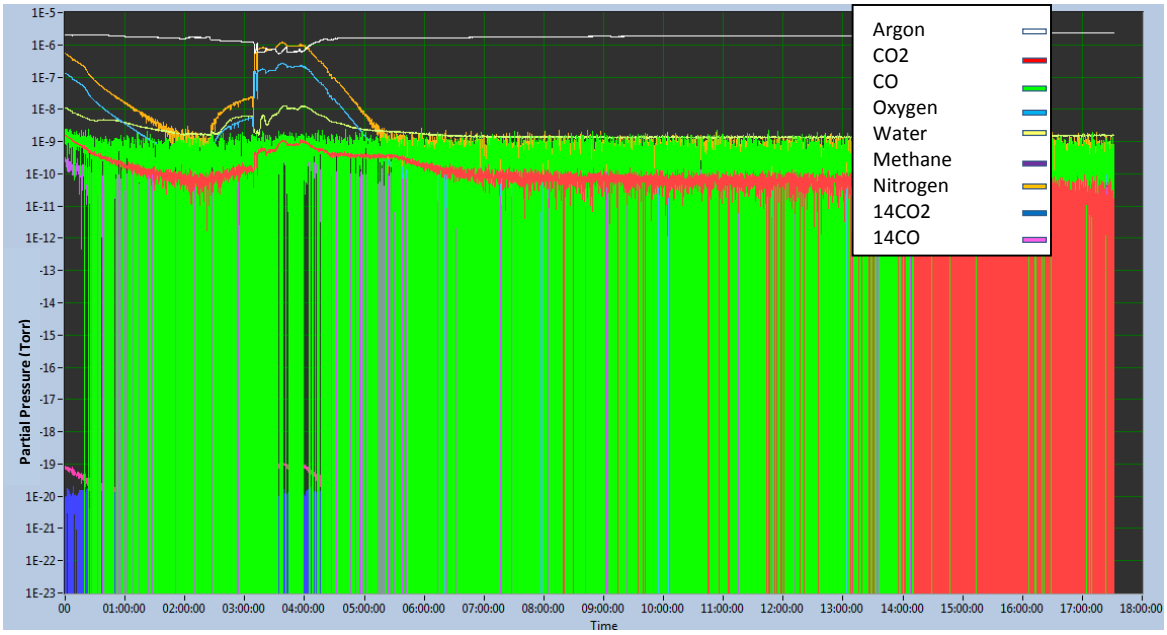

Figure 4.1: AE1 NBG18 +0%O_2 at 700°C for 8hrs with 2hr loading at 150°C

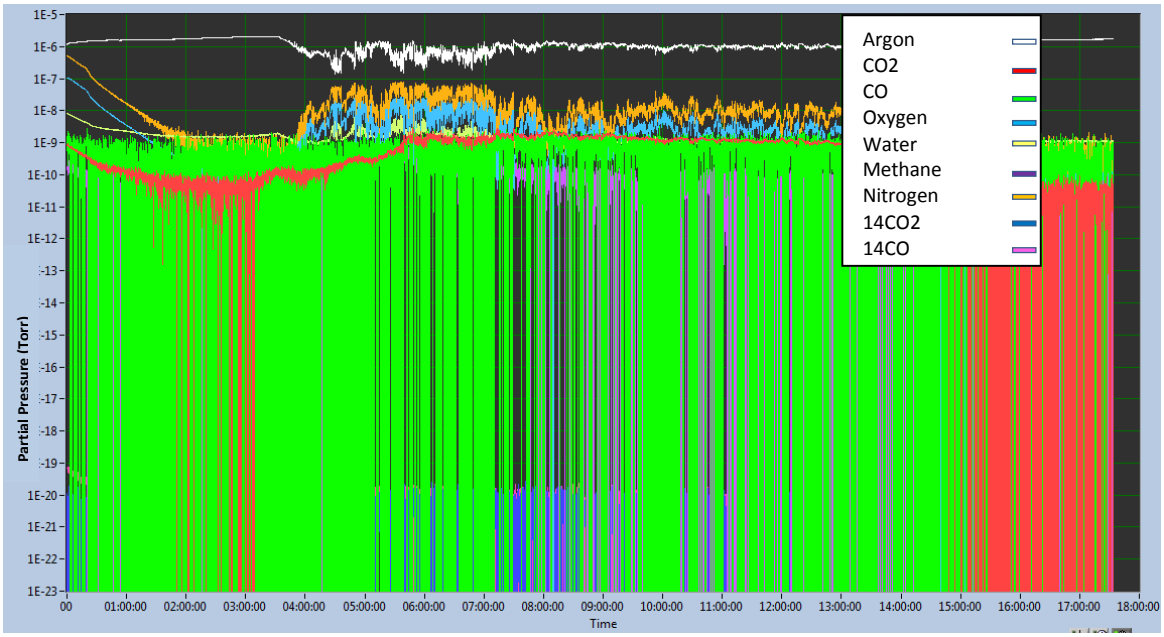

Figure 4.2: AE2 NBG18 +0%O_2 at 700°C for 8hrs with 2hr loading at 150°C

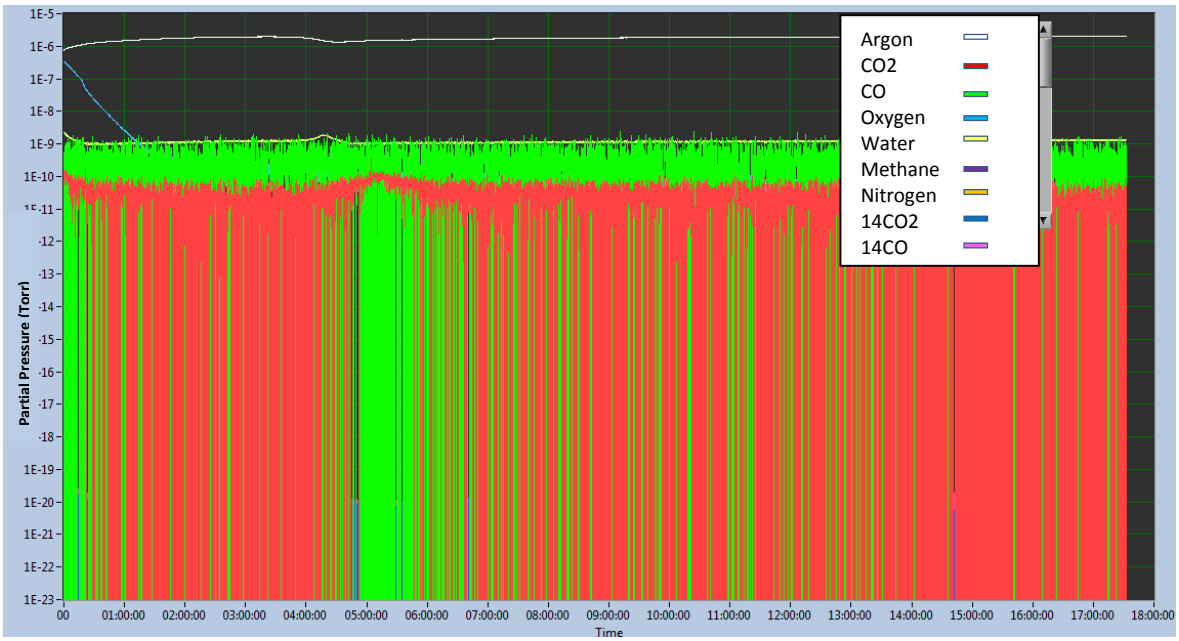

Figure 4.3: AE11 NBG25 +0%O_2 at 700°C for 8hrs with 2hr loading at 150°C

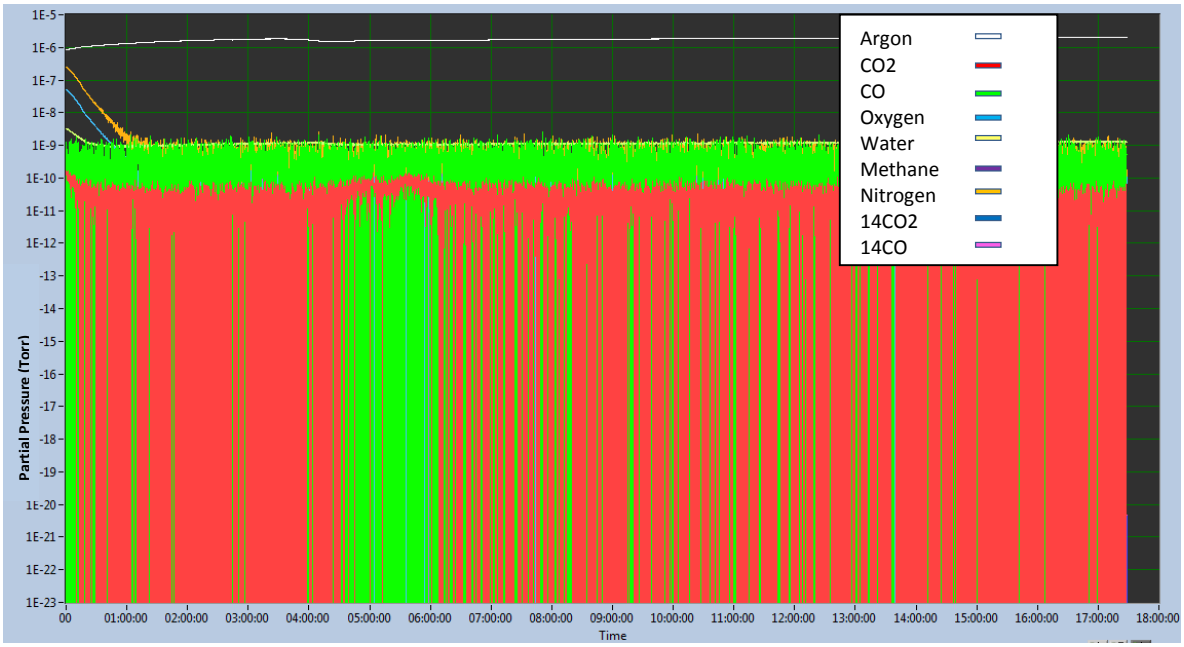

Figure 4.4: AE12 NBG25 +0%O_2 at 700°C for 8hrs with 2hr loading at 150°C

Water is present in all the experimental runs and peaks around 350-400°C then recedes. The water is believed to be intrinsic to the Gas Analyzer and has been unable to be removed by prior users (Cleaver, 2011; Smith, 2013).

The corrected gas analyzer data for the experiments of both NBG-18 and NBG-25, with argon + 2vol% O_2 and a pre-loading of 2 hours at 150°C and a thermal treatment for 8 hours at 700°C, can be seen in Figures 4.5-4.8. Corrected Data is in partial pressure (Torr).

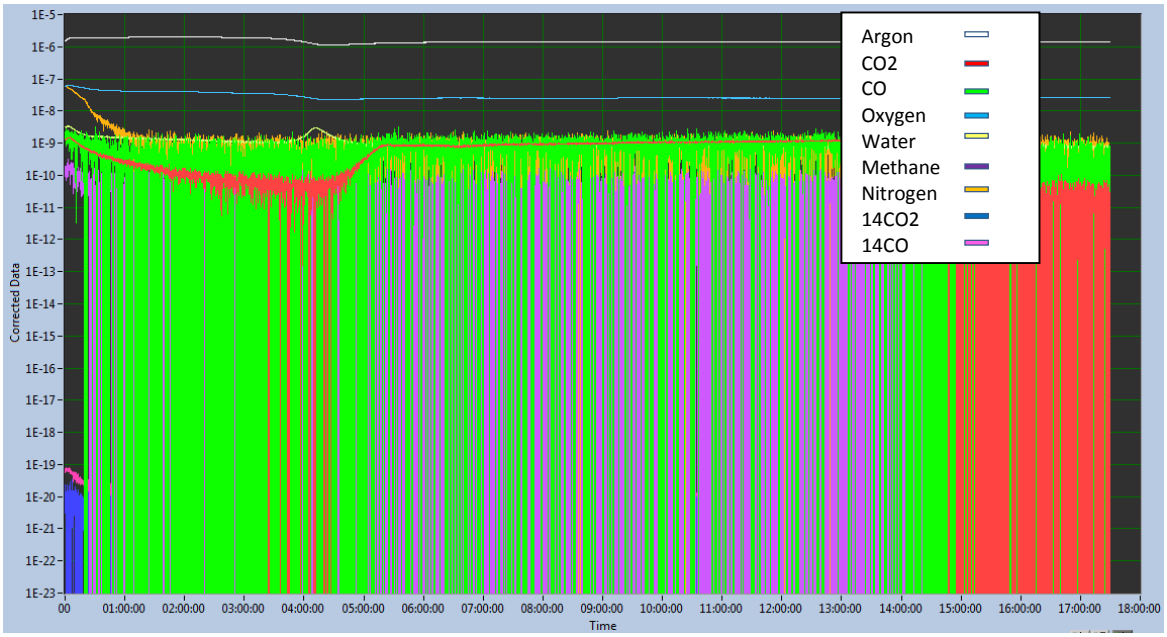

Figure 4.5: AE5 NBG18 +2%O_2 at 700°C for 8hrs with 2hr loading at 150°C

The curves representing Methane and Nitrogen were deleted from the screen shot in Figure 4.6 to allow visibility of the $^{14}CO_2$ and ^{14}CO gasification curves.

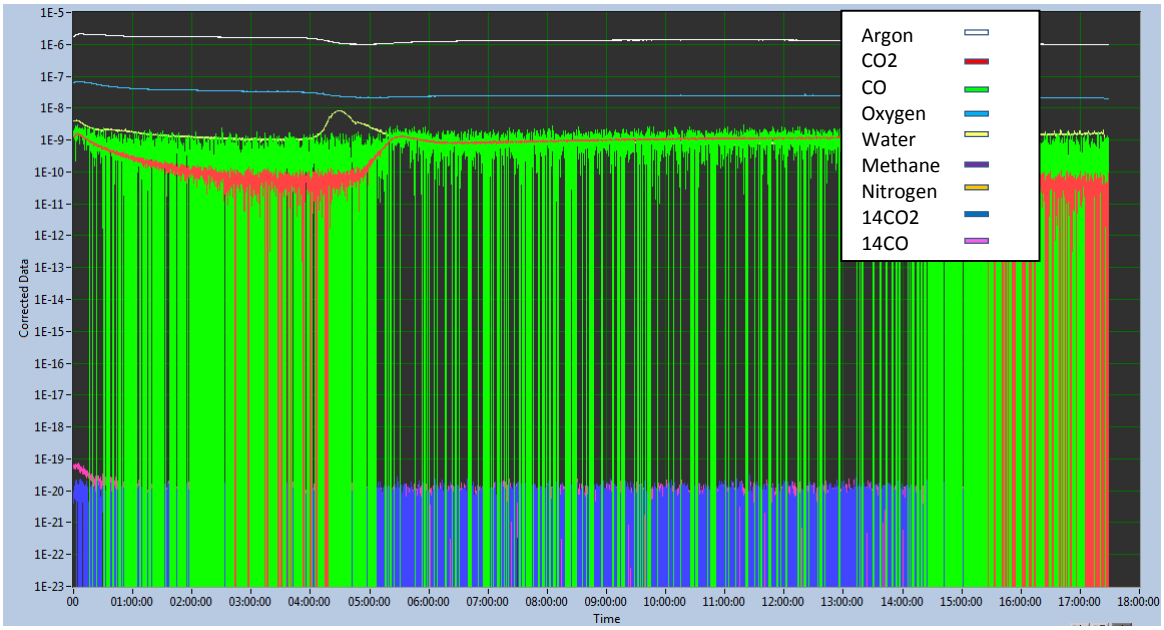

Figure 4.6: AE6 NBG18 +2% O_2 at 700°C for 8hrs with 2hr loading at 150°C

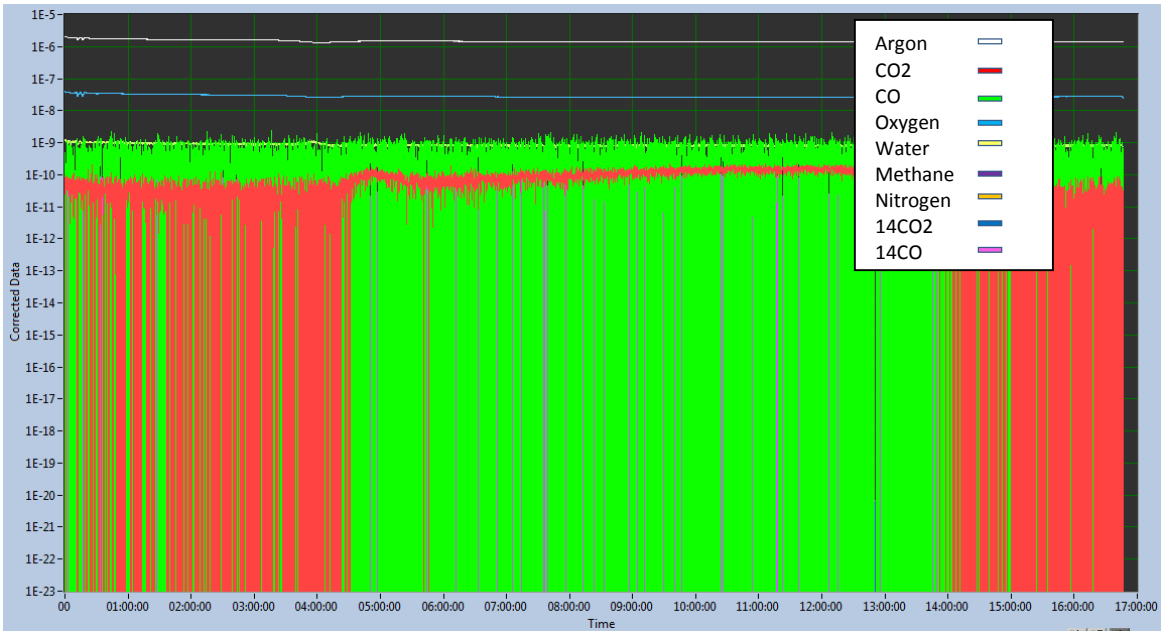

Figure 4.7: AE15 NBG25 +2%O_2 at 700°C for 8hrs with 2hr loading at 150°C

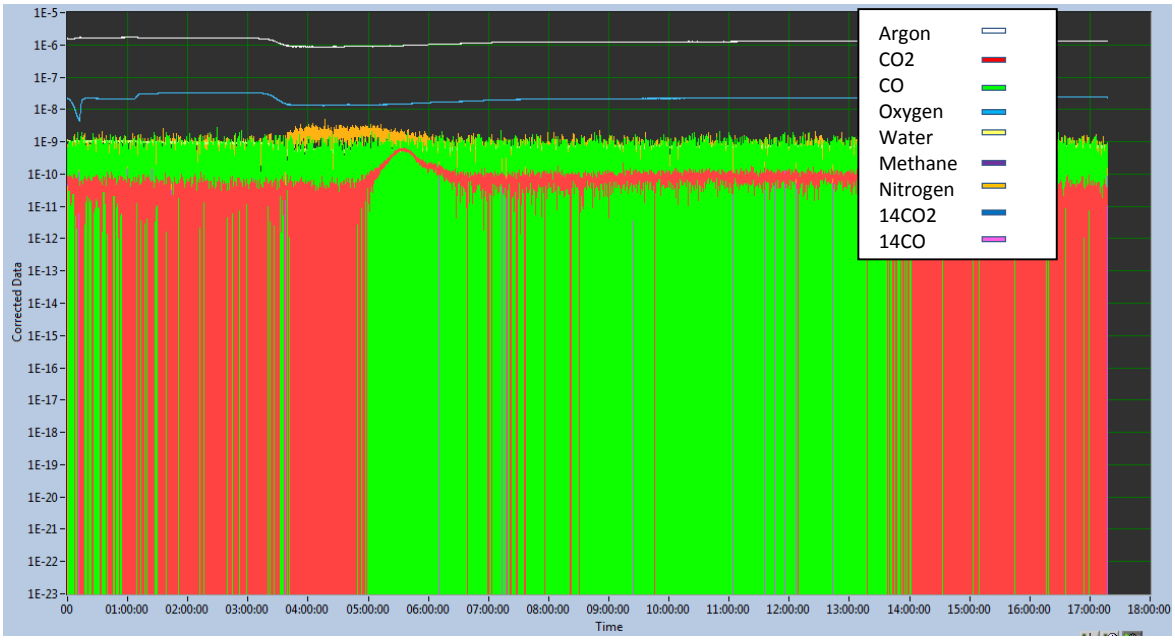

Figure 4.8: AE16 NBG25 +2%O_2 at 700°C for 8hrs with 2hr loading at 150°C

Figures 4.5-4.8 reveal CO remains the dominant desorption pathway for the gasification of both NBG-18 and NBG25. With the addition of 2vol% oxygen, the CO_2 curve increases during the oxidation process at thermal treatment temperature 700°C, from 5 hours and 30 minutes through 13 hours and 30 minutes (8 hours).

The corrected gas analyzer data for the experiments of both NBG-18 and NBG-25, with argon + 5vol% O_2 and a pre-loading of 2 hours at 150°C and a thermal treatment for 8 hours at 700°C, can be seen in Figures 4.9-4.10. Corrected Data is in partial pressure (Torr).

The curves representing Methane and Nitrogen were deleted from the screen shot in Figure 4.9 to allow visibility of the $^{14}CO_2$ and ^{14}CO gasification curves.

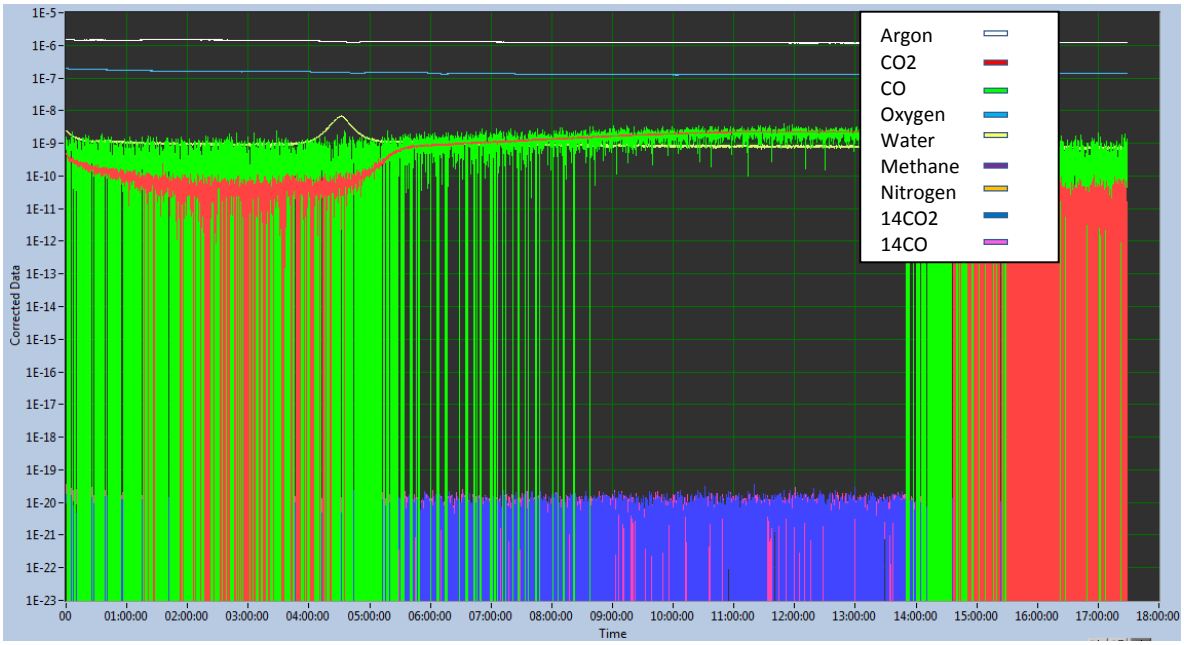

Figure 4.9: AE3 NBG18 +5%O_2 at 700°C for 8hrs with 2hr loading at 150°C

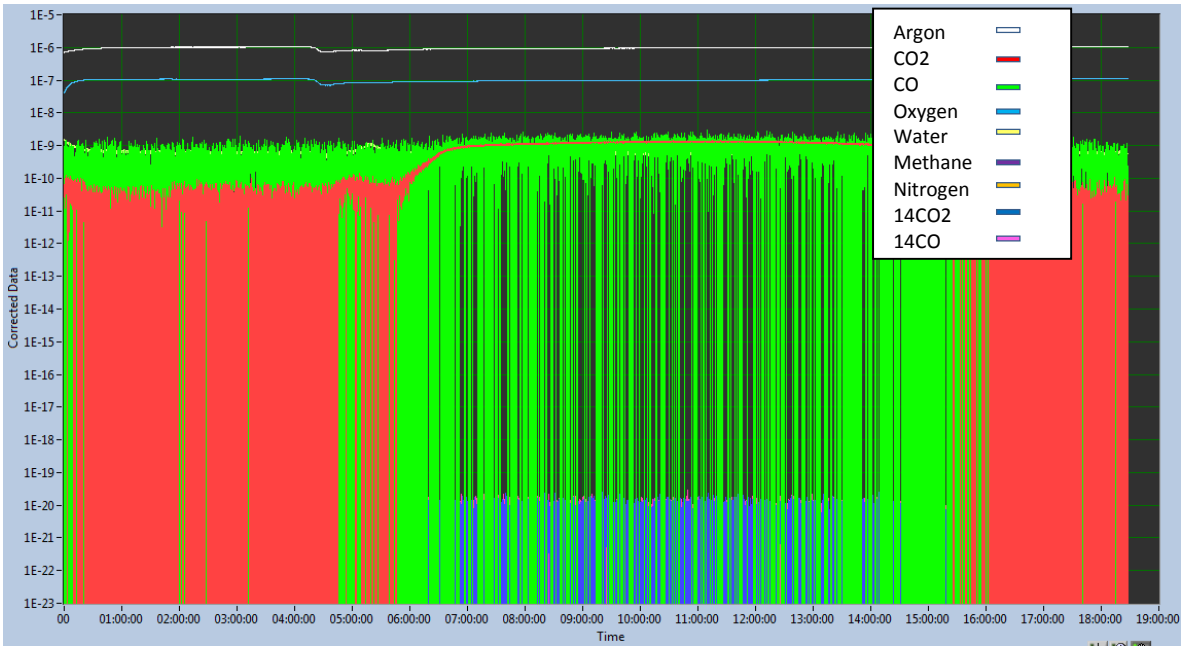

Figure 4.10: AE4 NBG18 +5%O_2 at 700°C for 8hrs with 2hr loading at 150°C

The percentage of carbon mass released during the gasification of both irradiated graphite types, N18 and N25, with the pre-loading process of varied oxygen levels for 2hr at 150°C prior to being thermally treated for 8 hours at 700°C is shown in Figure 4.11.

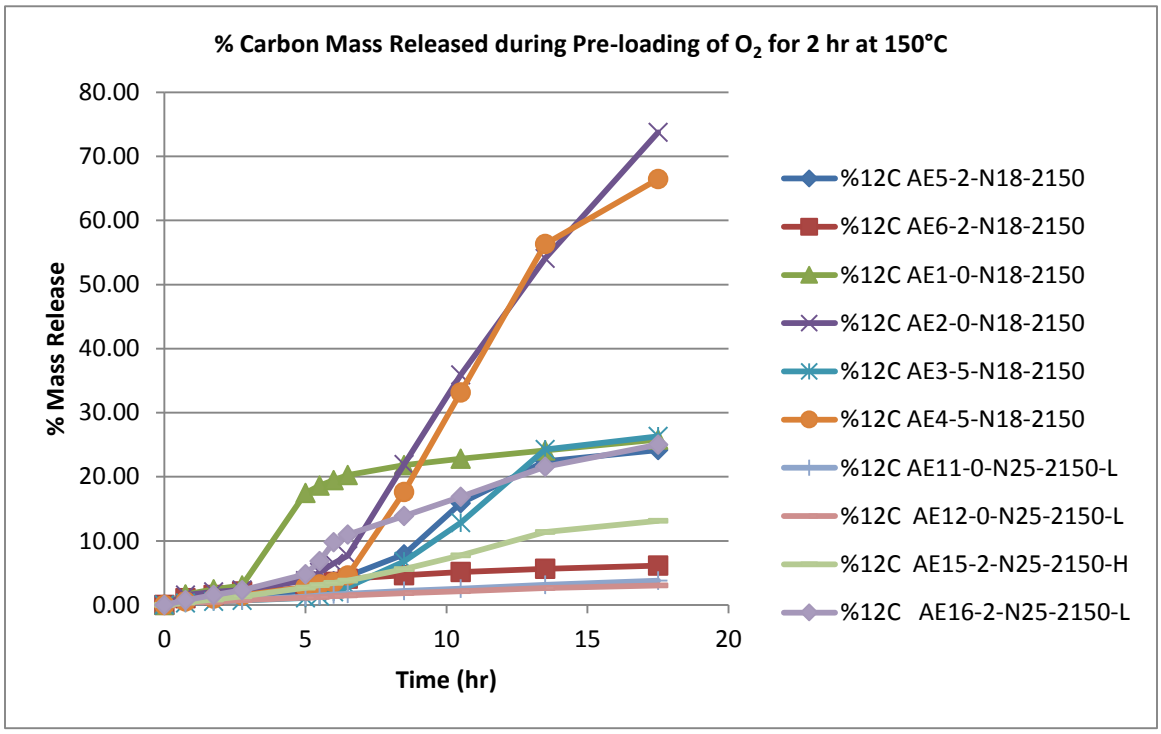

Figure 4.11: % Carbon Mass Released for O_2 pre-loading for 2 hr at 150°C

The NBG-25 graphite seems to release the least amount of carbon, (samples AE11, AE12, AE15 and AE16) with very low release in argon only, (samples AE11, and AE12) well below 10% of the total mass[1]. NBG-18 samples AE2 and AE4 experienced the greatest carbon mass loss. In the case of AE4, graphite oxidation is increased in the presence of higher levels of oxygen (5vol%), and therefore more mass loss is expected in comparison to samples with lower oxidant present. But it is inconsistent with its sample pair, AE3. AE2's behavior is inconsistent with that of AE1, processed under the same conditions, and with the other samples.

For the process involving 5vol% oxygen with 2 hours of preloading at 150°C, both the bulk graphite and ^{14}C exhibit large quantities of loss during thermal treatment. This suggests that there is an upper limit to the level of O_2 present for pre-loading that will maximize ^{14}C removal while concurrently minimizing the bulk graphite loss.

1. % mass loss contains a high degree of error due to method of calculation. Appendix G gives explanation and further data in Table G.1 for comparison.

Figure 4.12, shows that the greatest amount of ^{14}C released (above 90%) from the NBG-18 samples occurs in 5vol% O_2. This comes with a bulk graphite loss of over 20%, as seen in Figure 4.11. For the 5vol% pre-loading process, five of six NBG-18 samples nominally released between (40-90%) ^{14}C. The least percentage of ^{14}C loss from the NBG-18 samples was for pre-treatment with 0vol% O_2. The results of having such a low ^{14}C release with 0% oxygen (AE1 and AE2) pre-treatment at a temperature above room temperature, are inconsistent with Smith's results from pyrolysis treatment, argon only, with no pre-loading efforts (2hr at 38°C). Smith's best results for ^{14}C removal from NBG-18 were attained via thermal treatment for 13 hours at 700°C in argon only (Smith, 2013). As the only parameter difference is the pre-loading temperature, further study of this pre-loading temperature effect prompted the increased temperature to 300°C for more sample experimentation, which will be discussed in section 4.7.

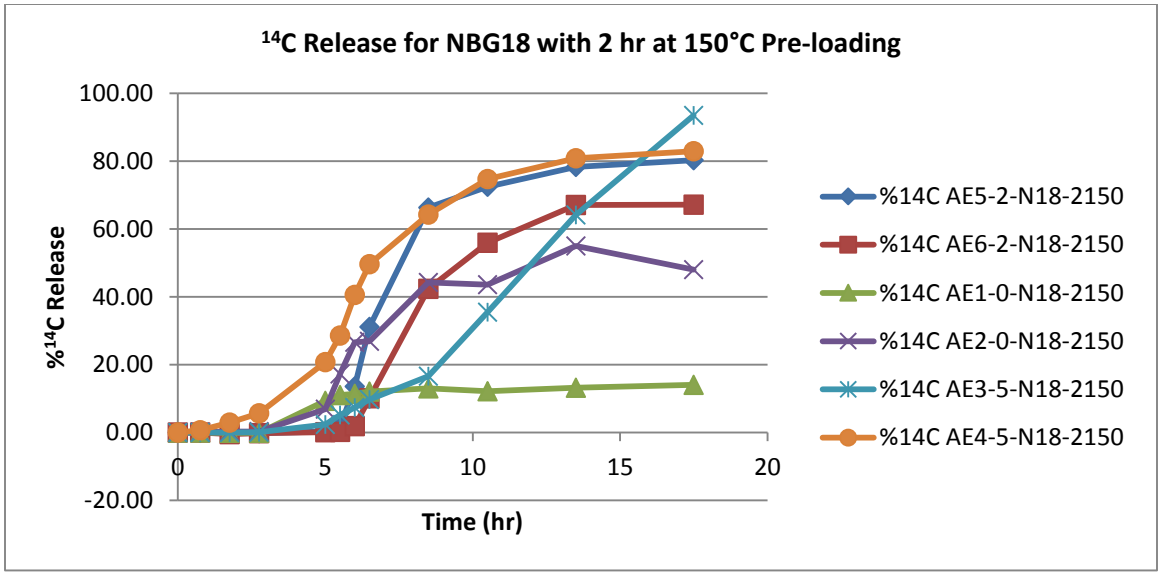

Figure 4.12: ^{14}C Release for NBG18 with 2 hr at 150°C

Looking at the behavior of NBG-25, separately, in Figure 4.13, results indicate that there is preferential release of ^{14}C under these pre-loading conditions (2hr at 150°C) and a 2% oxygen level. Clearly, the increased presence of oxygen results in larger percentage of ^{14}C released.

NBG-18 samples were immersed in liquid nitrogen prior to irradiation and irradiated for 120 days at MURR. NBG-25 samples were not liquid nitrogen immersed, and were irradiated in a sealed container between 350 - 400 days at ATR. The flux that the NBG-18 samples received was 6E+13 n/cm^{2}s, while NBG-25 samples were exposed to a flux of 3E+14 n/cm^{2}s. In comparison to the NBG-18 graphite, thermal treatment of NBG-25 with 2vol% O_2 was more effective. NBG-18 samples released an average of 74% ^{14}C, while NBG-25 samples released 88% ^{14}C average. This difference is likely due to the unique irradiation conditions of each graphite type rather than any fundamental material difference. In fact, the two graphites are physically quite similar.

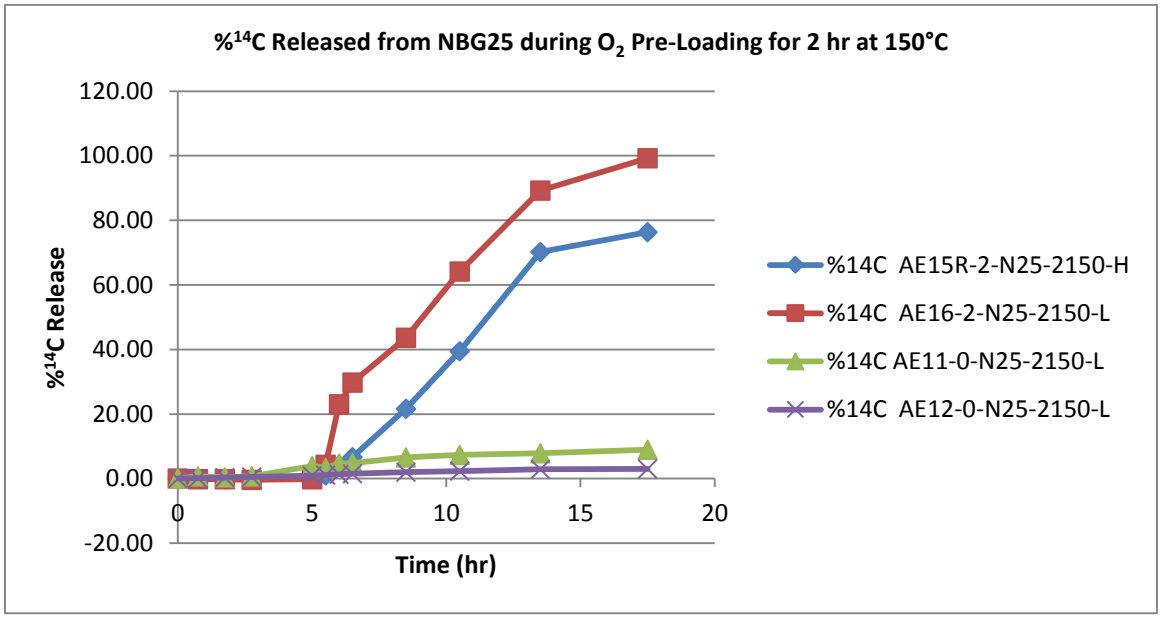

Figure 4.13: Carbon-14 Released from O_2 Pre-Loading for 2 hr at 150°C

In LaBrier's (2013) work on the characterization of carbon-14 in neutron irradiate graphite, he noted that substantial changes in elemental composition were observed for irradiated NBG-25 samples, including higher levels of oxygen (7% on surface, 20% at 30 nm sub-surface) and increased active site concentrations. This phenomenon could explain the increased release of ^{14}C if temperatures are being raised and held prior to thermal treatment, as this may allow for greater oxygen bonding to the irradiated graphite's active sites. Therefore, in the presence of oxygen, more carbon-oxygen bonds would form at the

defective lattice active sites (LaBrier, 2013). The pre-loading of the oxygen is within the chemical regime 1, <500°C, and in the chemical controlled regime, where carbon-oxygen bonds are forming and preparing to desorb as oxidation temperatures are reached closer to 700°C.

4.5 Graphite Experiments with Pre-Loading for 2 Hours at 300°C

4.5.1 Experimental Parameters

Experimental parameters are shown in Table 4.5 for all tests conducted with a pre-loading for 2 hours at 300°C. Oxygen levels of 0 vol% and 2 vol% were evaluated. Again, the argon and oxygen mixture for each experiment was allowed to flow through the system for approximately 30 minutes, prior to the start of the treatment, as the system was being checked and collection bottles were observed to function properly. These conditions were chosen to compare results with the pre-loading experiments performed at 150°C for 2 hours, section 4.4, to observe any preferential changes in release of either ^{14}C or the bulk graphite. Results from the experiments with pre-treatments performed at 150°C for 2 hours showed that during the oxygen loading (the first 3 hours of the experiment) the ^{14}C levels decreased. Because graphite oxidation at less than 600°C is relatively insignificant, it was thought that increasing the pre-loading temperature to 300°C might allow more oxygen to adhere to the surface and therefore become available for oxidation at the higher temperature than was observed at 150°C.

Table 4.5: Experimental Parameters for 2 hr at 300°C Pre-loading

Experimental ID	Graphite Type	Pre-Loading Time at Temp (hr) at (°C)	Thermal Treatment Time at Temperature (hr) at (°C)
Argon			
AE9-0-N18-2300	N18	2 at 300	8 at 700
AE10-0-N18-2300	N18	2 at 300	8 at 700
AE19-0-N25-2300-H	N25	2 at 300	8 at 700
AE110-0-N25-2300-M	N25	2 at 300	8 at 700
Argon + 2vol% O_2			
AE7-2-N18-2300	N18	2 at 300	8 at 700
AE8-2-N18-2300	N18	2 at 300	8 at 700
AE17-2-N25-2300-H	N25	2 at 300	8 at 700
AE18-2-N25-2300-L	N25	2 at 300	8 at 700

4.7.2 Experimental Results

The overview of the results for all experiments conducted under the parameters for pre-loading for 2 hours at 300°C and then thermally treating for 8 hours at 700°C can be seen in Table 4.6. The percentage of mass loss is widely varying due to differences in oxygen levels during pre-loading and graphite type.

Table 4.6: Summary of Experimental Results for 2 hr at 300°C Pre-loading

Experimental ID	Initial Mass (g)	Final Mass (g)	%Mass Loss	Mass Loss (g)
Argon				
AE9-0-N18-2300	0.0510	0.0506	0.7843	0.0004
AE10-0-N18-2300	0.0444	0.0443	0.2252	0.0001
AE19-0-N25-2300-H	0.0252	0.0242	3.968	0.0010
AE110-0-N25-2300-M	0.0346	0.0334	3.468	0.0012
Argon + 2vol% O_2				
AE7-2-N18-2300	0.0724	0.0557	23.07	0.0167
AE8-2-N18-2300	0.048	0.0375	21.88	0.0105
AE17-2-N25-2300-H	0.0526	0.0111	78.90	0.0415
AE18-2-N25-2300-L	0.0584	0.0156	73.29	0.0428

In general, NBG-25 lost more mass than NBG-18 and both types of graphite lost more mass when pre-treated with oxygen.

4.7.3 Gas Analyzer Data

The corrected gas analyzer data for the experiments for both NBG-18 and NBG-25, with argon only (0% O_2) and a pre-loading of 2 hours at 300°C and a thermal treatment for 8 hours at 700°C, can be seen in Figures 4.14-4.17. Corrected Data is in partial pressure (Torr).

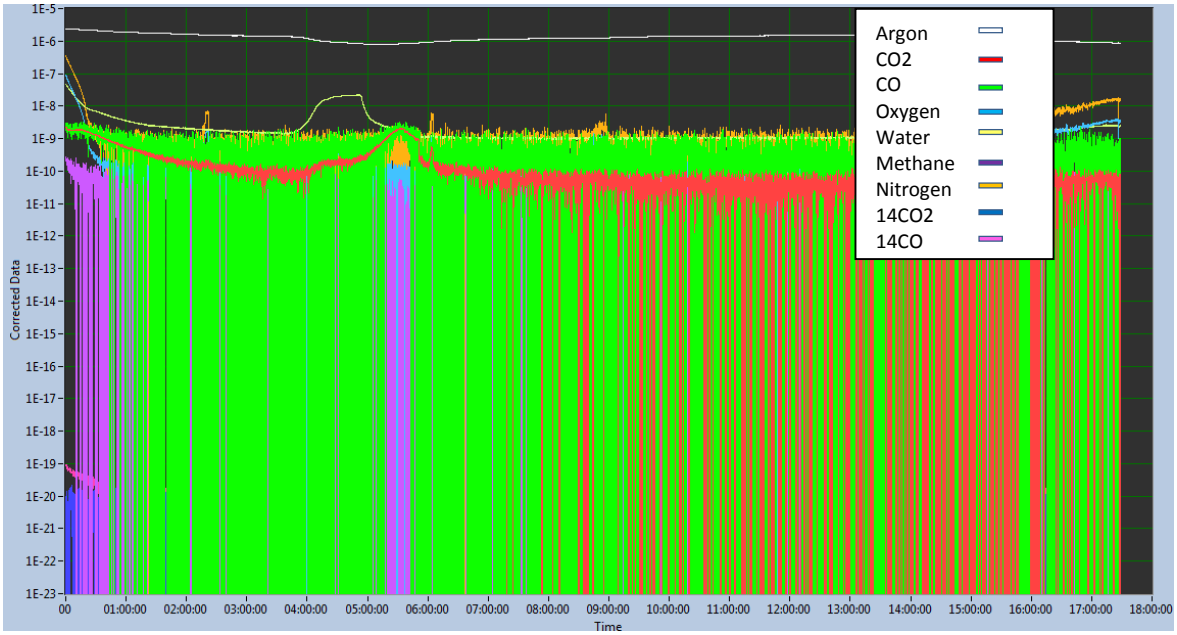

Figure 4.14: AE9 NBG18 +0%O_2 at 700°C for 8hrs with 2hr loading at 300°C

Figure 4.15: AE10 NBG18 +0%O_2 at 700°C for 8hrs with 2hr loading at 300°C

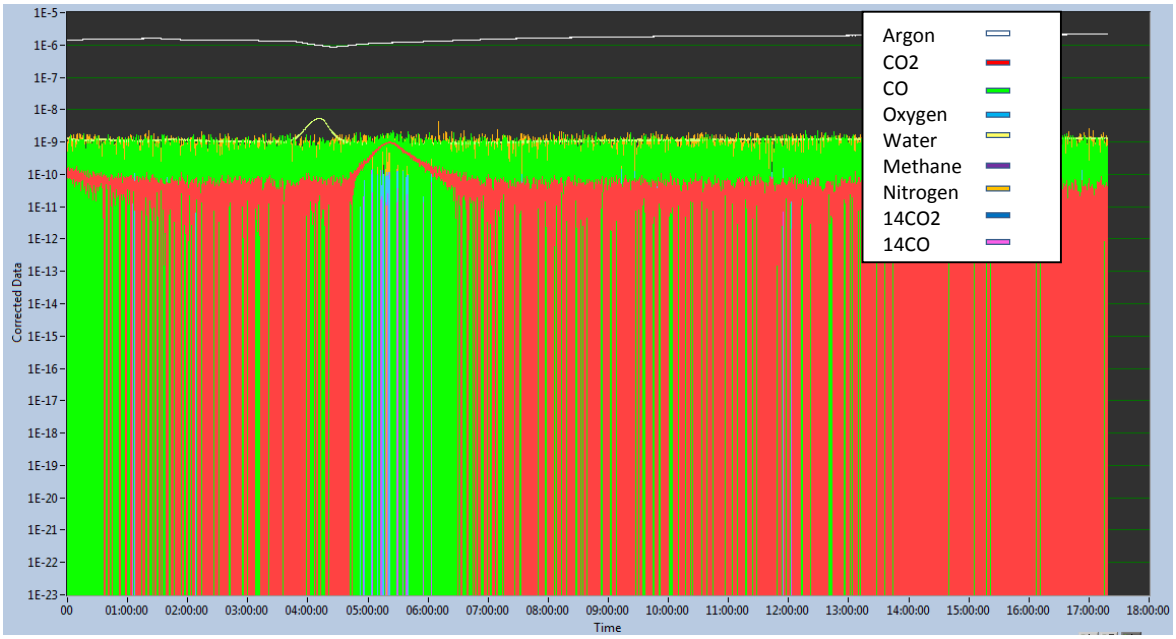

Figure 4.16: AE19 NBG25 +0%O_2 at 700°C for 8hrs with 2hr loading at 300°C

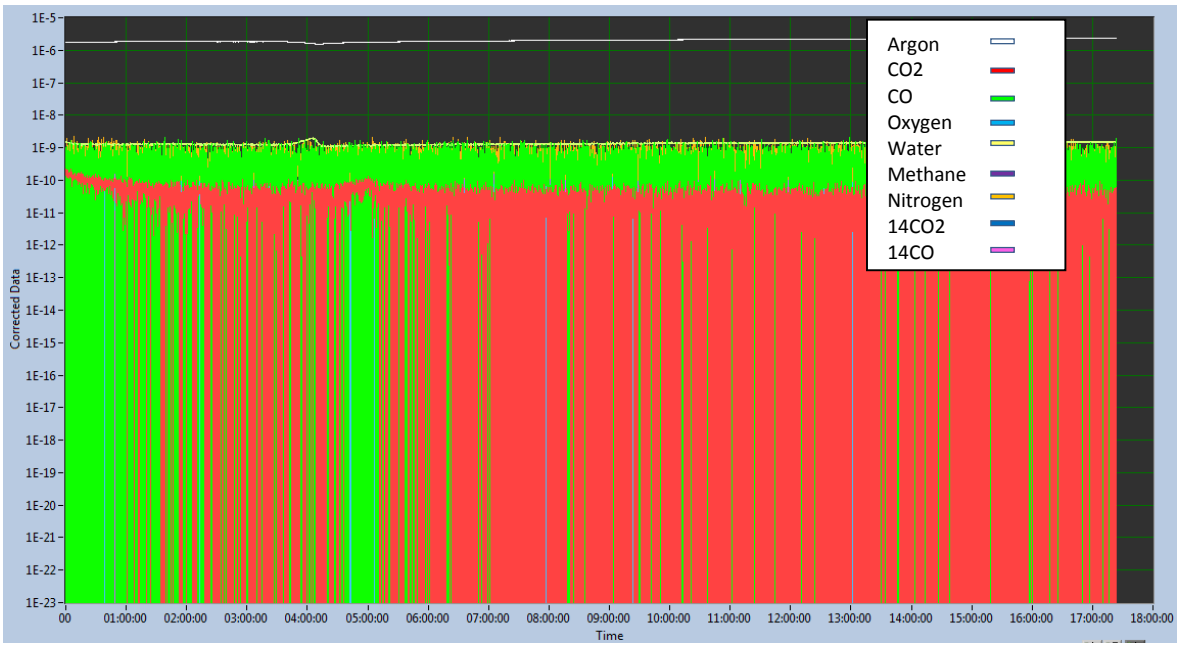

Figure 4.17: AE110 NBG25 +0%O_2 at 700°C for 8hrs with 2hr loading at 300°C

Experimental samples pre-treated at 300°C in 0vol% O_2 both NBG-18 (AE9, AE10) and NBG-25 (AE19, AE110) (Fig 4.14-4.17) exhibit similar thermal treatment gasification

curves. Data indicates that only 1-5% ^{14}C was removed for samples AE9, AE19, AE110. Sample AE10 did, however, release 25% ^{14}C and only 7% bulk graphite which is inconsistent with its experimental pair AE9 which only released 5.5% ^{14}C and 17% ^{12}C. An air ingress may account for the behavior discrepancy in data for sample AE9.

The data from both NBG-18 and NBG-25 samples pre-treated under pyrolysis is inconsistent with Smith's (2013) findings for NBG-18 at 0vol% and 700°C. Smith's study indicated that most of the ^{14}C was released during pyrolysis at 700°C. For this study, the pre-loading temperature is the only parameter change and, therefore, it might be concluded that the increased pre-loading temperature inhibits the release of the ^{14}C from the bulk graphite.

The corrected gas analyzer data for the experiments for both NBG-18 and NBG-25, with argon + 2vol% O_2 and a pre-loading of 2 hours at 300°C and a thermal treatment for 8 hours at 700°C, can be seen in Figures 4.18-4.21. Corrected Data is in partial pressure (Torr).

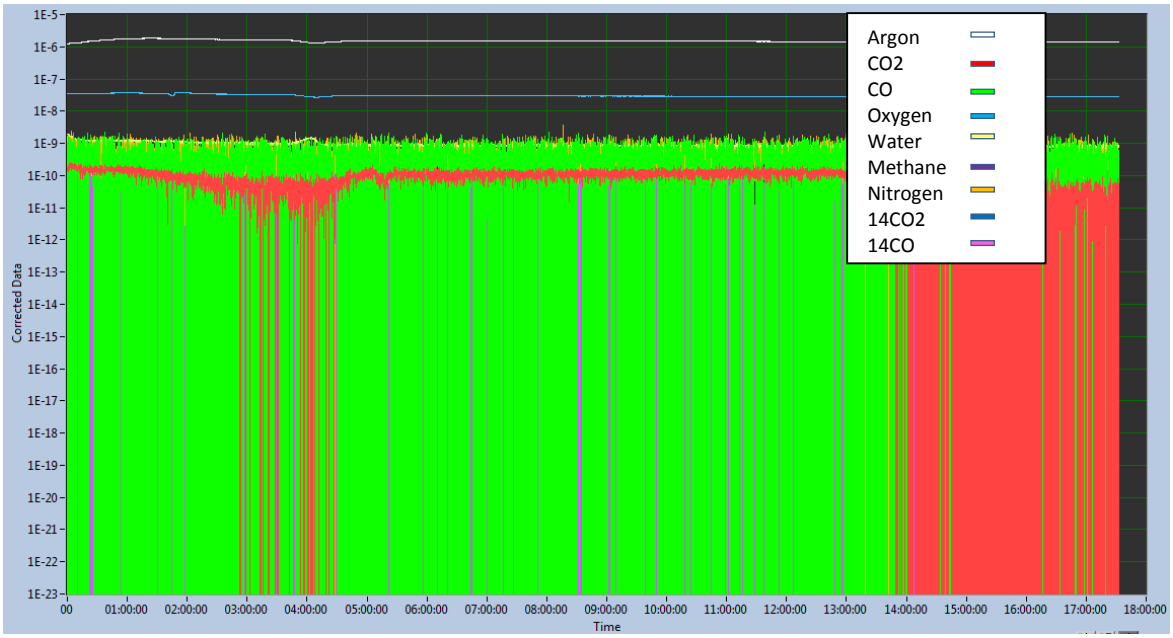

Figure 4.18: AE7 NBG18 +2%O_2 at 700°C for 8hrs with 2hr loading at 300°C

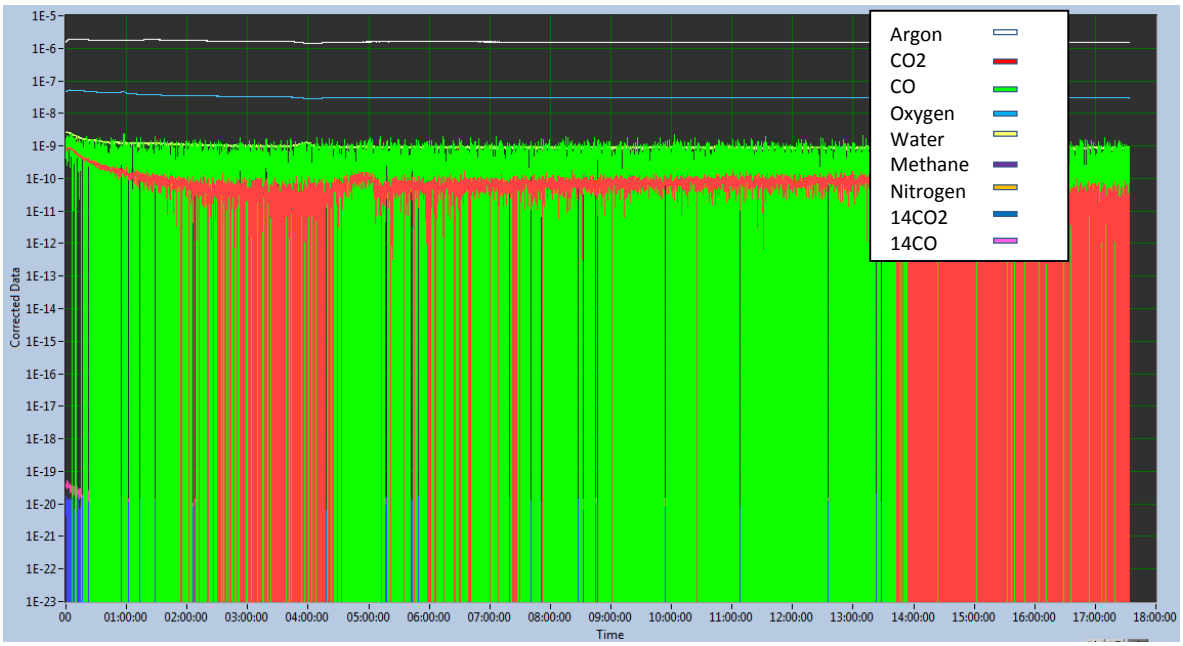

Figure 4.19: AE8 NBG18 +2%O_2 at 700°C for 8hrs with 2hr loading at 300°C

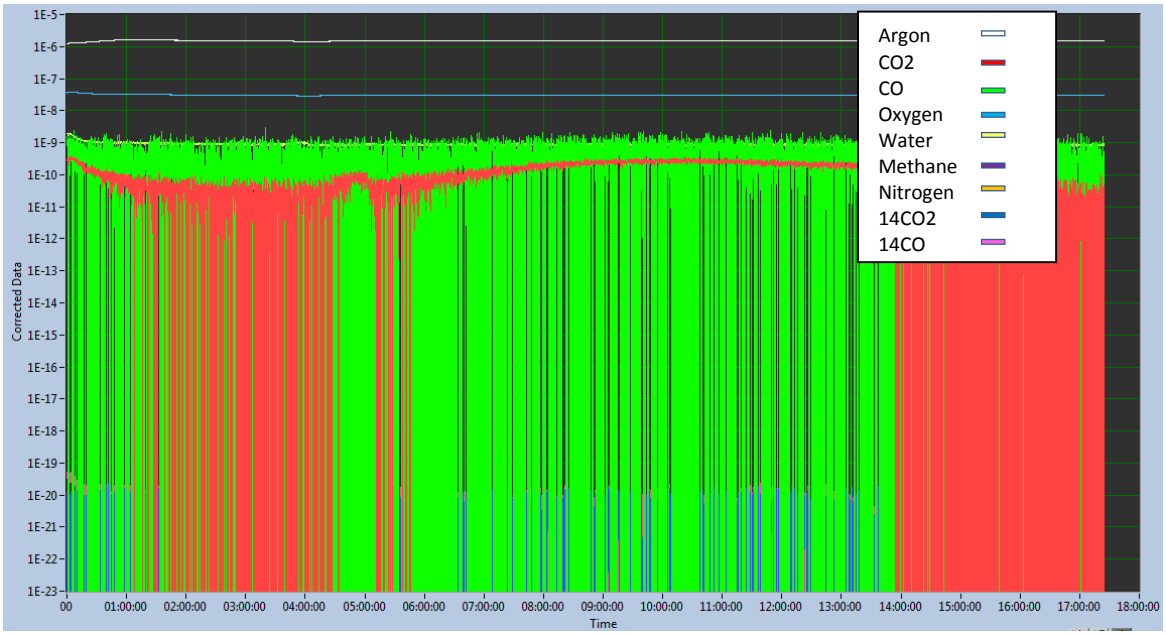

Figure 4.20: AE17 NBG25 +2%O_2 at 700°C for 8hrs with 2hr loading at 300°C

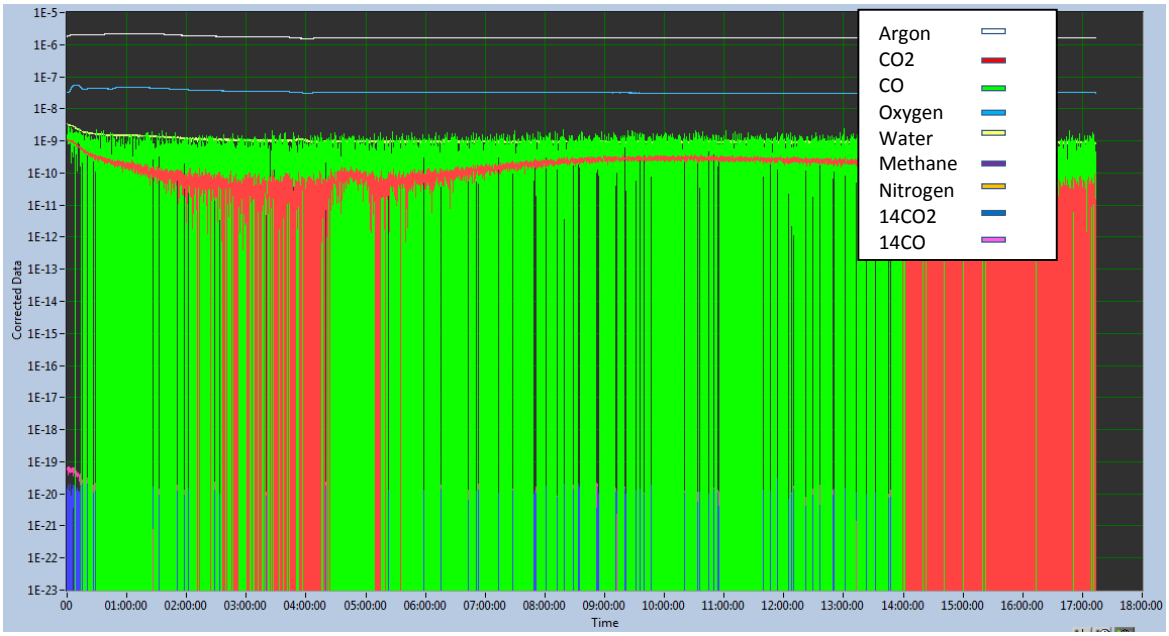

Figure 4.21: AE18 NBG25 +2%O_2 at 700°C for 8hrs with 2hr loading at 300°C

For the pre-loading process of 2vol% oxygen at 300°C prior to thermal treatment, the gasification curves for the two NBG-18 experiments are very similar suggesting the same desorption mechanism. Likewise, for NBG-25 experiments, the gasification curves are more rounded than for those of NBG-18, but similar to each other indicating a slightly different desorption mechanism. CO remains the dominant release pathway for both graphite types under these parameters. However, the release of ^{14}C increases to an average of 93% for all samples in this subset (AE7, AE8, AE17, AE18) and the % bulk graphite removed decreases to less than 11% for all samples in subset.

The percentage of carbon mass released during the gasification of NBG-18 and NBG-25, with the oxygen pre-loading for 2 hours at 300°C, is shown in Figure 4.22. The average % carbon mass loss for NBG-18 is 11%, while the average % carbon mass loss for NBG-25 is 10%. Both averages for this process are considerably

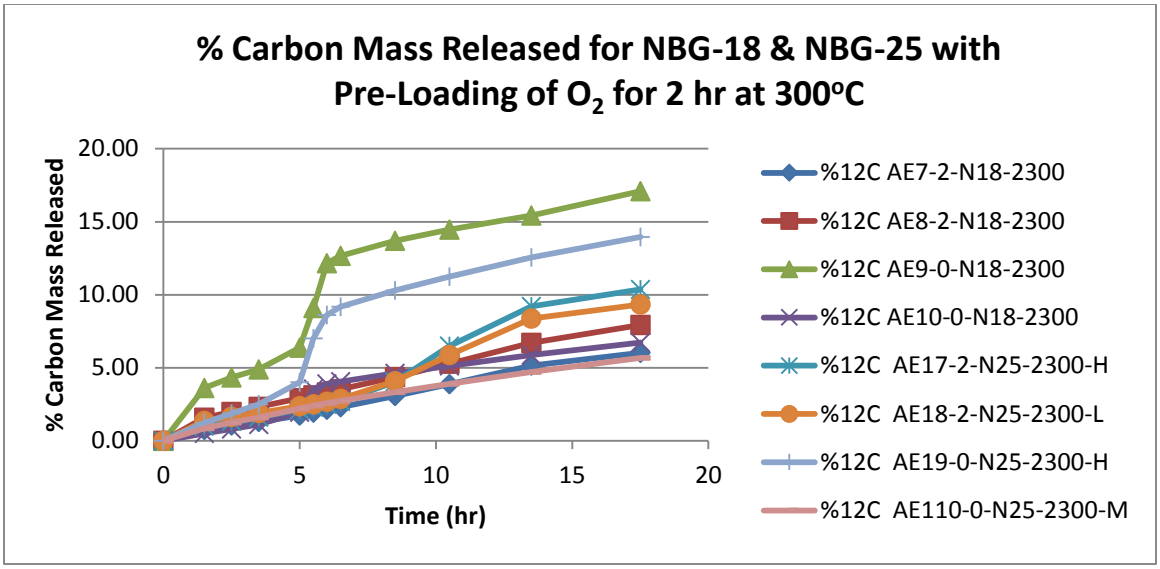

Figure 4.22: %Carbon Mass Released for NBG18 and NBG-25 with Pre-Loading of O_2 for 2 hr at 300°C

lower than the average %carbon mass loss for the O_2 pre-loading process of 2 hours at 150°C, which yielded averages for NBG-18 of 37% and for NBG-25 at 11% , or 27% for the process. See Figure 4.11. The carbon-14 release percentages for the pre-loading process of 2 hours at 300°C with 0vol% and 2vol% oxygen are shown in Figures 4.23 and 4.24.

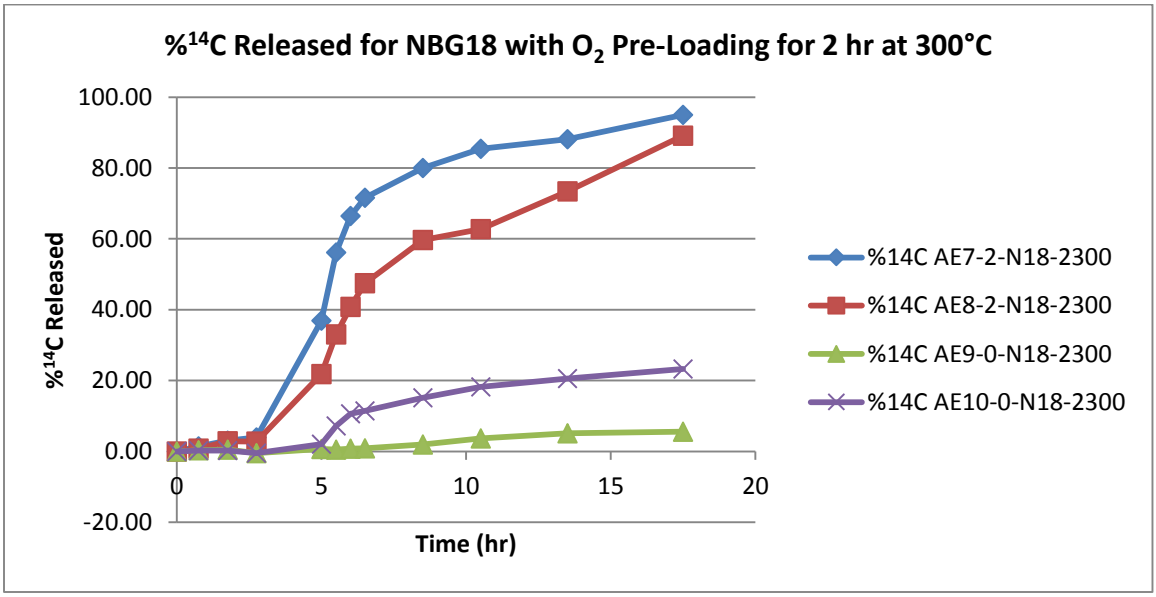

Figure 4.23: %^{14}C Released from NBG18 by O_2 Pre-Loading for 2 hr at 300°C

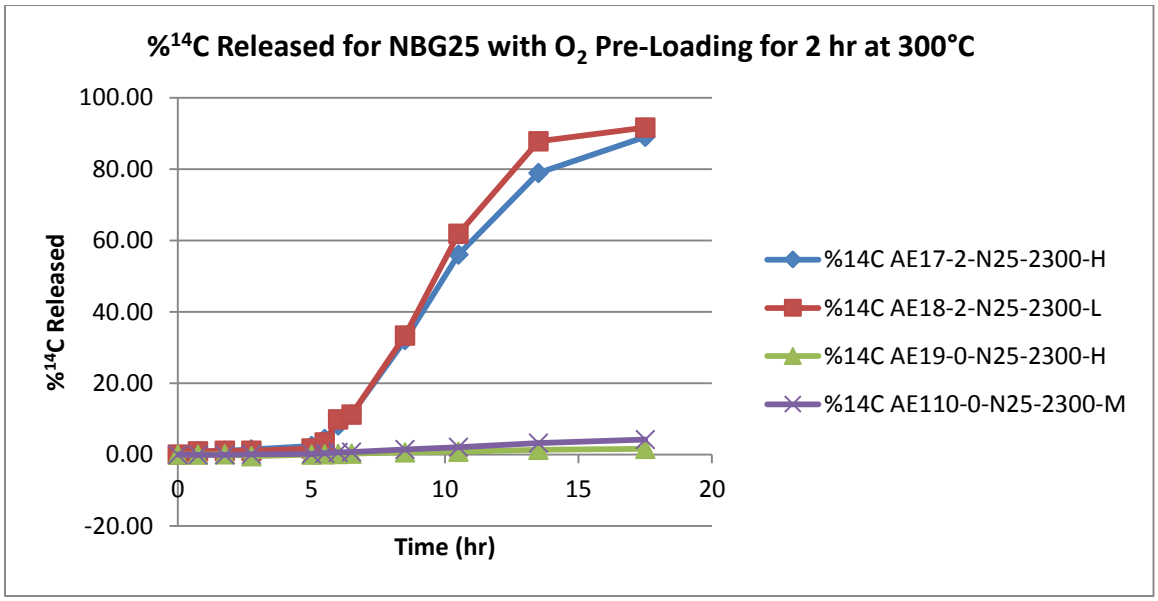

Figure 4.24: %^{14}C Released from NBG25 by O_2 Pre-Loading for 2 hr at 300°C

For the 300°C pre-loading experiments, both NBG-18 and NBG-25 exhibit preferential ^{14}C release for conditions with 2vol% oxygen. For this process, NBG-18 averaged 92% ^{14}C release in the presence of 2% oxygen, while similarly, NBG-25 averaged 90% ^{14}C release. As the pre-loading temperature increase is the only parameter change in process, it appears that as the pre-loading temperature increases, oxygen adsorbs to the graphite surface and is readily available for oxidation at the thermal treatment temperature of 700°C.

The average percentage of bulk graphite that is released from NBG-25, Figure 4.24, is 10% in conjunction with the ^{14}C release average of 90%; NBG-18, Figure 4.23, released slightly less bulk graphite, at 9%, while releasing an average of ^{14}C of 92%. Table 5.2 compares these release percentages.

4.8 Selective Release

The selective release of ^{14}C over ^{12}C is denoted by K and calculated by Equation 19. This value is a normalization that includes each sample's mass, activity and the experimental time. The experiments in this study were all sampled at the precise time

intervals and duration of treatments. These average selective release, K, values are shown in Table 4.8. Individual sample selective release values are shown in Tables F.1 and F.2 of Appendix F. Results indicate that both NBG-18 and NBG-25 show preferential release of ^{14}C with the thermal treatment process that includes the O_2 pre-loading for 2 hours at 300°C.

Table 4.8: ^{14}C Selective Release Averages for Experimental Subsets

AE-0-N18-2150	AE-2-N18-2150	AE-5-N18-2150
1.35	15.26	15.02
AE-0-N18-2300	**AE-2-N18-2300**	
2.11	58.69	
AE-0-N25-2150	**AE-2-N25-2150**	
1.86	20.08	
AE-0-N25-2300	**AE-2-N25-2300**	
0.42	20.68	

The selective release ratios from previous thermal treatment work can be seen in Tables 4.9-4.10. This data represents selective release values for thermal treatment conditions with no pre-loading of oxygen prior to treatment. However, Smith's best K value results of 195.49 yielded only a ^{14}C release of 46.39%. Whereas, for this study, the best K value of 58.69 yielded a 92% ^{14}C removal.

Table 4.9: Selective ^{14}C Release for Experimental Subsets Studied (Smith, 2013)

K: Selective Release of ^{14}C		
700-0-IE-N	**700-5-IE-N**	**1400-5-IE-N**
195.49	11.17	2.55

Table 1.10: Selective ^{14}C Release for Previous Thermal Treatment Work (Cleaver, 2011) (Podruhzina, 2004)

Selective Release of ^{14}C		
900°C, Ar, POCOFoam®	**1400°C, Ar, POCOFoam®**	**1060°C, Ar, Merlin**
42.14	38.49	26.9

Chapter 5.0 Conclusions

The objective of the research performed for this thesis was to refine the thermal treatment of neutron irradiated graphite towards maximizing the quantity of ^{14}C removed from the bulk graphite material, while minimizing the quantity of bulk graphite remaining after thermal treatment.

Previous thermal treatment experimental results for the NBG-18 samples studied by Smith (2013) are shown on Table 5.1. In Smith's experiments there was no pre-loading hold temperature, but rather the temperature was ramped up directly to the thermal treatment set point of 700°C and held for 9-13 hours. The prescribed argon-oxygen mixture was present during the temperature increase.

Table 2.1: Summary of Previous Experimental Results (Smith, 2013)

NBG-18	**Argon**	**Argon + 5vol% O_2**
	700	**700**
%^{12}C Removed	0.66	18.57
%^{14}C Removed	46.39	45.37

To optimize the relative release of ^{14}C with respect to ^{12}C, oxygen pre-loading was incorporated into the treatment process. For the purpose of comparison to previous results, tests were performed with 0vol% and 5vol% O_2. An intermediate level of 2vol% O_2 was also used. Pre-loading temperatures of 150°C and 300°C were tested, while the actual thermal treatment temperature (700°C) was kept the same as in previous experiments. Table 5.2 shows the experimental results from experiments completed for this thesis.

Table 5.2: Summary of Experimental Results for Current Study

Gas Mixture	Argon		Argon		Argon + 2vol% O_2		Argon + 2vol% O_2		Argon + 5vol% O_2	
Pre-Loading	2 Hr. @ 150°C		2 Hr. @ 300°C		2 Hr. @ 150°C		2 Hr. @ 300°C		2 Hr. @ 150°C	
Graphite	N18	N25	N18	N25	N18	N25	N18	N25	N18	N25
%^{12}C Removed	50	3	12	10	15	19	7	10	46	NA
%^{14}C Removed	32	6.0	14	2.9	74	88	92	90	88	NA

The data suggests that very small amounts of ^{14}C will desorb in pyrolysis, i.e. without O_2, with the addition of a pre-loading heating step at a temperature in the chemical controlled regime temperature region, <500°C, followed by oxidation at 700°C. These results are inconsistent with work by Smith (2013). The reason for inconsistency is unclear and is a subject for future investigation.

As both pre-loading oxygen concentration and temperature were increased, in sequential experiments, ^{14}C desorbed from the graphite in larger percentages with minimal bulk graphite removed in the treatment. The data from experiments using 5vol% O_2 pre-loading for 2 hours at 150°C, suggests that there is an upper limit for oxygen for pre-loading, because ^{14}C release decreased under this condition and increased amounts of bulk graphite were lost. This result is consistent with the findings of Smith (2013), who determined that temperature is more influential than oxygen level in selectively removing ^{14}C.

For the NBG-18 and NBG-25 samples studied for this thesis, the optimal conditions for release of ^{14}C while maintaining the highest quantity of bulk graphite are 2vol% O_2 pre-loading for 2 hours at 300°C, followed by thermal treatment for 8 hours at 700°C (Table 5.3).

Table 5.3: Summary of Optimal Thermal Treatment Process for Current Study

O_2 Pre-Loading Process	**2% O_2 2 Hr. at 300°C + 8Hr. at 700°C**	
Graphite	**N18**	**N25**
$\%^{12}C$ Removal	7	10
$\%^{14}C$ Removal	92	90

References

Banford, A.W., H. Eccles, M. J. Graves, W. von Lensa, and S. Norris. "CARBOWASTE-An Integrated Approach to Irradiated Graphite." Nuclear Future 4 (2008): 268-270.

Binford, Jesse S., Jr. "Kinetics of the Oxidation of Graphite." Advances in Chemistry Series 20 (1958): 39-48.

Cleaver, James. Thermal Treatment of Irradiated Graphite for the Removal of C-14. Masters Thesis. Idaho State University, 2011. Idaho Falls, 2011.

Davis Jr., Wallace. Carbon-14 Production in Nuclear Reactors. Oak Ridge: Oak Ridge National Laboratory, 1977.

Dunzik-Gougar . . "Removal of ^{14}C from Irradiated Graphite for Graphite Recycle and Waste Volume Reduction." NEUP Project Proposal, Department of Energy, 2009.

Electric Power Research Institute (EPRI). Graphite Decommissioning: Options for Graphite Treatment, Recycling, or Disposal, including a discussion of Safety-Related Issues. Palo Alto, CA: 2006. Technical Report 1013091.

El-Genk, M.S., and J.M.P. Tournier, "Development and validation of a model for the chemical kinetics of graphite oxidation." Journal of Nuclear Materials 411 (2011): 193-207.

El-Genk, M.S., and J.M.P. Tournier, "Comparison of Oxidation Model Predictions with Gasification Data of IG-110, IG-430 and NBG-25 Nuclear Graphite," Journal of Nuclear Material 420 (2012): 141-158.

Eto, M., and F. B. Growcock. Effect of Oxidizing Environment on the Strength and Oxidation Kinetics of HTGR Graphite: Part I: Reactivity and Strength Loss of H451. PCX and IG-11 Graphites. Upton, New York: Brookhaven National Labroatory, 1981.

Fachinger, Johannes, Werner von Lensa, and Tatjana Podruhzina. “Decontamination of Nuclear Graphite.” 3rd International Topical Meeting on High Temperature Reactor Technology. South Africa: North-West University, 2006.

Fachinger, J., Podruhzina, T., & Von Lensa, W. “Decontamination of Nuclear Graphite by Thermal Treatment.” Manchester: Solutions for Graphite Waste. 2007.

Gen-IV International Forum. The Very-High_Temperature Teactor (VHTR) is a graphite moderated, helium-coolde reactor with a thermal neutron spectrum. *Gen-4.* [Online] Gen-4. http://www.gen-4.org/Technology/systems/vhte.htm.

Haag, G., “Properties of ATR-2E Graphite and Property Changes Due to Fast Neutron Irradiation.” Institue for Sicherheitsforschung and Reaktortechnik Forschungszentrun, Julich. 1983.

Hagen, A., “Deep Sea Disposal: Protecting Fish and Man. s.l.”Vienna: International Atomic Energy Agency, 1988. 30405943840.

Idaho National Laboratory**.** HTGR Technology Course for the Nuclear Reglatory Commision. Idaho National Laboratory, 2010.

International Atomic Energy Agency (IAEA). Characterization, Treatment and Conditioning of Radioactive Graphite from Decomissioning of Nuclear Reactors*.* Vienna: IAEA, 2006.

International Atomic Energy Agency (IAEA). Irradiation Damage in Graphite due to Fast Neutrons in Fission and Fusion Systems. Vienna: IAEA, 2000.

International Atomic Energy Agency (IAEA). Management of Waste Containing Tritium and Carbon-14. Vienna: IAEA, 2004.

LaBrier, Daniel P. “Characterization of ^{14}C in Neutron Irradiated Graphite.” Phd. Dissertation. Idaho State University, 2013. Idaho Falls, 2013.

Mantell, C.L. Carbon and Graphite Handbook*.* New York : Intersicent, 1968.

Marsden, B. J., and K. L.Hopkinson. The Chemical Form of Carbon-14 within Graphite. Ed. K. L. Hopkinson and C J Wheatley. United Kingdom: Serco Assurance, 2002.

McCrory, Shilo. "Characterizing the Pathway to Formation of ^{14}C in Irradiated Graphite." Master's Thesis. Idaho State University, 2011. Idaho Falls, 2011.

Nuclear Energy Agency. Generation IV International Forum. s.l. : Technical Secretariat, 2009.

Podruzhina, Tatiana. Graphite as Radioactive Waste: Corrosion Behaviour Under Final Repository Conditions and Thermal Treatment. Diss. Rheinisch-Westfalischen Technischen Hochschule Aachen, 2004. Germany: Aachen, 2004.

Propp, W. A. Graphite Oxidation Thermodynamics/Reactions. Idaho Falls, Idaho: Idaho National Engineering and Environmental Laboratory, 1998.

Richards, M. B. "Combustibility of High-Purity, Nuclear-Grade Graphite." General Atomics. American Carbon Society 22nd Biennial Conference. San Diego: American Carbon Society, 1995. 598-599.

Smith, T. "Removal of ^{14}C from Irradiated Graphite for Waste Volume Reduction and Bulk Graphite Recycle: Thermal Treatment." Master's Thesis. Idaho State University, 2013. Idaho Falls, Idaho, 2013.

Smith, T., McCrory, S., Dunzik-Gougar., "Limited Oxidation of Irradiated Graphite Waste to Remove Surface Carbon-1 ." Nuclear Engineering and Technology, Vol. 45, No. 2. April 2013.

Snead, Lance, and Tim Burchell. "Oxidation of High-Quality Graphite for IFE". Proceedings of the DOE/NE High Average Power Laser Program Workshop, Pleasanton, CA, July 25-26, 2002.

Takahashi, R., S. Toyahara, S. Maruki, H. Ueda, and T. Yamamoto. "Investigation of Morphology and Impurity of Nuclear Grade Graphite, and Leaching Mechanism of Carbon-14." IAEA Technical Committee Meeting on "Nuclear Graphite Waste Management", Manchester, United Kingdom, October 18-20, 1999.

United States Department of Energy Office of Environmental Management Spent Fuel Management Office. “Graphite Oxidation Thermodynamics/Reactions”. s.l. : United States Department of Energy Office of Environmental Management, 1998. DOE/SNF/REP-018 Rev 0.

von Lensa, W., Vulpius, D., Steinmetz, H., Girke, N., Bosbach, D., Thomasuke, B., Banford, A., Bradbury, D., Grambow, B., Grave, M., Jones, A., Petit, L., Pina, G., “Treatment and Disposal of Irradiated Graphite and their Carbonaceous Waste.” Technical Report CARBOWASTE. 2010.

Vulpius, D., M. Florjan, and J. Fachinger. “Isotopic Decontamination of Neutron Irradiated Graphite.” Institute for Energy Research-Safety Research and Reactor Technology, 2008.

Wickham, A., Neighbour, G., Dubourg, . “The Uncertain Future for Nuclear Graphite Disposal Crisis or pportunity?” IAEA Workshop on Nuclear Graphite Waste Management. October 18-20, 1999. Manchester UK.

Xiaowei, L., R. Jean-Charles, and Y. Suyuan. *“*Effect of Temperature on Graphite Oxidation Behavior.*”* Nuclear Engineering and Design, 2004.

Yates, J.T. JR, T. Madey, and N. Erickson, “ESCA Study of Carbon Monoxide and Oxygen Adsorption on Tungsten,” XPS PhotoElectron Spectroscopy: Benchmark Papers in Physical Chemistry and Chemical Physics. Vol. *2*. Academic Press, Inc., 1978.

Appendix

Appendix A: Sample Release Rate Data

Table A1: AE1-0-18-2150 Release Rate

AE1							
f_{12C}	**mtj (g)**	**mtj-1 (g)**	**t-tj-1(hr)**	**Xtj (moles)**	**Xtj-1 (moles)**	**R' (mol/g hr)**	**NR' ^{12}C**
1.00	3.60E-02	3.63E-02	0.00E+00	2.83E-05	0.00E+00	0.00E+00	0.00E+00
1.00	3.57E-02	3.60E-02	7.50E-01	5.00E-05	2.83E-05	8.05E-04	8.05E-04
1.00	3.54E-02	3.57E-02	1.00E+00	7.35E-05	5.00E-05	6.58E-04	6.58E-04
1.00	3.52E-02	3.54E-02	1.00E+00	9.24E-05	7.36E-05	5.31E-04	5.31E-04
1.00	3.00E-02	3.52E-02	2.25E+00	5.28E-04	9.25E-05	5.50E-03	5.50E-03
1.00	2.95E-02	3.00E-02	5.00E-01	5.63E-04	5.29E-04	2.29E-03	2.29E-03
1.00	2.92E-02	2.95E-02	5.00E-01	5.89E-04	5.63E-04	1.69E-03	1.69E-03
1.00	2.89E-02	2.92E-02	5.00E-01	6.13E-04	5.89E-04	1.63E-03	1.63E-03
1.00	2.84E-02	2.89E-02	2.00E+00	6.59E-04	6.13E-04	7.92E-04	7.92E-04
1.00	2.80E-02	2.84E-02	2.00E+00	6.89E-04	6.60E-04	5.20E-04	5.20E-04
1.00	2.75E-02	2.80E-02	3.00E+00	7.29E-04	6.90E-04	4.64E-04	4.64E-04
1.00	2.69E-02	2.75E-02	4.00E+00	7.80E-04	7.29E-04	4.60E-04	4.60E-04
					Average:	1.28E-03	1.28E-03
f_{14C}	**mtj (g)**	**mtj-1 (g)**	**t-tj-1 (hr)**	**Xtj (moles)**	**Xtj-1 (moles)**	**R' (mol/g hr)**	**NR' ^{14}C**
0.00E+00	0.00E+00	0.00E+00	0.00E+00	0.00E+00	0.00E+00	0.00E+00	0.00E+00
9.93E-07	3.57E-02	3.60E-02	7.50E-01	1.15E-12	0.00E+00	4.27E-11	4.30E-05
1.00E-06	3.54E-02	3.57E-02	1.00E+00	-8.51E-13	1.15E-12	-5.61E-11	-5.60E-05
1.01E-06	3.52E-02	3.54E-02	1.00E+00	-8.51E-13	-8.51E-13	0.00E+00	0.00E+00
1.07E-06	3.00E-02	3.52E-02	2.25E+00	2.76E-10	-8.51E-13	3.49E-09	3.26E-03
1.07E-06	2.95E-02	3.00E-02	5.00E-01	3.26E-10	2.76E-10	3.36E-09	3.14E-03
1.07E-06	2.92E-02	2.95E-02	5.00E-01	3.39E-10	3.26E-10	8.74E-10	8.14E-04
1.08E-06	2.89E-02	2.92E-02	5.00E-01	3.56E-10	3.39E-10	1.19E-09	1.10E-03
1.09E-06	2.84E-02	2.89E-02	2.00E+00	3.85E-10	3.56E-10	4.97E-10	4.58E-04
1.11E-06	2.80E-02	2.84E-02	2.00E+00	3.59E-10	3.85E-10	-4.54E-10	-4.09E-04
1.12E-06	2.75E-02	2.80E-02	3.00E+00	3.90E-10	3.59E-10	3.67E-10	3.29E-04
1.13E-06	2.69E-02	2.75E-02	4.00E+00	4.17E-10	3.90E-10	2.43E-10	2.15E-04
					Average:	7.96E-10	7.41E-04

Table A2: AE2-0-18-2150 Release Rate

AE2							
f_{12C}	**mtj (g)**	**mtj-1 (g)**	**t-tj-1(hr)**	**Xtj (moles)**	**Xtj-1 (moles)**	**R' (mol/g hr)**	**NR' ^{12}C**
1.00E+00	4.43E-02	0.00E+00	0.00E+00	0.00E+00	0.00E+00	0.00E+00	0.00E+00
1.00E+00	4.36E-02	4.43E-02	7.50E-01	5.66E-05	3.86E-05	5.42E-04	5.42E-04
1.00E+00	4.34E-02	4.36E-02	1.00E+00	7.47E-05	5.66E-05	4.13E-04	4.13E-04
1.00E+00	4.33E-02	4.34E-02	1.00E+00	8.66E-05	7.47E-05	2.74E-04	2.74E-04
1.00E+00	4.26E-02	4.33E-02	2.25E+00	1.41E-04	8.66E-05	5.57E-04	5.57E-04
1.00E+00	4.21E-02	4.26E-02	5.00E-01	1.87E-04	1.41E-04	2.18E-03	2.18E-03
1.00E+00	4.14E-02	4.21E-02	5.00E-01	2.39E-04	1.87E-04	2.46E-03	2.46E-03
1.00E+00	4.09E-02	4.14E-02	5.00E-01	2.83E-04	2.39E-04	2.14E-03	2.14E-03
1.00E+00	3.46E-02	4.09E-02	2.00E+00	8.09E-04	2.83E-04	6.43E-03	6.43E-03
1.00E+00	2.84E-02	3.46E-02	2.00E+00	1.32E-03	8.09E-04	7.45E-03	7.45E-03
1.00E+00	2.03E-02	2.84E-02	3.00E+00	2.00E-03	1.32E-03	7.89E-03	7.89E-03
1.00E+00	1.16E-02	2.03E-02	4.00E+00	2.72E-03	2.00E-03	8.92E-03	8.92E-03
					Average:	3.27E-03	3.27E-03
f_{14C}	**mtj (g)**	**mtj-1 (g)**	**t-tj-1 (hr)**	**Xtj (moles)**	**Xtj-1 (moles)**	**R' (mol/g hr)**	**NR' ^{14}C**
	4.43E-02	0.00E+00	0.00E+00	0.00E+00	0.00E+00	0.00E+00	0.00E+00
8.67E-07	4.36E-02	4.43E-02	7.50E-01	3.96E-12	0.00E+00	1.19E-10	1.37E-04
8.69E-07	4.34E-02	4.36E-02	1.00E+00	1.08E-11	3.96E-12	1.58E-10	1.81E-04
8.72E-07	4.33E-02	4.34E-02	1.00E+00	1.03E-11	1.08E-11	-1.31E-11	-1.50E-05
8.27E-07	4.26E-02	4.33E-02	2.25E+00	2.18E-10	1.03E-11	2.14E-09	2.58E-03
7.44E-07	4.21E-02	4.26E-02	5.00E-01	5.46E-10	2.18E-10	1.54E-08	2.07E-02
6.71E-07	4.14E-02	4.21E-02	5.00E-01	8.39E-10	5.46E-10	1.39E-08	2.07E-02
6.77E-07	4.09E-02	4.14E-02	5.00E-01	8.49E-10	8.39E-10	4.76E-10	7.03E-04
6.10E-07	3.46E-02	4.09E-02	2.00E+00	1.40E-09	8.49E-10	6.69E-09	1.10E-02
7.53E-07	2.84E-02	3.46E-02	2.00E+00	1.37E-09	1.40E-09	-3.16E-10	-4.19E-04
8.38E-07	2.03E-02	2.84E-02	3.00E+00	1.74E-09	1.37E-09	4.24E-09	5.06E-03
1.70E-06	1.16E-02	2.03E-02	4.00E+00	1.51E-09	1.74E-09	-2.72E-09	-1.60E-03
					Average:	3.34E-09	4.92E-03

Table A3: AE11-0-25-2150-L Release Rate

AE11							
f_{12C}	**mtj (g)**	**mtj-1 (g)**	**t-tj-1(hr)**	**Xtj (moles)**	**Xtj-1 (moles)**	**R' (mol/g hr)**	**NR' ^{12}C**
1.00E+00	0.00E+00	0.00E+00	0.00E+00	0.00E+00	0.00E+00	0.00E+00	0.00E+00
1.00E+00	6.11E-02	6.13E-02	7.50E-01	1.87E-05	9.44E-06	2.01E-04	2.01E-04
1.00E+00	6.09E-02	6.11E-02	1.00E+00	3.08E-05	1.87E-05	1.99E-04	1.99E-04
1.00E+00	6.08E-02	6.09E-02	1.00E+00	4.06E-05	3.08E-05	1.60E-04	1.60E-04
1.00E+00	6.05E-02	6.08E-02	2.25E+00	6.63E-05	4.06E-05	1.88E-04	1.88E-04
1.00E+00	6.04E-02	6.05E-02	5.00E-01	7.58E-05	6.63E-05	3.15E-04	3.15E-04
1.00E+00	6.03E-02	6.04E-02	5.00E-01	8.32E-05	7.58E-05	2.46E-04	2.46E-04
1.00E+00	6.02E-02	6.03E-02	5.00E-01	8.90E-05	8.32E-05	1.92E-04	1.92E-04
1.00E+00	6.00E-02	6.02E-02	2.00E+00	1.11E-04	8.90E-05	1.81E-04	1.81E-04
1.00E+00	5.97E-02	6.00E-02	2.00E+00	1.30E-04	1.11E-04	1.61E-04	1.61E-04
1.00E+00	5.94E-02	5.97E-02	3.00E+00	1.59E-04	1.30E-04	1.63E-04	1.63E-04
1.00E+00	5.90E-02	5.94E-02	4.00E+00	1.93E-04	1.59E-04	1.41E-04	1.41E-04
					Average:	1.79E-04	1.79E-04
f_{14C}	**mtj (g)**	**mtj-1 (g)**	**t-tj-1 (hr)**	**Xtj (moles)**	**Xtj-1 (moles)**	**R' (mol/g hr)**	**NR' ^{14}C**
	0.00E+00	0.00E+00	0.00E+00	0.00E+00	0.00E+00	0.00E+00	0.00E+00
4.59E-07	6.11E-02	6.13E-02	7.50E-01	1.78E-11	0.00E+00	3.87E-10	8.42E-04
4.62E-07	6.09E-02	6.11E-02	1.00E+00	1.04E-11	1.78E-11	-1.21E-10	-2.63E-04
4.61E-07	6.08E-02	6.09E-02	1.00E+00	1.77E-11	1.04E-11	1.21E-10	2.62E-04
4.49E-07	6.05E-02	6.08E-02	2.25E+00	9.22E-11	1.77E-11	5.44E-10	1.21E-03
4.52E-07	6.04E-02	6.05E-02	5.00E-01	7.81E-11	9.22E-11	-4.64E-10	-1.03E-03
4.46E-07	6.03E-02	6.04E-02	5.00E-01	1.11E-10	7.81E-11	1.10E-09	2.46E-03
4.47E-07	6.02E-02	6.03E-02	5.00E-01	1.12E-10	1.11E-10	3.16E-11	7.07E-05
4.40E-07	6.00E-02	6.02E-02	2.00E+00	1.55E-10	1.12E-10	3.56E-10	8.08E-04
4.38E-07	5.97E-02	6.00E-02	2.00E+00	1.74E-10	1.55E-10	1.60E-10	3.65E-04
4.38E-07	5.94E-02	5.97E-02	3.00E+00	1.86E-10	1.74E-10	6.69E-11	1.53E-04
4.36E-07	5.90E-02	5.94E-02	4.00E+00	2.11E-10	1.86E-10	1.03E-10	2.36E-04
					Average:	1.90E-10	4.27E-04

Table A4: AE12-0-25-2150-L Release Rate

AE12							
f_{12C}	**m_{tj} (g)**	**m_{tj-1} (g)**	**t-t_{j-1}(hr)**	**X_{tj} (moles)**	**X_{tj-1} (moles)**	**R' (mol/g hr)**	**NR' ^{12}C**
1.00E+00	7.31E-02			0.00E+00			
1.00E+00	7.28E-02	7.31E-02	7.50E-01	2.28E-05	1.35E-05	1.71E-04	1.71E-04
1.00E+00	7.28E-02	7.28E-02	1.00E+00	2.89E-05	2.28E-05	8.39E-05	8.39E-05
1.00E+00	7.25E-02	7.28E-02	1.00E+00	4.59E-05	2.89E-05	2.34E-04	2.34E-04
1.00E+00	7.23E-02	7.25E-02	2.25E+00	6.98E-05	4.59E-05	1.46E-04	1.46E-04
1.00E+00	7.22E-02	7.23E-02	5.00E-01	7.68E-05	6.98E-05	1.96E-04	1.96E-04
1.00E+00	7.21E-02	7.22E-02	5.00E-01	8.51E-05	7.68E-05	2.29E-04	2.29E-04
1.00E+00	7.20E-02	7.21E-02	5.00E-01	9.09E-05	8.51E-05	1.62E-04	1.62E-04
1.00E+00	7.18E-02	7.20E-02	2.00E+00	1.12E-04	9.09E-05	1.49E-04	1.49E-04
1.00E+00	7.15E-02	7.18E-02	2.00E+00	1.32E-04	1.12E-04	1.37E-04	1.37E-04
1.00E+00	7.12E-02	7.15E-02	3.00E+00	1.61E-04	1.32E-04	1.35E-04	1.35E-04
1.00E+00	7.09E-02	7.12E-02	4.00E+00	1.86E-04	1.61E-04	8.68E-05	8.68E-05
					Average:	1.57E-04	1.57E-04
f_{14C}	**m_{tj} (g)**	**m_{tj-1} (g)**	**t-t_{j-1} (hr)**	**X_{tj} (moles)**	**X_{tj-1} (moles)**	**R' (mol/g hr)**	**NR' ^{14}C**
0.00E+00	7.31E-02		0.00E+00	0.00E+00			
3.26E-07	7.28E-02	7.31E-02	7.50E-01	2.56E-12	0.00E+00	4.67E-11	1.43E-04
3.26E-07	7.28E-02	7.28E-02	1.00E+00	6.56E-12	2.56E-12	5.49E-11	1.69E-04
3.26E-07	7.25E-02	7.28E-02	1.00E+00	1.11E-11	6.56E-12	6.30E-11	1.93E-04
3.26E-07	7.23E-02	7.25E-02	2.25E+00	1.92E-11	1.11E-11	4.94E-11	1.52E-04
3.26E-07	7.22E-02	7.23E-02	5.00E-01	2.28E-11	1.92E-11	9.92E-11	3.04E-04
3.26E-07	7.21E-02	7.22E-02	5.00E-01	2.66E-11	2.28E-11	1.04E-10	3.20E-04
3.25E-07	7.20E-02	7.21E-02	5.00E-01	3.03E-11	2.66E-11	1.03E-10	3.17E-04
3.25E-07	7.18E-02	7.20E-02	2.00E+00	4.06E-11	3.03E-11	7.16E-11	2.21E-04
3.25E-07	7.15E-02	7.18E-02	2.00E+00	4.52E-11	4.06E-11	3.17E-11	9.74E-05
3.25E-07	7.12E-02	7.15E-02	3.00E+00	5.75E-11	4.52E-11	5.75E-11	1.77E-04
3.26E-07	7.09E-02	7.12E-02	4.00E+00	6.01E-11	5.75E-11	9.02E-12	2.77E-05
					Average:	6.28E-11	1.93E-04

Table A5: AE3R-5-18-2150 Release Rate

AE3R							
f_{12C}	**m_{tj} (g)**	**m_{tj-1} (g)**	**t-t_{j-1}(hr)**	**X_{tj} (moles)**	**X_{tj-1} (moles)**	**R' (mol/g hr)**	**NR' ^{12}C**
1.00E+00	1.26E-01		0.00E+00	0.00E+00			
1.00E+00	1.25E-01	1.26E-01	7.50E-01	3.29E-05	1.46E-05	1.94E-04	1.94E-04
1.00E+00	1.25E-01	1.25E-01	1.00E+00	5.56E-05	3.29E-05	1.82E-04	1.82E-04
1.00E+00	1.25E-01	1.25E-01	1.00E+00	7.26E-05	5.56E-05	1.36E-04	1.36E-04
1.00E+00	1.24E-01	1.25E-01	2.25E+00	1.15E-04	7.26E-05	1.52E-04	1.52E-04
1.00E+00	1.24E-01	1.24E-01	5.00E-01	1.46E-04	1.15E-04	4.97E-04	4.97E-04
1.00E+00	1.23E-01	1.24E-01	5.00E-01	2.12E-04	1.46E-04	1.07E-03	1.07E-03
1.00E+00	1.22E-01	1.23E-01	5.00E-01	2.90E-04	2.12E-04	1.27E-03	1.27E-03
1.00E+00	1.17E-01	1.22E-01	2.00E+00	7.09E-04	2.90E-04	1.71E-03	1.71E-03
1.00E+00	1.10E-01	1.17E-01	2.00E+00	1.34E-03	7.09E-04	2.70E-03	2.70E-03
1.00E+00	9.52E-02	1.10E-01	3.00E+00	2.54E-03	1.34E-03	3.65E-03	3.65E-03
1.00E+00	9.26E-02	9.52E-02	4.00E+00	2.76E-03	2.54E-03	5.59E-04	5.59E-04
					Average:	1.10E-03	1.10E-03
f_{14C}	**m_{tj} (g)**	**m_{tj-1} (g)**	**t-t_{j-1} (hr)**	**X_{tj} (moles)**	**X_{tj-1} (moles)**	**R' (mol/g hr)**	**NR' ^{14}C**
0.00E+00	1.26E-01		0.00E+00	0.00E+00			
2.05E-06	1.25E-01	1.26E-01	7.50E-01	5.93E-12	0.00E+00	6.29E-11	3.07E-05
2.06E-06	1.25E-01	1.25E-01	1.00E+00	1.42E-11	5.93E-12	6.61E-11	3.22E-05
2.06E-06	1.25E-01	1.25E-01	1.00E+00	2.00E-11	1.42E-11	4.64E-11	2.25E-05
2.02E-06	1.24E-01	1.25E-01	2.25E+00	5.11E-10	2.00E-11	1.75E-09	8.66E-04
1.97E-06	1.24E-01	1.24E-01	5.00E-01	1.11E-09	5.11E-10	9.68E-09	4.92E-03
1.93E-06	1.23E-01	1.24E-01	5.00E-01	1.58E-09	1.11E-09	7.59E-09	3.93E-03
1.90E-06	1.22E-01	1.23E-01	5.00E-01	2.09E-09	1.58E-09	8.27E-09	4.35E-03
1.83E-06	1.17E-01	1.22E-01	2.00E+00	3.56E-09	2.09E-09	5.98E-09	3.27E-03
1.51E-06	1.10E-01	1.17E-01	2.00E+00	7.60E-09	3.56E-09	1.73E-08	1.14E-02
9.69E-07	9.52E-02	1.10E-01	3.00E+00	1.37E-08	7.60E-09	1.87E-08	1.93E-02
1.79E-07	9.26E-02	9.52E-02	4.00E+00	2.00E-08	1.37E-08	1.65E-08	9.25E-02
					Average:	7.81E-09	1.28E-02

Table A6: AE4R-5-18-2150 Release Rate

AE4R							
f_{12C}	**m_{tj} (g)**	**m_{tj-1} (g)**	**t-t_{j-1}(hr)**	**X_{tj} (moles)**	**X_{tj-1} (moles)**	**R' (mol/g hr)**	**NR' ^{12}C**
1.00E+00	4.42E-02			0.00E+00			
1.00E+00	4.40E-02	4.42E-02	7.50E-01	2.07E-05	9.97E-06	3.24E-04	3.24E-04
1.00E+00	4.38E-02	4.40E-02	1.00E+00	3.68E-05	2.07E-05	3.67E-04	3.67E-04
1.00E+00	4.35E-02	4.38E-02	1.00E+00	5.54E-05	3.68E-05	4.25E-04	4.25E-04
1.00E+00	4.30E-02	4.35E-02	2.25E+00	1.03E-04	5.54E-05	4.88E-04	4.88E-04
1.00E+00	4.28E-02	4.30E-02	5.00E-01	1.17E-04	1.03E-04	6.43E-04	6.43E-04
1.00E+00	4.26E-02	4.28E-02	5.00E-01	1.31E-04	1.17E-04	6.38E-04	6.38E-04
1.00E+00	4.22E-02	4.26E-02	5.00E-01	1.69E-04	1.31E-04	1.80E-03	1.80E-03
1.00E+00	3.64E-02	4.22E-02	2.00E+00	6.48E-04	1.69E-04	5.68E-03	5.68E-03
1.00E+00	2.95E-02	3.64E-02	2.00E+00	1.22E-03	6.48E-04	7.86E-03	7.86E-03
1.00E+00	1.93E-02	2.95E-02	3.00E+00	2.07E-03	1.22E-03	9.63E-03	9.63E-03
1.00E+00	1.48E-02	1.93E-02	4.00E+00	2.45E-03	2.07E-03	4.85E-03	4.85E-03
					Average:	2.97E-03	2.97E-03
f_{14C}	**m_{tj} (g)**	**m_{tj-1} (g)**	**t-t_{j-1} (hr)**	**X_{tj} (moles)**	**X_{tj-1} (moles)**	**R' (mol/g hr)**	**NR' ^{14}C**
	4.42E-02			0.00E+00			
1.03E-06	4.40E-02	4.42E-02	7.50E-01	2.75E-11	0.00E+00	8.30E-10	8.06E-04
1.01E-06	4.38E-02	4.40E-02	1.00E+00	1.14E-10	2.75E-11	1.96E-09	1.94E-03
9.87E-07	4.35E-02	4.38E-02	1.00E+00	2.16E-10	1.14E-10	2.34E-09	2.38E-03
8.40E-07	4.30E-02	4.35E-02	2.25E+00	7.88E-10	2.16E-10	5.84E-09	6.95E-03
7.60E-07	4.28E-02	4.30E-02	5.00E-01	1.09E-09	7.88E-10	1.38E-08	1.82E-02
6.35E-07	4.26E-02	4.28E-02	5.00E-01	1.54E-09	1.09E-09	2.13E-08	3.35E-02
5.44E-07	4.22E-02	4.26E-02	5.00E-01	1.88E-09	1.54E-09	1.60E-08	2.95E-02
4.47E-07	3.64E-02	4.22E-02	2.00E+00	2.44E-09	1.88E-09	6.58E-09	1.47E-02
3.89E-07	2.95E-02	3.64E-02	2.00E+00	2.84E-09	2.44E-09	5.48E-09	1.41E-02
4.52E-07	1.93E-02	2.95E-02	3.00E+00	3.07E-09	2.84E-09	2.60E-09	5.74E-03
5.25E-07	1.48E-02	1.93E-02	4.00E+00	3.15E-09	3.07E-09	1.03E-09	1.96E-03
					Average:	7.08E-09	1.18E-02

Table A7: AE5-2-18-2150 Release Rate

AE5							
f_{12C}	**m_{tj} (g)**	**m_{tj-1} (g)**	**t-t_{j-1}(hr)**	**X_{tj} (moles)**	**X_{tj-1} (moles)**	**R' (mol/g hr)**	**NR' ^{12}C**
1.00E+00	9.62E-02	0.00E+00		0.00E+00			
1.00E+00	9.53E-02	9.62E-02	7.50E-01	7.74E-05	4.27E-05	4.81E-04	4.81E-04
1.00E+00	9.49E-02	9.53E-02	1.00E+00	1.08E-04	7.74E-05	3.21E-04	3.21E-04
1.00E+00	9.47E-02	9.49E-02	1.00E+00	1.25E-04	1.08E-04	1.80E-04	1.80E-04
1.00E+00	9.42E-02	9.47E-02	2.25E+00	1.70E-04	1.25E-04	2.13E-04	2.13E-04
1.00E+00	9.35E-02	9.42E-02	5.00E-01	2.28E-04	1.70E-04	1.22E-03	1.22E-03
1.00E+00	9.27E-02	9.35E-02	5.00E-01	2.96E-04	2.28E-04	1.45E-03	1.45E-03
1.00E+00	9.19E-02	9.27E-02	5.00E-01	3.60E-04	2.96E-04	1.40E-03	1.40E-03
1.00E+00	8.86E-02	9.19E-02	2.00E+00	6.32E-04	3.60E-04	1.48E-03	1.48E-03
1.00E+00	8.09E-02	8.86E-02	2.00E+00	1.27E-03	6.32E-04	3.62E-03	3.62E-03
1.00E+00	7.47E-02	8.09E-02	3.00E+00	1.80E-03	1.27E-03	2.15E-03	2.15E-03
1.00E+00	7.30E-02	7.47E-02	4.00E+00	1.94E-03	1.80E-03	4.74E-04	4.74E-04
					Average:	1.18E-03	1.18E-03
f_{14C}	**m_{tj} (g)**	**m_{tj-1} (g)**	**t-t_{j-1} (hr)**	**X_{tj} (moles)**	**X_{tj-1} (moles)**	**R' (mol/g hr)**	**NR' ^{14}C**
	9.62E-02			0.00E+00			
1.26E-07	9.53E-02	9.62E-02	7.50E-01	-1.08E-12	0.00E+00	-1.50E-11	-1.19E-04
1.27E-07	9.49E-02	9.53E-02	1.00E+00	-1.26E-12	-1.08E-12	-1.87E-12	-1.48E-05
1.27E-07	9.47E-02	9.49E-02	1.00E+00	-1.93E-12	-1.26E-12	-7.09E-12	-5.57E-05
1.27E-07	9.42E-02	9.47E-02	2.25E+00	3.28E-12	-1.93E-12	2.45E-11	1.92E-04
1.26E-07	9.35E-02	9.42E-02	5.00E-01	1.72E-11	3.28E-12	2.97E-10	2.35E-03
1.12E-07	9.27E-02	9.35E-02	5.00E-01	1.37E-10	1.72E-11	2.55E-09	2.28E-02
9.02E-08	9.19E-02	9.27E-02	5.00E-01	3.12E-10	1.37E-10	3.78E-09	4.19E-02
4.56E-08	8.86E-02	9.19E-02	2.00E+00	6.65E-10	3.12E-10	1.92E-09	4.21E-02
4.09E-08	8.09E-02	8.86E-02	2.00E+00	7.26E-10	6.65E-10	3.44E-10	8.41E-03
3.49E-08	7.47E-02	8.09E-02	3.00E+00	7.85E-10	7.26E-10	2.44E-10	6.99E-03
3.24E-08	7.30E-02	7.47E-02	4.00E+00	8.04E-10	7.85E-10	6.61E-11	2.04E-03
					Average:	8.37E-10	1.15E-02

Table A8: AE6-2-18-2150 Release Rate

AE6							
f_{12C}	m_{tj} (g)	m_{tj-1} (g)	$t\text{-}t_{j-1}$(hr)	X_{tj} (moles)	X_{tj-1} (moles)	R' (mol/g hr)	NR' ^{12}C
1.00E+00	9.15E-02	0.00E+00		0.00E+00			
1.00E+00	9.05E-02	9.15E-02	7.50E-01	7.95E-05	3.98E-05	5.78E-04	5.78E-04
1.00E+00	9.01E-02	9.05E-02	1.00E+00	1.19E-04	7.95E-05	4.36E-04	4.36E-04
1.00E+00	8.96E-02	9.01E-02	1.00E+00	1.58E-04	1.19E-04	4.36E-04	4.36E-04
1.00E+00	8.91E-02	8.96E-02	2.25E+00	1.97E-04	1.58E-04	1.94E-04	1.94E-04
1.00E+00	8.87E-02	8.91E-02	5.00E-01	2.36E-04	1.97E-04	8.74E-04	8.74E-04
1.00E+00	8.82E-02	8.87E-02	5.00E-01	2.75E-04	2.36E-04	8.75E-04	8.75E-04
1.00E+00	8.77E-02	8.82E-02	5.00E-01	3.14E-04	2.75E-04	8.75E-04	8.75E-04
1.00E+00	8.73E-02	8.77E-02	2.00E+00	3.52E-04	3.14E-04	2.19E-04	2.19E-04
1.00E+00	8.68E-02	8.73E-02	2.00E+00	3.90E-04	3.52E-04	2.19E-04	2.19E-04
1.00E+00	8.64E-02	8.68E-02	3.00E+00	4.28E-04	3.90E-04	1.46E-04	1.46E-04
1.00E+00	8.59E-02	8.64E-02	4.00E+00	4.66E-04	4.28E-04	1.10E-04	1.10E-04
					Average:	4.51E-04	4.51E-04
f_{14C}	m_{tj} (g)	m_{tj-1} (g)	$t\text{-}t_{j-1}$ (hr)	X_{tj} (moles)	X_{tj-1} (moles)	R' (mol/g hr)	NR' ^{14}C
	9.15E-02			0.00E+00			
7.62E-08	9.05E-02	9.15E-02	7.50E-01	3.11E-13	0.00E+00	4.53E-12	5.95E-05
7.70E-08	9.01E-02	9.05E-02	1.00E+00	-2.52E-12	3.11E-13	-3.12E-11	-4.06E-04
7.72E-08	8.96E-02	9.01E-02	1.00E+00	-1.04E-12	-2.52E-12	1.64E-11	2.12E-04
7.74E-08	8.91E-02	8.96E-02	2.25E+00	5.20E-13	-1.04E-12	7.75E-12	1.00E-04
7.77E-08	8.87E-02	8.91E-02	5.00E-01	1.02E-12	5.20E-13	1.13E-11	1.45E-04
7.68E-08	8.82E-02	8.87E-02	5.00E-01	1.10E-11	1.02E-12	2.24E-10	2.92E-03
7.07E-08	8.77E-02	8.82E-02	5.00E-01	5.82E-11	1.10E-11	1.07E-09	1.51E-02
4.56E-08	8.73E-02	8.77E-02	2.00E+00	2.43E-10	5.82E-11	1.06E-09	2.32E-02
3.50E-08	8.68E-02	8.73E-02	2.00E+00	3.22E-10	2.43E-10	4.50E-10	1.29E-02
2.63E-08	8.64E-02	8.68E-02	3.00E+00	3.86E-10	3.22E-10	2.45E-10	9.31E-03
2.64E-08	8.59E-02	8.64E-02	4.00E+00	3.86E-10	3.86E-10	1.22E-12	4.63E-05
					Average:	2.78E-10	5.77E-03

Table A9: AE15R-2-25-2150-H Release Rate

AE15R							
f_{12C}	**m_{tj} (g)**	**m_{tj-1} (g)**	**t-t_{j-1}(hr)**	**X_{tj} (moles)**	**X_{tj-1} (moles)**	**R' (mol/g hr)**	**NR' ^{12}C**
1.00E+00	2.96E-02	0.00E+00		0.00E+00			
1.00E+00	2.95E-02	2.96E-02	7.50E-01	9.56E-06	3.20E-06	2.86E-04	2.86E-04
1.00E+00	2.93E-02	2.95E-02	1.00E+00	2.14E-05	9.56E-06	4.01E-04	4.01E-04
1.00E+00	2.92E-02	2.93E-02	1.00E+00	3.32E-05	2.14E-05	4.03E-04	4.03E-04
1.00E+00	2.88E-02	2.92E-02	2.25E+00	6.63E-05	3.32E-05	5.03E-04	5.03E-04
1.00E+00	2.87E-02	2.88E-02	5.00E-01	7.62E-05	6.63E-05	6.93E-04	6.93E-04
1.00E+00	2.86E-02	2.87E-02	5.00E-01	8.46E-05	7.62E-05	5.84E-04	5.84E-04
1.00E+00	2.85E-02	2.86E-02	5.00E-01	9.38E-05	8.46E-05	6.41E-04	6.41E-04
1.00E+00	2.80E-02	2.85E-02	2.00E+00	1.37E-04	9.38E-05	7.65E-04	7.65E-04
1.00E+00	2.73E-02	2.80E-02	2.00E+00	1.91E-04	1.37E-04	9.59E-04	9.59E-04
1.00E+00	2.62E-02	2.73E-02	3.00E+00	2.80E-04	1.91E-04	1.09E-03	1.09E-03
1.00E+00	2.57E-02	2.62E-02	4.00E+00	3.23E-04	2.80E-04	4.11E-04	4.11E-04
					Average:	6.12E-04	6.12E-04
f_{14C}	**m_{tj} (g)**	**m_{tj-1} (g)**	**t-t_{j-1} (hr)**	**X_{tj} (moles)**	**X_{tj-1} (moles)**	**R' (mol/g hr)**	**NR' ^{14}C**
	2.96E-02			0.00E+00			
3.74E-07	2.95E-02	2.96E-02	7.50E-01	-7.84E-13	0.00E+00	-3.53E-11	-9.43E-05
3.76E-07	2.93E-02	2.95E-02	1.00E+00	-1.51E-12	-7.84E-13	-2.47E-11	-6.55E-05
3.79E-07	2.92E-02	2.93E-02	1.00E+00	-2.34E-12	-1.51E-12	-2.83E-11	-7.48E-05
3.82E-07	2.88E-02	2.92E-02	2.25E+00	1.07E-12	-2.34E-12	5.19E-11	1.36E-04
3.81E-07	2.87E-02	2.88E-02	5.00E-01	9.36E-12	1.07E-12	5.76E-10	1.51E-03
3.69E-07	2.86E-02	2.87E-02	5.00E-01	3.94E-11	9.36E-12	2.09E-09	5.67E-03
3.61E-07	2.85E-02	2.86E-02	5.00E-01	6.13E-11	3.94E-11	1.53E-09	4.25E-03
3.09E-07	2.80E-02	2.85E-02	2.00E+00	1.99E-10	6.13E-11	2.41E-09	7.79E-03
2.44E-07	2.73E-02	2.80E-02	2.00E+00	3.63E-10	1.99E-10	2.94E-09	1.20E-02
1.25E-07	2.62E-02	2.73E-02	3.00E+00	6.45E-10	3.63E-10	3.44E-09	2.75E-02
1.01E-07	2.57E-02	2.62E-02	4.00E+00	7.01E-10	6.45E-10	5.37E-10	5.30E-03
					Average:	1.23E-09	5.81E-03

Table A10: AE16-2-25-2150-L Release Rate

AE16							
f_{12C}	**m_{tj} (g)**	**m_{tj-1} (g)**	**$t\text{-}t_{j-1}$(hr)**	**X_{tj} (moles)**	**X_{tj-1} (moles)**	**R' (mol/g hr)**	**NR' ^{12}C**
1.00E+00	1.82E-02	0.00E+00		0.00E+00			
1.00E+00	1.81E-02	1.82E-02	7.50E-01	1.10E-05	4.27E-06	4.96E-04	4.96E-04
1.00E+00	1.79E-02	1.81E-02	1.00E+00	2.35E-05	1.10E-05	6.91E-04	6.91E-04
1.00E+00	1.78E-02	1.79E-02	1.00E+00	3.51E-05	2.35E-05	6.49E-04	6.49E-04
1.00E+00	1.73E-02	1.78E-02	2.25E+00	7.29E-05	3.51E-05	9.44E-04	9.44E-04
1.00E+00	1.70E-02	1.73E-02	5.00E-01	1.04E-04	7.29E-05	3.56E-03	3.56E-03
1.00E+00	1.64E-02	1.70E-02	5.00E-01	1.49E-04	1.04E-04	5.31E-03	5.31E-03
1.00E+00	1.62E-02	1.64E-02	5.00E-01	1.66E-04	1.49E-04	2.16E-03	2.16E-03
1.00E+00	1.57E-02	1.62E-02	2.00E+00	2.11E-04	1.66E-04	1.37E-03	1.37E-03
1.00E+00	1.51E-02	1.57E-02	2.00E+00	2.56E-04	2.11E-04	1.45E-03	1.45E-03
1.00E+00	1.43E-02	1.51E-02	3.00E+00	3.27E-04	2.56E-04	1.56E-03	1.56E-03
1.00E+00	1.37E-02	1.43E-02	4.00E+00	3.79E-04	3.27E-04	9.10E-04	9.10E-04
					Average:	1.74E-03	1.74E-03
f_{14C}	**m_{tj} (g)**	**m_{tj-1} (g)**	**$t\text{-}t_{j-1}$ (hr)**	**X_{tj} (moles)**	**X_{tj-1} (moles)**	**R' (mol/g hr)**	**NR' ^{14}C**
	1.82E-02			0.00E+00			
3.71E-07	1.81E-02	1.82E-02	7.50E-01	-1.06E-12	0.00E+00	-7.73E-11	-2.08E-04
3.74E-07	1.79E-02	1.81E-02	1.00E+00	-1.05E-12	-1.06E-12	4.44E-13	1.19E-06
3.78E-07	1.78E-02	1.79E-02	1.00E+00	-1.86E-12	-1.05E-12	-4.55E-11	-1.20E-04
3.87E-07	1.73E-02	1.78E-02	2.25E+00	-9.64E-13	-1.86E-12	2.25E-11	5.81E-05
3.78E-07	1.70E-02	1.73E-02	5.00E-01	2.37E-11	-9.64E-13	2.85E-09	7.55E-03
3.14E-07	1.64E-02	1.70E-02	5.00E-01	1.28E-10	2.37E-11	1.23E-08	3.93E-02
2.90E-07	1.62E-02	1.64E-02	5.00E-01	1.66E-10	1.28E-10	4.58E-09	1.58E-02
2.40E-07	1.57E-02	1.62E-02	2.00E+00	2.43E-10	1.66E-10	2.39E-09	9.95E-03
1.59E-07	1.51E-02	1.57E-02	2.00E+00	3.57E-10	2.43E-10	3.63E-09	2.29E-02
5.07E-08	1.43E-02	1.51E-02	3.00E+00	4.97E-10	3.57E-10	3.08E-09	6.07E-02
3.78E-09	1.37E-02	1.43E-02	4.00E+00	5.53E-10	4.97E-10	9.79E-10	2.59E-01
					Average:	2.70E-09	3.77E-02

Table A11: AE7-2-18-2300 Release Rate

AE7							
f_{12C}	**m_{tj} (g)**	**m_{tj-1} (g)**	**t-t_{j-1}(hr)**	**X_{tj} (moles)**	**X_{tj-1} (moles)**	**R' (mol/g hr)**	**NR' ^{12}C**
1.00E+00	7.24E-02	0.00E+00	0.00E+00	0.00E+00			
1.00E+00	7.19E-02	7.24E-02	1.50E+00	4.54E-05	1.17E-05	3.10E-04	3.10E-04
1.00E+00	7.16E-02	7.19E-02	1.00E+00	6.34E-05	4.54E-05	2.51E-04	2.51E-04
1.00E+00	7.15E-02	7.16E-02	1.00E+00	7.79E-05	6.34E-05	2.03E-04	2.03E-04
1.00E+00	7.11E-02	7.15E-02	1.50E+00	1.05E-04	7.79E-05	2.49E-04	2.49E-04
1.00E+00	7.10E-02	7.11E-02	5.00E-01	1.16E-04	1.05E-04	3.18E-04	3.18E-04
1.00E+00	7.09E-02	7.10E-02	5.00E-01	1.28E-04	1.16E-04	3.34E-04	3.34E-04
1.00E+00	7.07E-02	7.09E-02	5.00E-01	1.39E-04	1.28E-04	3.21E-04	3.21E-04
1.00E+00	7.02E-02	7.07E-02	2.00E+00	1.85E-04	1.39E-04	3.24E-04	3.24E-04
1.00E+00	6.96E-02	7.02E-02	2.00E+00	2.34E-04	1.85E-04	3.50E-04	3.50E-04
1.00E+00	6.87E-02	6.96E-02	3.00E+00	3.11E-04	2.34E-04	3.69E-04	3.69E-04
1.00E+00	6.80E-02	6.87E-02	4.00E+00	3.64E-04	3.11E-04	1.93E-04	1.93E-04
					Average:	2.93E-04	2.93E-04
f_{14C}	**m_{tj} (g)**	**m_{tj-1} (g)**	**t-t_{j-1} (hr)**	**X_{tj} (moles)**	**X_{tj-1} (moles)**	**R' (mol/g hr)**	**NR' ^{14}C**
	7.24E-02		0.00E+00	0.00E+00			
3.43E-07	7.19E-02	7.24E-02	1.50E+00	2.88E-11	0.00E+00	2.65E-10	7.73E-04
3.38E-07	7.16E-02	7.19E-02	1.00E+00	6.35E-11	2.88E-11	4.84E-10	1.43E-03
3.36E-07	7.15E-02	7.16E-02	1.00E+00	8.18E-11	6.35E-11	2.56E-10	7.62E-04
2.22E-07	7.11E-02	7.15E-02	1.50E+00	7.67E-10	8.18E-11	6.39E-09	2.88E-02
1.54E-07	7.10E-02	7.11E-02	5.00E-01	1.17E-09	7.67E-10	1.13E-08	7.32E-02
1.18E-07	7.09E-02	7.10E-02	5.00E-01	1.38E-09	1.17E-09	6.04E-09	5.12E-02
1.00E-07	7.07E-02	7.09E-02	5.00E-01	1.49E-09	1.38E-09	3.00E-09	2.99E-02
7.13E-08	7.02E-02	7.07E-02	2.00E+00	1.66E-09	1.49E-09	1.23E-09	1.73E-02
5.23E-08	6.96E-02	7.02E-02	2.00E+00	1.78E-09	1.66E-09	8.08E-10	1.55E-02
4.30E-08	6.87E-02	6.96E-02	3.00E+00	1.83E-09	1.78E-09	2.73E-10	6.33E-03
1.82E-08	6.80E-02	6.87E-02	4.00E+00	1.98E-09	1.83E-09	5.21E-10	2.86E-02
					Average:	2.78E-09	2.31E-02

Table A12: AE8-2-18-2300 Release Rate

AE8							
f_{12C}	m_{tj} (g)	m_{tj-1} (g)	$t\text{-}t_{j-1}$(hr)	X_{tj} (moles)	X_{tj-1} (moles)	R' (mol/g hr)	NR' ^{12}C
1.00E+00	4.80E-02	0.00E+00		0.00E+00			
1.00E+00	4.72E-02	4.80E-02	1.50E+00	6.31E-05	2.42E-05	5.41E-04	5.41E-04
1.00E+00	4.71E-02	4.72E-02	1.00E+00	7.89E-05	6.31E-05	3.34E-04	3.34E-04
1.00E+00	4.69E-02	4.71E-02	1.00E+00	9.25E-05	7.89E-05	2.89E-04	2.89E-04
1.00E+00	4.66E-02	4.69E-02	1.50E+00	1.16E-04	9.25E-05	3.37E-04	3.37E-04
1.00E+00	4.65E-02	4.66E-02	5.00E-01	1.25E-04	1.16E-04	3.56E-04	3.56E-04
1.00E+00	4.64E-02	4.65E-02	5.00E-01	1.33E-04	1.25E-04	3.50E-04	3.50E-04
1.00E+00	4.63E-02	4.64E-02	5.00E-01	1.41E-04	1.33E-04	3.50E-04	3.50E-04
1.00E+00	4.59E-02	4.63E-02	2.00E+00	1.74E-04	1.41E-04	3.64E-04	3.64E-04
1.00E+00	4.55E-02	4.59E-02	2.00E+00	2.11E-04	1.74E-04	3.96E-04	3.96E-04
1.00E+00	4.48E-02	4.55E-02	3.00E+00	2.68E-04	2.11E-04	4.21E-04	4.21E-04
1.00E+00	4.42E-02	4.48E-02	4.00E+00	3.17E-04	2.68E-04	2.74E-04	2.74E-04
					Average:	3.65E-04	3.65E-04
f_{14C}	m_{tj} (g)	m_{tj-1} (g)	$t\text{-}t_{j-1}$ (hr)	X_{tj} (moles)	X_{tj-1} (moles)	R' (mol/g hr)	NR' ^{14}C
	4.80E-02			0.00E+00			
1.90E-07	4.72E-02	4.80E-02	1.50E+00	5.60E-12	0.00E+00	7.78E-11	4.10E-04
1.87E-07	4.71E-02	4.72E-02	1.00E+00	2.13E-11	5.60E-12	3.32E-10	1.78E-03
1.87E-07	4.69E-02	4.71E-02	1.00E+00	2.08E-11	2.13E-11	-1.04E-11	-5.53E-05
1.52E-07	4.66E-02	4.69E-02	1.50E+00	1.64E-10	2.08E-11	2.03E-09	1.34E-02
1.30E-07	4.65E-02	4.66E-02	5.00E-01	2.48E-10	1.64E-10	3.62E-09	2.78E-02
1.15E-07	4.64E-02	4.65E-02	5.00E-01	3.07E-10	2.48E-10	2.51E-09	2.18E-02
1.02E-07	4.63E-02	4.64E-02	5.00E-01	3.57E-10	3.07E-10	2.17E-09	2.12E-02
7.93E-08	4.59E-02	4.63E-02	2.00E+00	4.49E-10	3.57E-10	9.93E-10	1.25E-02
7.40E-08	4.55E-02	4.59E-02	2.00E+00	4.72E-10	4.49E-10	2.53E-10	3.42E-03
5.36E-08	4.48E-02	4.55E-02	3.00E+00	5.52E-10	4.72E-10	5.86E-10	1.09E-02
2.22E-08	4.42E-02	4.48E-02	4.00E+00	6.70E-10	5.52E-10	6.60E-10	2.97E-02
					Average:	1.20E-09	1.30E-02

Table A13: AE17-2-5-2300-H Release Rate

AE17							
f_{12C}	**m_{tj} (g)**	**m_{tj-1} (g)**	**t-t_{j-1}(hr)**	**X_{tj} (moles)**	**X_{tj-1} (moles)**	**R' (mol/g hr)**	**NR' ^{12}C**
1.00E+00	5.26E-02	0.00E+00		0.00E+00			
1.00E+00	5.21E-02	5.26E-02	1.50E+00	4.44E-05	1.75E-05	3.40E-04	3.40E-04
1.00E+00	5.19E-02	5.21E-02	1.00E+00	5.84E-05	4.44E-05	2.68E-04	2.68E-04
1.00E+00	5.18E-02	5.19E-02	1.00E+00	7.08E-05	5.84E-05	2.40E-04	2.40E-04
1.00E+00	5.15E-02	5.18E-02	1.50E+00	9.36E-05	7.08E-05	2.93E-04	2.93E-04
1.00E+00	5.14E-02	5.15E-02	5.00E-01	1.01E-04	9.36E-05	2.87E-04	2.87E-04
1.00E+00	5.13E-02	5.14E-02	5.00E-01	1.09E-04	1.01E-04	3.14E-04	3.14E-04
1.00E+00	5.12E-02	5.13E-02	5.00E-01	1.18E-04	1.09E-04	3.68E-04	3.68E-04
1.00E+00	5.05E-02	5.12E-02	2.00E+00	1.77E-04	1.18E-04	5.71E-04	5.71E-04
1.00E+00	4.92E-02	5.05E-02	2.00E+00	2.84E-04	1.77E-04	1.06E-03	1.06E-03
1.00E+00	4.78E-02	4.92E-02	3.00E+00	4.03E-04	2.84E-04	8.09E-04	8.09E-04
1.00E+00	4.71E-02	4.78E-02	4.00E+00	4.55E-04	4.03E-04	2.69E-04	2.69E-04
					Average:	4.38E-04	4.38E-04
f_{14C}	**m_{tj} (g)**	**m_{tj-1} (g)**	**t-t_{j-1} (hr)**	**X_{tj} (moles)**	**X_{tj-1} (moles)**	**R' (mol/g hr)**	**NR' ^{14}C**
	5.26E-02			0.00E+00			
4.38E-07	5.21E-02	5.26E-02	1.50E+00	1.56E-11	0.00E+00	1.98E-10	4.51E-04
4.39E-07	5.19E-02	5.21E-02	1.00E+00	2.06E-11	1.56E-11	9.56E-11	2.18E-04
4.38E-07	5.18E-02	5.19E-02	1.00E+00	2.75E-11	2.06E-11	1.34E-10	3.06E-04
4.36E-07	5.15E-02	5.18E-02	1.50E+00	4.71E-11	2.75E-11	2.53E-10	5.80E-04
4.28E-07	5.14E-02	5.15E-02	5.00E-01	8.48E-11	4.71E-11	1.46E-09	3.42E-03
4.12E-07	5.13E-02	5.14E-02	5.00E-01	1.57E-10	8.48E-11	2.81E-09	6.81E-03
3.99E-07	5.12E-02	5.13E-02	5.00E-01	2.17E-10	1.57E-10	2.33E-09	5.84E-03
3.09E-07	5.05E-02	5.12E-02	2.00E+00	6.15E-10	2.17E-10	3.90E-09	1.26E-02
2.06E-07	4.92E-02	5.05E-02	2.00E+00	1.07E-09	6.15E-10	4.54E-09	2.21E-02
1.02E-07	4.78E-02	4.92E-02	3.00E+00	1.51E-09	1.07E-09	2.97E-09	2.92E-02
5.36E-08	4.71E-02	4.78E-02	4.00E+00	1.71E-09	1.51E-09	1.02E-09	1.89E-02
					Average:	1.79E-09	9.13E-03

Table A14: AE18-2-5-2300-L Release Rate

AE18							
f_{12C}	**m_{tj} (g)**	**m_{tj-1} (g)**	**t-t_{j-1}(hr)**	**X_{tj} (moles)**	**X_{tj-1} (moles)**	**R' (mol/g hr)**	**NR' ^{12}C**
1.00E+00	5.84E-02	0.00E+00		0.00E+00			
1.00E+00	5.76E-02	5.84E-02	1.50E+00	6.56E-05	2.82E-05	4.27E-04	4.27E-04
1.00E+00	5.74E-02	5.76E-02	1.00E+00	8.01E-05	6.56E-05	2.53E-04	2.53E-04
1.00E+00	5.73E-02	5.74E-02	1.00E+00	9.27E-05	8.01E-05	2.19E-04	2.19E-04
1.00E+00	5.70E-02	5.73E-02	1.50E+00	1.15E-04	9.27E-05	2.56E-04	2.56E-04
1.00E+00	5.69E-02	5.70E-02	5.00E-01	1.22E-04	1.15E-04	2.47E-04	2.47E-04
1.00E+00	5.68E-02	5.69E-02	5.00E-01	1.30E-04	1.22E-04	2.87E-04	2.87E-04
1.00E+00	5.67E-02	5.68E-02	5.00E-01	1.39E-04	1.30E-04	3.27E-04	3.27E-04
1.00E+00	5.60E-02	5.67E-02	2.00E+00	1.99E-04	1.39E-04	5.24E-04	5.24E-04
1.00E+00	5.50E-02	5.60E-02	2.00E+00	2.85E-04	1.99E-04	7.74E-04	7.74E-04
1.00E+00	5.35E-02	5.50E-02	3.00E+00	4.08E-04	2.85E-04	7.40E-04	7.40E-04
1.00E+00	5.29E-02	5.35E-02	4.00E+00	4.55E-04	4.08E-04	2.20E-04	2.20E-04
					Average:	3.89E-04	3.89E-04
f_{14C}	**m_{tj} (g)**	**m_{tj-1} (g)**	**t-t_{j-1} (hr)**	**X_{tj} (moles)**	**X_{tj-1} (moles)**	**R' (mol/g hr)**	**NR' ^{14}C**
	5.84E-02			0.00E+00			
3.79E-07	5.76E-02	5.84E-02	1.50E+00	1.63E-11	0.00E+00	1.86E-10	4.90E-04
3.80E-07	5.74E-02	5.76E-02	1.00E+00	1.97E-11	1.63E-11	5.97E-11	1.57E-04
3.81E-07	5.73E-02	5.74E-02	1.00E+00	2.03E-11	1.97E-11	9.41E-12	2.47E-05
3.80E-07	5.70E-02	5.73E-02	1.50E+00	3.20E-11	2.03E-11	1.37E-10	3.60E-04
3.74E-07	5.69E-02	5.70E-02	5.00E-01	6.32E-11	3.20E-11	1.09E-09	2.92E-03
3.49E-07	5.68E-02	5.69E-02	5.00E-01	1.82E-10	6.32E-11	4.17E-09	1.19E-02
3.45E-07	5.67E-02	5.68E-02	5.00E-01	2.05E-10	1.82E-10	8.32E-10	2.41E-03
2.62E-07	5.60E-02	5.67E-02	2.00E+00	6.13E-10	2.05E-10	3.59E-09	1.37E-02
1.53E-07	5.50E-02	5.60E-02	2.00E+00	1.13E-09	6.13E-10	4.66E-09	3.04E-02
5.04E-08	5.35E-02	5.50E-02	3.00E+00	1.61E-09	1.13E-09	2.89E-09	5.73E-02
3.47E-08	5.29E-02	5.35E-02	4.00E+00	1.68E-09	1.61E-09	3.34E-10	9.61E-03
					Average:	1.63E-09	1.18E-02

Table A15: AE9-0-18-2300 Release Rate

AE9							
f_{12C}	m_{tj} (g)	m_{tj-1} (g)	$t\text{-}t_{j-1}$(hr)	X_{tj} (moles)	X_{tj-1} (moles)	R' (mol/g hr)	NR' ^{12}C
1.00E+00	5.10E-02	0.00E+00		0.00E+00			
1.00E+00	4.92E-02	5.10E-02	1.50E+00	1.54E-04	4.45E-05	1.42E-03	1.42E-03
1.00E+00	4.88E-02	4.92E-02	1.00E+00	1.84E-04	1.54E-04	6.29E-04	6.29E-04
1.00E+00	4.85E-02	4.88E-02	1.00E+00	2.08E-04	1.84E-04	4.77E-04	4.77E-04
1.00E+00	4.78E-02	4.85E-02	1.50E+00	2.71E-04	2.08E-04	8.64E-04	8.64E-04
1.00E+00	4.64E-02	4.78E-02	5.00E-01	3.86E-04	2.71E-04	4.84E-03	4.84E-03
1.00E+00	4.48E-02	4.64E-02	5.00E-01	5.17E-04	3.86E-04	5.63E-03	5.63E-03
1.00E+00	4.45E-02	4.48E-02	5.00E-01	5.38E-04	5.17E-04	9.51E-04	9.51E-04
1.00E+00	4.40E-02	4.45E-02	2.00E+00	5.82E-04	5.38E-04	4.99E-04	4.99E-04
1.00E+00	4.36E-02	4.40E-02	2.00E+00	6.15E-04	5.82E-04	3.66E-04	3.66E-04
1.00E+00	4.31E-02	4.36E-02	3.00E+00	6.55E-04	6.15E-04	3.11E-04	3.11E-04
1.00E+00	4.23E-02	4.31E-02	4.00E+00	7.27E-04	6.55E-04	4.13E-04	4.13E-04
					Average:	1.49E-03	1.49E-03
f_{14C}	m_{tj} (g)	m_{tj-1} (g)	$t\text{-}t_{j-1}$ (hr)	X_{tj} (moles)	X_{tj-1} (moles)	R' (mol/g hr)	NR' ^{14}C
	5.10E-02			0.00E+00			
8.73E-08	4.92E-02	5.10E-02	1.50E+00	1.10E-12	0.00E+00	1.44E-11	1.65E-04
8.78E-08	4.88E-02	4.92E-02	1.00E+00	1.76E-12	1.10E-12	1.34E-11	1.53E-04
8.91E-08	4.85E-02	4.88E-02	1.00E+00	-1.71E-12	1.76E-12	-7.12E-11	-7.99E-04
8.95E-08	4.78E-02	4.85E-02	1.50E+00	2.44E-12	-1.71E-12	5.70E-11	6.37E-04
9.23E-08	4.64E-02	4.78E-02	5.00E-01	1.82E-12	2.44E-12	-2.58E-11	-2.79E-04
9.53E-08	4.48E-02	4.64E-02	5.00E-01	2.82E-12	1.82E-12	4.30E-11	4.52E-04
9.58E-08	4.45E-02	4.48E-02	5.00E-01	3.14E-12	2.82E-12	1.46E-11	1.52E-04
9.59E-08	4.40E-02	4.45E-02	2.00E+00	7.06E-12	3.14E-12	4.39E-11	4.58E-04
9.50E-08	4.36E-02	4.40E-02	2.00E+00	1.32E-11	7.06E-12	7.03E-11	7.40E-04
9.47E-08	4.31E-02	4.36E-02	3.00E+00	1.81E-11	1.32E-11	3.74E-11	3.95E-04
9.62E-08	4.23E-02	4.31E-02	4.00E+00	1.98E-11	1.81E-11	9.53E-12	9.91E-05
					Average:	1.88E-11	1.98E-04

Table A16: AE10-0-18-2300 Release Rate

AE10							
f_{12C}	**m_{tj} (g)**	**m_{tj-1} (g)**	**t-t_{j-1}(hr)**	**X_{tj} (moles)**	**X_{tj-1} (moles)**	**R' (mol/g hr)**	**NR' ^{12}C**
1.00E+00	4.44E-02	0.00E+00		0.00E+00			
1.00E+00	4.42E-02	4.44E-02	1.50E+00	1.83E-05	3.35E-06	2.24E-04	2.24E-04
1.00E+00	4.40E-02	4.42E-02	1.00E+00	2.97E-05	1.83E-05	2.59E-04	2.59E-04
1.00E+00	4.39E-02	4.40E-02	1.00E+00	4.13E-05	2.97E-05	2.63E-04	2.63E-04
1.00E+00	4.35E-02	4.39E-02	1.50E+00	7.21E-05	4.13E-05	4.69E-04	4.69E-04
1.00E+00	4.28E-02	4.35E-02	5.00E-01	1.31E-04	7.21E-05	2.70E-03	2.70E-03
1.00E+00	4.27E-02	4.28E-02	5.00E-01	1.44E-04	1.31E-04	6.30E-04	6.30E-04
1.00E+00	4.26E-02	4.27E-02	5.00E-01	1.50E-04	1.44E-04	2.70E-04	2.70E-04
1.00E+00	4.23E-02	4.26E-02	2.00E+00	1.71E-04	1.50E-04	2.45E-04	2.45E-04
1.00E+00	4.21E-02	4.23E-02	2.00E+00	1.90E-04	1.71E-04	2.21E-04	2.21E-04
1.00E+00	4.18E-02	4.21E-02	3.00E+00	2.17E-04	1.90E-04	2.15E-04	2.15E-04
1.00E+00	4.14E-02	4.18E-02	4.00E+00	2.49E-04	2.17E-04	1.92E-04	1.92E-04
					Average:	5.17E-04	5.17E-04
f_{14C}	**m_{tj} (g)**	**m_{tj-1} (g)**	**t-t_{j-1} (hr)**	**X_{tj} (moles)**	**X_{tj-1} (moles)**	**R' (mol/g hr)**	**NR' ^{14}C**
	4.44E-02			0.00E+00			
1.35E-07	4.42E-02	4.44E-02	1.50E+00	9.80E-13	0.00E+00	1.47E-11	1.09E-04
1.35E-07	4.40E-02	4.42E-02	1.00E+00	9.36E-13	9.80E-13	-9.90E-13	-7.31E-06
1.37E-07	4.39E-02	4.40E-02	1.00E+00	-2.38E-12	9.36E-13	-7.53E-11	-5.51E-04
1.34E-07	4.35E-02	4.39E-02	1.50E+00	1.03E-11	-2.38E-12	1.92E-10	1.43E-03
1.30E-07	4.28E-02	4.35E-02	5.00E-01	3.57E-11	1.03E-11	1.17E-09	9.01E-03
1.25E-07	4.27E-02	4.28E-02	5.00E-01	5.30E-11	3.57E-11	8.09E-10	6.47E-03
1.24E-07	4.26E-02	4.27E-02	5.00E-01	5.68E-11	5.30E-11	1.78E-10	1.43E-03
1.20E-07	4.23E-02	4.26E-02	2.00E+00	7.52E-11	5.68E-11	2.16E-10	1.80E-03
1.16E-07	4.21E-02	4.23E-02	2.00E+00	9.06E-11	7.52E-11	1.81E-10	1.56E-03
1.14E-07	4.18E-02	4.21E-02	3.00E+00	1.02E-10	9.06E-11	9.26E-11	8.15E-04
1.11E-07	4.14E-02	4.18E-02	4.00E+00	1.16E-10	1.02E-10	8.12E-11	7.33E-04
					Average:	2.60E-10	2.07E-03

Table A17: AE19-0-25-2300-H Release Rate

AE19							
f_{12C}	**m_{tj} (g)**	**m_{tj-1} (g)**	**t-t_{j-1}(hr)**	**X_{tj} (moles)**	**X_{tj-1} (moles)**	**R' (mol/g hr)**	**NR' ^{12}C**
1.00E+00	2.52E-02	0.00E+00		0.00E+00			
1.00E+00	2.49E-02	2.52E-02	1.50E+00	2.57E-05	6.05E-06	5.18E-04	5.18E-04
1.00E+00	2.47E-02	2.49E-02	1.00E+00	3.90E-05	2.57E-05	5.37E-04	5.37E-04
1.00E+00	2.46E-02	2.47E-02	1.00E+00	5.23E-05	3.90E-05	5.38E-04	5.38E-04
1.00E+00	2.42E-02	2.46E-02	1.50E+00	8.42E-05	5.23E-05	8.65E-04	8.65E-04
1.00E+00	2.34E-02	2.42E-02	5.00E-01	1.47E-04	8.42E-05	5.21E-03	5.21E-03
1.00E+00	2.30E-02	2.34E-02	5.00E-01	1.81E-04	1.47E-04	2.85E-03	2.85E-03
1.00E+00	2.29E-02	2.30E-02	5.00E-01	1.93E-04	1.81E-04	1.05E-03	1.05E-03
1.00E+00	2.26E-02	2.29E-02	2.00E+00	2.16E-04	1.93E-04	5.13E-04	5.13E-04
1.00E+00	2.24E-02	2.26E-02	2.00E+00	2.36E-04	2.16E-04	4.35E-04	4.35E-04
1.00E+00	2.20E-02	2.24E-02	3.00E+00	2.63E-04	2.36E-04	4.12E-04	4.12E-04
1.00E+00	2.17E-02	2.20E-02	4.00E+00	2.93E-04	2.63E-04	3.39E-04	3.39E-04
					Average:	1.21E-03	1.21E-03
f_{14C}	**m_{tj} (g)**	**m_{tj-1} (g)**	**t-t_{j-1} (hr)**	**X_{tj} (moles)**	**X_{tj-1} (moles)**	**R' (mol/g hr)**	**NR' ^{14}C**
	2.52E-02			0.00E+00			
4.40E-07	2.49E-02	2.52E-02	1.50E+00	-1.75E-13	0.00E+00	-4.62E-12	-1.05E-05
4.43E-07	2.47E-02	2.49E-02	1.00E+00	9.33E-13	-1.75E-13	4.45E-11	1.00E-04
4.48E-07	2.46E-02	2.47E-02	1.00E+00	-3.55E-12	9.33E-13	-1.81E-10	-4.05E-04
4.53E-07	2.42E-02	2.46E-02	1.50E+00	3.69E-13	-3.55E-12	1.06E-10	2.35E-04
4.67E-07	2.34E-02	2.42E-02	5.00E-01	1.06E-12	3.69E-13	5.74E-11	1.23E-04
4.75E-07	2.30E-02	2.34E-02	5.00E-01	1.41E-12	1.06E-12	2.99E-11	6.30E-05
4.78E-07	2.29E-02	2.30E-02	5.00E-01	2.38E-12	1.41E-12	8.35E-11	1.75E-04
4.82E-07	2.26E-02	2.29E-02	2.00E+00	5.92E-12	2.38E-12	7.75E-11	1.61E-04
4.86E-07	2.24E-02	2.26E-02	2.00E+00	7.82E-12	5.92E-12	4.21E-11	8.66E-05
4.91E-07	2.20E-02	2.24E-02	3.00E+00	1.22E-11	7.82E-12	6.56E-11	1.34E-04
4.98E-07	2.17E-02	2.20E-02	4.00E+00	1.45E-11	1.22E-11	2.57E-11	5.17E-05
					Average:	3.15E-11	6.49E-05

Table A18: AE110-0-25-2300-M Release Rate

AE110							
f_{12C}	**m_{tj} (g)**	**m_{tj-1} (g)**	**$t\text{-}t_{j-1}$(hr)**	**X_{tj} (moles)**	**X_{tj-1} (moles)**	**R' (mol/g hr)**	**NR' ^{12}C**
1.00E+00	3.46E-02	0.00E+00		0.00E+00			
1.00E+00	3.43E-02	3.46E-02	1.50E+00	2.47E-05	6.35E-06	3.53E-04	3.53E-04
1.00E+00	3.42E-02	3.43E-02	1.00E+00	3.57E-05	2.47E-05	3.21E-04	3.21E-04
1.00E+00	3.40E-02	3.42E-02	1.00E+00	4.59E-05	3.57E-05	2.98E-04	2.98E-04
1.00E+00	3.38E-02	3.40E-02	1.50E+00	6.38E-05	4.59E-05	3.50E-04	3.50E-04
1.00E+00	3.38E-02	3.38E-02	5.00E-01	6.94E-05	6.38E-05	3.34E-04	3.34E-04
1.00E+00	3.37E-02	3.38E-02	5.00E-01	7.43E-05	6.94E-05	2.88E-04	2.88E-04
1.00E+00	3.37E-02	3.37E-02	5.00E-01	7.88E-05	7.43E-05	2.71E-04	2.71E-04
1.00E+00	3.34E-02	3.37E-02	2.00E+00	9.63E-05	7.88E-05	2.59E-04	2.59E-04
1.00E+00	3.32E-02	3.34E-02	2.00E+00	1.13E-04	9.63E-05	2.43E-04	2.43E-04
1.00E+00	3.30E-02	3.32E-02	3.00E+00	1.36E-04	1.13E-04	2.31E-04	2.31E-04
1.00E+00	3.26E-02	3.30E-02	4.00E+00	1.64E-04	1.36E-04	2.14E-04	2.14E-04
					Average:	2.88E-04	2.88E-04
f_{14C}	**m_{tj} (g)**	**m_{tj-1} (g)**	**$t\text{-}t_{j-1}$ (hr)**	**X_{tj} (moles)**	**X_{tj-1} (moles)**	**R' (mol/g hr)**	**NR' ^{14}C**
	3.46E-02			0.00E+00			
3.74E-07	3.43E-02	3.46E-02	1.50E+00	-9.66E-13	0.00E+00	-1.86E-11	-4.98E-05
3.75E-07	3.42E-02	3.43E-02	1.00E+00	-9.43E-13	-9.66E-13	6.57E-13	1.75E-06
3.76E-07	3.40E-02	3.42E-02	1.00E+00	6.71E-13	-9.43E-13	4.72E-11	1.26E-04
3.78E-07	3.38E-02	3.40E-02	1.50E+00	2.08E-12	6.71E-13	2.75E-11	7.28E-05
3.78E-07	3.38E-02	3.38E-02	5.00E-01	3.85E-12	2.08E-12	1.05E-10	2.78E-04
3.78E-07	3.37E-02	3.38E-02	5.00E-01	6.51E-12	3.85E-12	1.57E-10	4.17E-04
3.78E-07	3.37E-02	3.37E-02	5.00E-01	7.93E-12	6.51E-12	8.44E-11	2.23E-04
3.77E-07	3.34E-02	3.37E-02	2.00E+00	1.59E-11	7.93E-12	1.18E-10	3.14E-04
3.77E-07	3.32E-02	3.34E-02	2.00E+00	2.18E-11	1.59E-11	8.88E-11	2.35E-04
3.76E-07	3.30E-02	3.32E-02	3.00E+00	3.44E-11	2.18E-11	1.26E-10	3.36E-04
3.76E-07	3.26E-02	3.30E-02	4.00E+00	4.47E-11	3.44E-11	7.81E-11	2.08E-04
					Average:	7.41E-11	1.96E-04

Appendix B: Equipment and Supply List

EQUIPMENT USED:

- Mellen SD Series Split Furnace
    - Model Number: SD16-3.125X12H-1Z
    - Serial Number: 04075530
    - Maximum Temperature: 1600 °C
  - Mellen Control Box
    - Model Number: PS400-240-25CLT-P-B-OT
    - Serial Number: 04075530
    - UDC 100L Limit Controller
    - UDC 3000 Temperature Controller
- Cooling Fans
  - Honeywell Air Circulator, Turbo Force Power
  - Model HT-900 Series
  - Part No. 30LBT900UA0
- Graphite Sample Placement Device/Holder for Graphite Samples
  - Constructed from the following pieces:
    - Alumina Rod
      - ¼" diameter, 27" length, double bore 1/16" holes
    - Alumina "Dee Tube"
      - For 1.75" inner diameter tubes, 5" length
    - High Temperature Zirconia Adhesive
      - Cotronics corporation
      - 904 Zirconia Ultra Hi-Temp Ceramic Adhesive
      - Use up to 2200°C
- Alumina Tubes for Furnaces
  - Main furnace
    - 2" OD, 1.75" ID, 42" length and 40" length
  - Oxidizer furnace
    - 1" OD, 0.75" ID, 41" length
- End Caps
  - Custom made previously at the Idaho National Laboratory
  - Main Furnace end caps fit 2 in. O.D. tubes
  - Oxidizer Furnace end caps fit 1 in. O.D. tubes
  - Assumed to be stainless steel
  - VITON O-rings size 328
- Non-hardening Clay
  - Purchased from local craft store
- PTFE Thread Tape
  - Blue Monster
  - ½" x 1,429"
- Mass Flow Controllers
  - MKS Type M100B MFC
    - Calibrated for: O_2

        - Range: 1000 sccm
        - Model Number: M100B01513CS1BV
        - Serial Number: 021660381
    - MKS Type M100B MFC
        - Calibrated for: Ar
        - Range: 1000 sccm
        - Model Number: M100B00413CS1BV
        - Serial Number: 021689944
    - Maximum Inlet Pressure: 150 psig
    - Control Range: 2% to 100% of Full Scale
    - Accuracy: ± 1% of Full Scale
    - Repeatability: ± 0.2% of Full Scale
    - Resolution: ± 0.1% of Full Scale
- Thermocouples
    - Custom made by Idaho Laboratories Corporation
        - Type K, 3 ft., ¼" diameter rod, mini male plug
        - (4) Type K, 1 ft., 1/16" diameter, mini male plug
        - Type S, 30" length, 1/16" diameter, mini male plug
            - 062-S(010)-PY10%RH/I600-H-UNG-30" IMM
            - 12" length of PT10%RH sheath at the hot tip
            - 18" length of I600 sheath
            - Ungrounded junction
            - Transition with spring relief and 36" of Teflon leads
            - High temperature epoxy
- Thermometers
        - Bontron BT-811
            - Resolution: K-type
                - 0.1°C below 1000°C
                - 1°C above 1000°C
            - Accuracy: K-type, not including error of the thermocouple
                - ± 0.1% reading + 0.7°C (-100°C ~ 1372°C)
            - Measurement Range: K-type
                - -200°C ~ 1372°C
            - Sample Rate: 1 time/sec
        - Bontron BT-727D
            - RS-232 Data Logger
            - 2 channel, hand held
            - Serial number: 09021989
            - Range:
                - K-type: -100°C ~ 1300°C
                - S-type: 0°C ~ 1700°C
            - Accuracy: (18°C ~ 28°C ambient)
                - K-type: ± (0.1% rdg + 0.7°C)
                - S-type: ± (0.1% rdg + 2°C)
- Oxidizer Furnace
    - Lindberg/Blue M Tube Furnace
        - Model Number: 55332

        - Serial Number: 937408
        - Maximum Temperature: 1200 °C
    - Controller
        - Model Number: 58114
        - Serial Number: Z10C-152808-ZC
- Copper Oxide
    - Perkin Elmer Instruments
    - Wire Form
    - Material Number: 0240-1092
    - Lot Number: H18161
    - Date: 07/12/10
- Copper Mesh
    - TWP Inc.
    - 30 mesh copper 0.012 diameter wire
    - Part #: 030X030C0120W36T
- Collection/Washing Bottles
    - Chemglass 125 mL 3-neck European Style Flasks
    - 24/40-14/20 Joints
    - CG-1570-04
- Rubber Laboratory Stoppers
    - Fisherbrand
        - One-hole rubber stoppers
            - Size #5, hole size 5mm
            - Size #0, hole size 3mm
        - Solid rubber stopper
            - Size #0
- Stopper/Tubing connector
    - Bel-Art Scienceware Reducing Quick-Disconnects
        - Fits tubing I.D. 1/8 in. – 1/4 in.
- Disposable Syringes
    - Excel Int.
        - Without needle
        - 5 mL
        - Ref 26231
        - Model 5mlSlipTip
        - 5mlwo120202
- Sodium Hydroxide (NaOH)
    - Acros Organics
    - Reagent ACS
    - Pellets 97+%
    - Used to make 4 M solutions
- Graduated Cylinder
    - PUREX® USA
    - 50 mL
    - No. 3075
    - TC 20°C
- “Rubber” Tubing

    - Fisherbrand 3/16” ID x 1/16” wall, clear
- Glass Tubing
    - Standard Laboratory Glass Tubing
        - 5 mm OD, ~3 mm ID
- Diffusers
    - PETCO Bubbling Airstone
- Luer lock adapter
    - Cole-Parmer Instrument Company
    - One-way stopcocks with luer connections
- Septum
    - Ace Glass Inc
    - Septum stopper
    - 14/20 Jts Red
- Needle
    - Popper
    - Deflected noncoring septum penetration needles
    - Gauge 20, 6 in. length
    - Stainless steel
- Balance
    - Adventurer™ OHAUS
    - Maximum capacity: 210 g
    - Serial number: H041 120 235 1092 P
    - ID#: H0411202351
    - Item #: AR2140
- Liquid Scintillation Counter
    - Beckman LS 6500
    - Multi-purpose scintillation counter
    - System ID # 302115
- Scintillation Cocktail
    - Scintisafe Plus 50% Cocktail
- Bottle-Top Dispenser
    - Fisherbrand
    - 1-30mL in 1mL increments
    - ±0.7% accuracy; ±0.1% repeatability
    - Used to dispense scintillation cocktail
- Glass Vials
    - Fisherbrand
    - 20 mL Borosilicate glass
    - White urea caps, Cork-backed metal foil liner
- Gas Cylinders and Regulators
    - From NorLAB, a division of Norco Inc.
        - O_2
            - Item Number: SPG TSNRES76
            - Research Grade
            - Concentration 99.999%
                - < 0.5 ppm THC < 0.5 ppm CO
                - < 0.5 ppm CO_2 < 1 ppm H_2O

        - < 5 ppm Ar < 2 ppm N_2
    - Size T
    - Valve connection CGA 540
  - Harris High Purity Regulator
    - Item Number: HAR HP722125540
    - 0-125 psi, 2-Stage, CGA 540
  - Ar
    - Item Number: SPG TSNRES16
    - Research Grade
    - Minimum purity 99.9999%
      < 1 ppm H_2O < 0.2 ppm O_2
      < 0.1 ppm THC < 1 ppm N_2
      < 0.1 ppm CO < 0.1 ppm CO_2
    - Size 300
    - Valve connection CGA580
  - Harris High Purity Regulator
    - Item Number: HAR HP722125580
    - 0-125 psi, 2-Stage, CGA 580
  - Extra dry compressed air
    - 20.95±0.45% O_2
    - Balance N_2
    - SPG TSNED14
  - Used air regulator
    - CGA 590 nut
    - W/E CGA 510 nipple with filter
  - Calibration mixture
    - 10% CO_2
    - 10% CO
    - 10% CH_4
    - Balance N_2
  - Harris High Purity Regulator
    - Item Number: HAP HP7220503500
  - Compressed Helium
- Swagelok (Idaho Valve & Fitting) Parts
  - SS-4BHT-36 Teflon Lined Hose 1/4 in. Tube Stub Ends, 36 in. long
  - SS-4BHT-24 Teflon Lined Hose 1/4 in. Tube Stub Ends, 24 in. long
  - SS-400-3 SS Swagelok Tube Fitting, Union Tee, 1/4 in. Tube OD
  - SS-FM4SL4SL4-36 316L SS Convoluted (Flex Metal) Hose, 1/4 in., 316L SS Braid, 1/4 in. Tube Fittings, 36 in. Length
  - SS-4C-1/3 SS Poppet Check Valve, Fixed Pressure, 1/4 in. Swagelok Tube Fitting, 1/3 psig
  - SS-400-P 316 Stainless Steel Plug for 1/4 in. Swagelok Tube Fitting
  - SS-401-PC SS Swagelok Tube Fitting, Port Connector, 1/4 in. Tube OD
  - SS-43GS4 SS 1-Piece 40 Series Ball Valve, 1.4 Cv, 1/4 in. Swagelok Tube Fitting
  - SS-400-9 SS Swagelok Tube Fitting, Union Elbow, 1/4 in. Tube OD
  - SS-T4-S-035-20D SS Tubing 1/4 in.

- T-400-SET PTFE Ferrule Set (1 Front Ferrule/1 Back Ferrule) for 1/4 in. Swagelok Tube Fitting
- SS-810-6-4BT Reducing Union, Bored Through, 1/2 in. Swage x 1/4 in. Swage
- SS-810-6-4 SS Swagelok Tube Fitting, Reducing Union, 1/2 in. x 1/4 in. Tube OD
- SS-400-3TFT Female run Tee 1/4 in. Swage x 1/8 in. Female NPT
- SS-3-HC-1-2 SS Hose Connector, 1/8 in. Male NPT, 3/16 in. Hose ID
- SS-400-1-4 SS Swagelok Tube Fitting, Male Connector, 1/4 in. Tube OD x 1/4 in. Male NPT
- SS-100-R-4BT SS Swagelok Tube Fitting, Bored-Through Reducer, 1/16 in. x 1/4 in. Tube OD

- Graphite Samples
  - NBG-18
    - Listed Density: 1.85 g/cm^3
    - Average Porosity: 17-18%
    - Total Impurity: <100 ppm
    - Sample Size: ~ 0.5 cm x 0.50 cm
    - Flux Exposure: 6.7E+13 neutrons/cm^2s from MURR, U of Missouri, 120 days
  - NBG-25 from SGL, Germany
    - Listed Density: 1.82 g/cm^3
    - Average Porosity: 10-15%
    - Total Impurity: <100 ppm
    - Sample Size: Varied
    - Flux Exposure: 3.0E+14 neutrons/ cm^2s from ATR, Idaho National Laboratory <400 days

- Gas Analyzer
  - HIDEN ANALYTICAL QGA
    - Model No: HAS-301-941
    - Reference No: WR13757
    - RC Interface
      - S/n: 781902/E-13757
      - MAC Address: 00:01:CO:06:83:3F
    - RF Head
      - S/N: 6/81902/E
    - Gauge Head
      - S/N: HAM 71-5-7152
  - Software
    - MASsoft 7 Professional
    - QGA Professional -V 1.29
- ^{14}C Liquid Source
  - Eckert and Ziegler Analytics
  - 0.1 M NaOH, 1000.65 g, 1 L
  - ~30 µg C in Na_2CO_3/g of NaOH
  - $t_{1/2}$: 2.082×10^6 days
  - Activity: 3.707×10^4 Bq
  - Date: 07/19/2011, 12:00 pm EST

    - Uncertainty (%): u_A 0.2, u_B 2.0, u 4.0
- Volumetric Pipets
    - Reusable Class A
    - 0.5mL, Standard
    - Accuracy: ±0.006mL
- Syringe
    - B-D Becton Dickinson & Company
    - 1cc Tuberculin Syring ST™ Slip Tip
    - No. 309602
- Needle
    - B-D Becton Dickinson & Company
    - 20G1 PrecisionGlide®
    - No. 305175

Appendix C: Gas Specifications

The manufacturer specifications of the carrier gas (argon) and the oxidation agent (oxygen) added to the carrier gas can be seen in Table .

Table C.1: Properties of Gases Used

Gas	Molecular Weight g/mol	Density g/cc	Manufacture	Type, Purity	Impurities
Ar	39.948	1.784	NorLab	Research, 99.9999%	< 1 ppm H2O < 0.2 ppm O_2 < 0.1 ppm THC < 1 ppm N2 < 0.1 ppm CO < 0.1 ppm C O_2
O_2	31.988	1.429	NorLab	Research, 99.999%	< 0.5 ppm THC < 0.5 ppm CO < 0.5 ppm C O_2 < 1 ppm H2O < 5 ppm Ar < 2 ppm N2

Appendix D: Gas Analyzer Calculations to Correct Raw Data

Figures D.1a and D.1b show the settings for the QGA's gas detection screen with the gas species to be monitored entered.

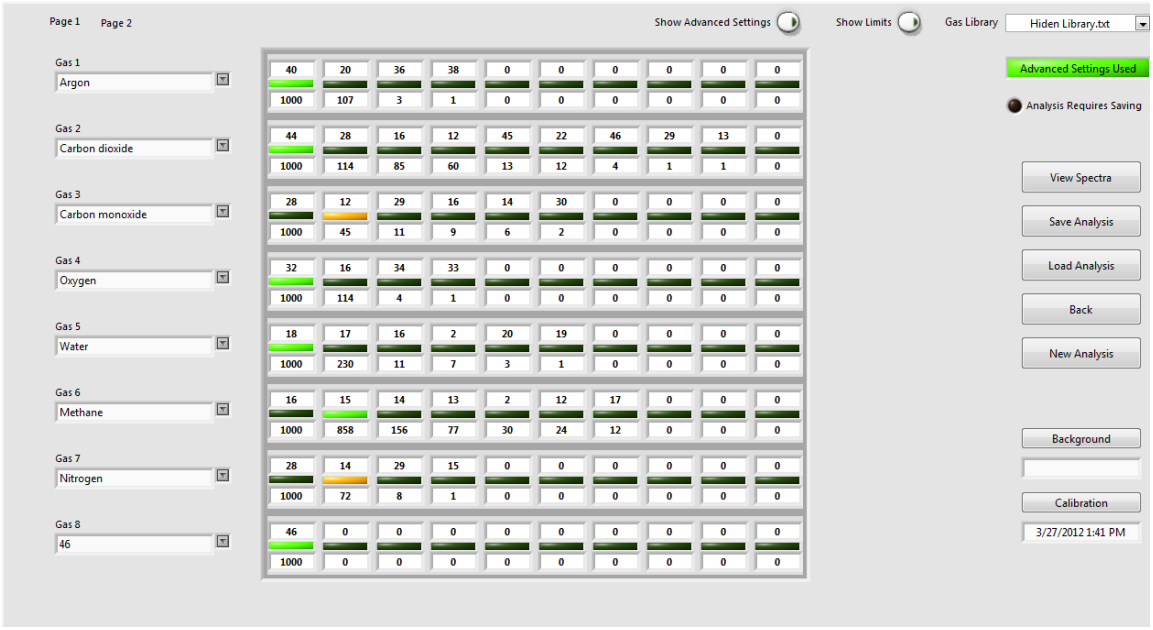

Figure D.1a: Gas Analyzer Limits Chosen for Experiment (Smith, 2013)

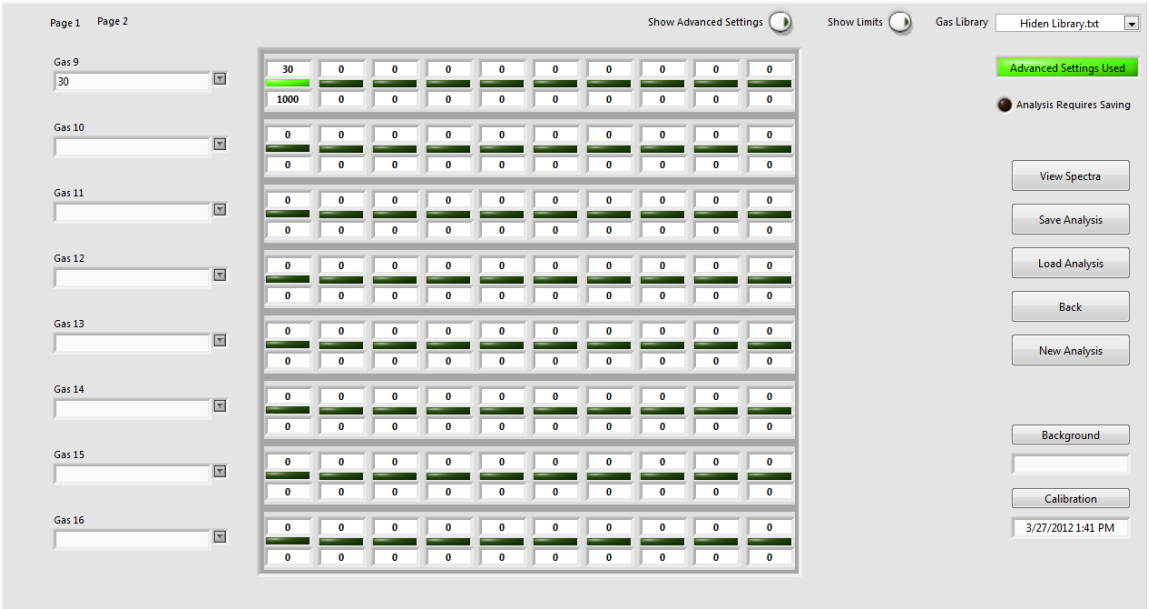

Figure D.1b: Gas Analyzer Limits Chosen for Experiment (Smith, 2013)

If a gas is not being analyzed on its 1000 intensity peak, and the peak is not overlapping with another gas peak, then the conversion calculation to the 1000 intensity peak pressure is shown in Equation 20.

$$P_{1000} = P_{I_i} \times (\frac{1000}{I_i}) \quad \text{Equation 20}$$

Where P_{1000} is the gas pressure of the 1000 intensity peak, P_{I_i} is the gas pressure of the *i* intensity peak, and I_i is the intensity of peak *i*.

If two gases have an overlapping peak must be resolved in order to find the 1000 intensity peak pressure for a gas without a unique peak, the calculation is shown in Equation 21.

$$P_{1000_z} = P_{I_{i_z}} \times \left(\frac{1000}{I_{i_z}}\right) - P_{I_{i_y}} \times \left(\frac{I_{o_y}}{I_{i_y}}\right) \quad \text{Equation 21}$$

Where z is the gas that has an overlapping peak but does not have a unique peak, and y is the gas with a unique peak and an overlapping peak. I_{o_y} is the intensity of the overlapping peak of gas y, and I_{i_z} and I_{i_y}.are the intensities of the peaks used for analysis for gas z and y respectively.

The software calibration factors obtained were used by the QGA software as multipliers in correcting the raw data.

Table D.1: Calibration Factors

Gas Setup							
Gas Names	**Unique Peaks Above**	**Ignore Peaks Below**	**Detector**	**Electron Energy**	**Emission Current**	**Minor Peaks**	**Calibration Values**
Argon	200	5	Faraday	70	250	No	9.99E-01
Carbon dioxide	200	20	Faraday	70	250	No	1.36E+00
Carbon monoxide	40	40	Faraday	70	250	No	1.43E+00
Oxygen	200	5	Faraday	70	250	No	9.98E-01
Water	200	10	Faraday	70	250	No	1.00E+00
Methane	200	70	Faraday	70	250	No	8.16E-01
Nitrogen	70	5	Faraday	70	250	No	9.04E-01
$^{14}CO_2$	100	5	Faraday	70	250	No	5.50E+09
^{14}CO	100	5	Faraday	70	250	No	5.66E+09

Appendix E: Liquid Scintillation Counter Calculations

To evaluate the change in activity with respect to time, the measured activity in a sample (dpm/mL) reported by the LSC was multiplied by the total volume from which the sample was taken. The activity was summed during the entire experiment to evaluate the increase in activity with respect to time and the total activity within the sample. The samples, backgrounds, and the standard were counted for 60 minutes with the LSC. The LUMEX% from LSC results was significant.

The true activity in a sample was determined using the minimum detectable activity (MDA) using Equation 22 Knoll (2000).

$$MDA = L_D/(f\varepsilon T) \quad \text{Equation 22}$$

For ^{14}C, f = 1, ε is the efficiency, and T is the count time. L_D is the minimum number of counts needed to ensure a false-negative rate no larger than 5% when using a specific L_c that ensures a false-positive rate less than 5%.

$$L_D = 4.653(\sigma_{N_B}) + 2.706 \quad \text{Equation 23}$$

$$L_c = 2.326(\sigma_{N_B})$$ Equation 24

Where NB is the background counts and σ_{N_B} is the square root of the background counts. Table E.1 shows the results of LSC counting of standards, backgrounds, and active experiment samples.

Table E.1: Efficiency based on Paired Counting

	cpm (raw)	LUMEX%	dpm
Standard	1187.82	0.02	1187.58
Background	42.13	4.15	40.38

Appendix F: ^{14}C Selective Release, K, Data

Table F.1: ^{14}C Selective Release, K, for NBG 18 Treated at 700°C for 8hrs

14C Selective Release, K, for NBG 18 Treated at 700oC for 8 hrs																			
AE5-2-N18-2150		AE6-2-N18-2150		AE7-2-N18-2300		AE8-2-N18-2300		AE9-0-N18-2300		AE10-0-N18-2300		AE1-0-N18-2150		AE2-0-N18-2150		AE3R-5-N18-2150		AE4R-5-N18-2150	
Time (hr)	K	Time (hr)	K	Time (hr)	K	Time (hr)	K	Time (hr)	K	Time (hr)	K	Time (hr)	K	Time (hr)	K	Time (hr)	K	Time (hr)	K
0.00	0.00	0.00	0.00	0.00	0.00	0.00	0.00	0.00	0.00	0.00	0.00	0.00	0.05	0.00	0.00	0.00	0.00	0.00	
0.75	-0.25	0.75	0.10	1.50	2.49	1.50	0.76	1.50	0.12	1.50	0.49	0.75	-0.09	0.75	0.25	0.75	0.16	0.75	2.49
1.75	-0.05	1.75	-0.93	2.50	5.70	2.50	5.33	2.50	0.24	2.50	-0.03	1.75	0.00	1.75	0.44	1.75	0.18	1.75	5.29
2.75	-0.31	2.75	0.49	3.50	3.76	3.50	-0.19	3.50	-1.68	3.50	-2.10	2.75	0.59	2.75	-0.05	2.75	0.17	2.75	5.59
5.00	0.90	5.00	0.52	5.00	115.86	5.00	39.78	5.00	0.74	5.00	3.05	5.00	1.37	5.00	4.64	5.00	5.70	5.00	14.24
5.50	1.92	5.50	0.17	5.50	230.40	5.50	78.10	5.50	-0.06	5.50	3.33	5.50	0.48	5.50	9.48	5.50	9.91	5.50	28.30
6.00	15.71	6.00	3.34	6.00	153.31	6.00	62.27	6.00	0.08	6.00	10.27	6.00	0.68	6.00	8.45	6.00	3.68	6.00	52.56
6.50	29.97	6.50	17.29	6.50	93.10	6.50	60.50	6.50	0.16	6.50	5.29	6.50	0.58	6.50	0.33	6.50	3.43	6.50	16.37
8.50	28.44	8.50	105.81	8.50	53.34	8.50	34.40	8.50	0.92	8.50	7.37	8.50	-0.79	8.50	1.70	8.50	1.91	8.50	2.59
10.50	2.33	10.50	58.62	10.50	44.09	10.50	8.62	10.50	2.02	10.50	7.08	10.50	0.71	10.50	-0.06	10.50	4.21	10.50	1.79
13.50	3.25	13.50	63.62	13.50	17.17	13.50	25.96	13.50	1.27	13.50	3.79	13.50	0.47	13.50	0.64	13.50	5.29	13.50	0.60
17.50	4.30	17.50	0.42	17.50	148.11	17.50	108.25	17.50	0.24	17.50	3.81	17.50	0.37	17.50	-0.18	17.50	165.59	17.50	0.41
Ave K	7.84	*Ave K*	22.68	*Ave K*	78.85	*Ave K*	38.53	*Ave K*	0.37	*Ave K*	3.85	*Ave K*	0.37	*Ave K*	2.33	*Ave K*	18.20	*Ave K*	11.84
Subset Average K		15.26		***Subset Average K***		58.69		***Subset Average K***		2.11		***Subset Average K***		1.35		***Subset Average K***		15.02	

Table F.2: ^{14}C Selective Release, K, for NBG 25 Treated at 700°C for 8hrs

14C Selective Release, K, for NBG 25 Treated at 700oC for 8 hrs															
AE15R-2-N25-2150-High		AE16-2-N25-2150-Low		AE17-2-N25-2300-High		AE18-2-N25-2300-Low		AE19-0-N25-2300-High		AE110-0-N25-2300-Mid		AE11-0-N25-2150		AE12-0-N25-2150	
Time (hr)	K	Time (hr)	K	Time (hr)	K	Time (hr)	K	Time (hr)	K	Time (hr)	K	Time (hr)	K	Time (hr)	K
0	0.00	0	0.00	0	0.00	0	0.00	0	0.00	0	0.00	0.00	0.00	0.00	
0.75	-0.33	0.75	-0.42	1.5	1.32	1.5	1.15	1.5	-0.02	1.5	-0.14	1.50	4.19	1.50	0.84
1.75	-0.16	1.75	0.00	2.5	0.81	2.5	0.62	2.5	0.19	2.5	0.01	2.50	-1.32	2.50	2.01
2.75	-0.19	2.75	-0.19	3.5	1.27	3.5	0.11	3.5	-0.75	3.5	0.42	3.50	1.63	3.50	0.83
5	0.27	5	0.06	5	1.98	5	1.40	5	0.27	5	0.21	5.00	6.46	5.00	1.04
5.5	2.18	5.5	2.12	5.5	11.93	5.5	11.83	5.5	0.02	5.5	0.83	5.50	-3.26	5.50	1.56
6	9.72	6	7.40	6	21.72	6	41.53	6	0.02	6	1.45	6.00	10.02	6.00	1.40
6.5	6.62	6.5	7.31	6.5	15.88	6.5	7.38	6.5	0.17	6.5	0.82	6.50	0.37	6.50	1.95
8.5	10.19	8.5	7.29	8.5	22.07	8.5	26.12	8.5	0.31	8.5	1.21	8.50	4.46	8.50	1.48
10.5	12.53	10.5	15.78	10.5	20.82	10.5	39.32	10.5	0.20	10.5	0.97	10.50	2.27	10.50	0.71
13.5	25.21	13.5	38.82	13.5	36.11	13.5	77.46	13.5	0.32	13.5	1.45	13.50	0.94	13.50	1.31
17.5	12.90	17.5	284.55	17.5	70.42	17.5	43.63	17.5	0.15	17.5	0.97	17.50	1.67	17.50	0.32
Ave K	7.18	*Ave K*	32.98	*Ave K*	18.58	*Ave K*	22.78	*Ave K*	0.08	*Ave K*	0.75	*Ave K*	2.49	*Ave K*	1.22
Subset Average K		20.08		***Subset Average K***		20.68		***Subset Average K***		0.42		***Subset Average K***		1.86	

Appendix G: Uncertainty of Values for Carbon-12 Mass Loss

Carbon-12 mass loss data came from two different sources. The first was from the physical weighing of the graphite samples prior to and immediately after thermal treatment. *(Samples were then returned to the furnace and completely oxidized to obtain the full activity of each sample for carbon-14 calculations).* The weight difference was divided by the initial sample weight to achieve % mass loss. The second carbon-12 mass loss value came from the Hiden Quadrupole Gas Analyzer (QGA) which monitored the carbon species released during thermal treatment. The sensitivity of the QGA was to 100 PPB. The values obtained from the QGA for the carbon species was less than 1 PPB, therefore, a high percentage of error is associated with these carbon-12 values.

The QGA values were used in the % mass loss calculations of this study, in order to compare the mass loss with previous studies which used the QGA values in this manner. Table G.1 shows the physical mass loss and the QGA mass loss values for comparison.

Table G.1: Carbon Mass Data

Sample Type & O2 Level	Initial Mass (g)	Post Thermal Treat. Mass (g)	Thermal Treat. Mass Loss (g)	Therm Treat. %Mass Loss	QGA Thermal Treat. Mass Loss (g)	QGA Thermal Treat. %Mass Loss
AE1-0-N18-2150	0.0363	0.0358	0.0005	1.38	0.0093700	25.80
AE2-0-N18-2150	0.0443	0.0437	0.0006	1.35	0.0327000	73.74
AE11-0-N25-L	0.0613	0.0611	0.0002	0.33	0.0023200	3.78
AE12-0-N25-L	0.0731	0.0725	0.0006	0.82	0.0022300	3.10
AE3-5-N18-2150	0.1257	0.0788	0.0469	37.31	0.0331000	26.30
AE4-5-N18-2150	0.0442	0.0034	0.0408	92.31	0.0249000	66.49
AE5-2-N18-2150	0.0962	0.0837	0.0125	12.99	0.0232428	24.16
AE6-2-N18-2150	0.0915	0.0817	0.0098	10.71	0.0055968	6.12
AE15-2-N25-2150-H	0.0296	0.0124	0.0172	58.11	0.0038817	13.11
AE16-2-N25-2150-L	0.0182	0.0078	0.0104	57.14	0.0045494	25.00
AE7-2-N18-2300	0.0724	0.0557	0.0167	23.07	0.0043700	6.04
AE8-2-N18-2300	0.048	0.0375	0.0105	21.88	0.0038100	7.94
AE17-2-N25-2300-H	0.0526	0.0111	0.0415	78.90	0.0054600	10.40
AE18-2-N25-2300-L	0.0584	0.0156	0.0428	73.29	0.0054600	9.34
AE9-0-N18-2300	0.051	0.0506	0.0004	0.78	0.0087194	17.10
AE10-0-N18-2300	0.0444	0.0443	0.0001	0.23	0.0029899	6.73
AE19-0-N25-2300-H	0.0252	0.0242	0.001	3.97	0.0035204	13.97
AE110-0-N25-2300-M	0.0346	0.0334	0.0012	3.47	0.0019656	5.68